Parkinson's Disease: Structural Integrity of Four Cognitive Networks

Jeremy Jao Yang Goh

Submitted in partial fulfillment of the requirement for the degree of

Master of Science in Psychology

University of Canterbury

2013

Acknowledgements

Let me start by saying that the journey here has not been easy with multiple delays and false starts along the way, on which blame falls squarely on my shoulder, and no one else. The motivation to continue has been dampened several times, because of personal reasons.

Therefore, I would like to express my deepest gratitude to my primary supervisor, Professor John Dalrymple-Alford, who has continually inspired and encouraged me stay on target and to finally reach the finish line. His invaluable knowledge and wisdom, coupled with his infectious enthusiasm for the topic, has evidently rubbed off on me and I feel truly honored to have had the opportunity to work with him. My sincerest thanks also go to Dr. Tracy Melzer, who continues to amaze me with his broad technical knowledge, for his expertise and sound advice in all neuroimaging related topics. I must also recognize the considerable contributions made by the researchers at the New Zealand Brain Research Institute who have worked tirelessly so on finding ways to further improve the quality of life and cognition of patients with neurodegenerative disorders. Your work is a constant reminder that my research is relevant in the 'real world'.

I would also like to thank my family for being there as support and for believing in my abilities to finish when I couldn't believe in myself. To my parents, you both are the greatest inspiration for me to finish this thesis and to show that I'm capable of pushing myself beyond my limits as you have always taught us to do. To my sister, thank you for understanding and helping whenever I struggled with personal issues. To my twin brother, your greatest help to me is just being there when I needed someone to talk to and believing in me when no one else does. To my two younger brothers, both of you inspired me to set a good example for you to follow when you come into the academic world in the future. A very special thanks to my uncle as well, for sponsoring me throughout my study life and never doubting my abilities to go as high as I can go.

Finally, I would also like to thank my partner, Angeline, for her love and support throughout the period of this research. I also acknowledge the sacrifices that she has had to make and appreciate everything she has done for me.

Table of Contents

1. Introduction

2. Method

3. Results

4. Discussion

5. References

Individuals with Parkinson's disease (PD) often show cognitive impairments in addition to motor symptoms, with the majority of PD patients converting to dementia as the disease progresses. The changes in the microstructural integrity of key nodes in resting state networks (RSNs) could be a good indicator of the cognitive effects of PD on brain regions as it progresses to dementia. To assess the association between cognitive effects and microstructural change, the microstructural integrity of the regions of interest (ROIs) in 4 resting state networks (RSN), specifically the default mode network (DMN), based on DTI were obtained in three separate groups of patients with PD. One group of patients (PD-N) were cognitively normal, while the second group of patients (PD-MCI) reflect the transitional phase of mild cognitive impairment prior to dementia, and the third group of patients (PD-D) possessed a clear diagnosis of dementia. A comparison group of healthy controls (HC) were included, matched across the three patient groups. The PD-D group showed worse microstructural integrity for the majority of the ROIs across the 4 networks. The loss of structural integrity in the PD-MCI group was more selective, with some ROIs showing similar changes to PD-D, and others showing similar changes to the PD-N group. The PD-N group fail to show any changes in the structural integrity of any ROIs, relative to HC. For future study, a combined structural / functional study should be performed to examine if there are similar changes across both measures.

1. Introduction

1.1 Parkinson's Disease

Parkinson's disease (PD) is the second most common aging-related neurodegenerative disorder, following Alzheimer's Disease (AD), with a male to female ratio of 2:1 in most studies (Meireles & Massano, 2012; Wirdefeldt, Adami, Cole, Trichopoulos, & Mandel, 2012). PD is an idiopathic motor disorder that is associated with the degeneration of nigrostriatal dopamine neurons, related to the presence of Lewy bodies in brain-stem nigral and extranigral neurons (Wirdefeldt et al., 2012). Various risk factors are implicated in the development of PD, including exposure to pesticides and other toxics, positive family history of PD and aging, which is the most significant risk factor documented so far (Hindle, 2010; Schapira & Jenner, 2011; Thal, Del Tredici, & Braak, 2004; Wirdefeldt et al., 2012). PD is diagnosed by identifying the classical motor symptoms of bradykinesia, rigidity, tremor, and postural instability (Guttman, Kish, & Furukawa, 2003 ; Jankovic, 2008). Other manifestations of PD include psychiatric symptoms such as anxiety and depression and dysautonomic symptoms such as orthostatic hypotension, constipation, sexual dysfunction and weight loss (Jankovic, 2008; Meireles & Massano, 2012). In addition, cognitive impairment is now recognised as a major feature of PD (Svenningsson, Westman, Ballard, & Aarsland, 2012).

1.2 Cognitive Impairments in PD

A growing body of neuropsychological evidence shows that patients with PD have diverse cognitive problems affecting visuospatial abilities, memory, and executive functioning, even at relatively early stages of the disease (Bosboom, Stoffers, & Wolters, 2004; Dagher & Nagano-Saito, 2007; Goldman, Baty, Buckles, Sahrmann, & Morris, 1998; Ibarrexte-Bilbao, Junque , Marti, & Tolosa, 2011; Williams-Gray, Foltynie, Brayne, Robbins, & Barker, 2007).

Many patients with PD endure cognitive decline, often sufficient to be categorized as mild cognitive impairment (PD-MCI), a diagnosis that can be defined as cognitive deterioration that is considered abnormal for the patient's age, but with retention of daily functioning (Aarsland et al., 2010; Barone et al., 2011; Goldman & Litvan, 2011 ; Jellinger, 2013). PD-MCI can include not only memory impairment, but impairments in language, attention, executive function and visuospatial function as well (Caviness et al., 2007).

As the specific criteria of PD-MCI vary widely across different groups based on different populations and methodology (Dalrymple-Alford et al., 2011), there has been a recent proposal of consensus criteria for PD-MCI (Litvan et al., 2012; see Method for definition). The prevalence of PD-MCI is estimated to be approximately 20 – 30% of non-demented PD patients (Aarsland et al., 2010; Goldman & Litvan, 2011; Meireles & Massano, 2012). Patients with PD-MCI are at an increased risk of developing dementia, compared to those without MCI (Broeders et al., 2013; Janvin , Larsen, Aarsland, & Hugdahl, 2006; Weintraub et al., 2012).

A highly important facet of PD is that cognitive decline in the majority results in a cumulative prevalence of dementia as high as 75% - 85% of patients, such that PD patients have a four- to six-fold chance of developing dementia, compared to healthy elderly people (Aarsland

et al., 2007; Emre et al., 2007; Hobson & Meara, 2007). Dementia has a substantial impact on both caregivers and is associated with increased mortality and morbidity rate as well as a higher risk for nursing home placement (Callahan et al., 2012; Gaugler, Mittelman, Hepburn, & Newcomer, 2010; Hughes, Ross, Mindham, & Spokes, 2004; Posada et al., 2011).

Therefore, it is important to elucidate the underlying neurobiological changes that may be implicated in the progression to dementia in patients with PD. One such neurobiological mechanism is the impairment of key resting-state cognitive networks.

1.3 Resting-State Networks

Functional magnetic resonance imaging (fMRI) studies when participants are not engaged in an external task (resting state, RS) have demonstrated that spontaneous fluctuations in activity within separate brain regions (‘nodes’) exhibit a strong temporal correlation, which suggests that these regions form different functional cognitive networks (Damoiseaux et al., 2006; Deco, Jirsa, & McIntosh, 2011; Fox & Raichle, 2007; Mantini, Perrucci, Gratta, Romani, & Corbetta, 2007). Several such networks have been identified, and these networks are spatially consistent across subjects and across different testing sessions (Jeong, Choi, & Kim, 2012; Shehzad et al., 2009). These networks, each termed a ‘resting-state network’ (RSN), have been suggested to represent the fundamental functional organization of the brain that represents various cognitive processes (van den Heuvel & Pol, 2010; Rosazza & Minati, 2011).

During the last decade, one RSN and its associated set of brain regions has become the object of intensive focus and research in neuroscience. This particular RSN is often referred to as the default mode network (DMN), which has been identified in an emerging body of evidence

that demonstrates a consistent pattern of activity across a network of specific brain nodal regions that include the posterior cingulate cortex (PCC), medial prefrontal cortex - both ventral and dorsal regions (vMPFC/dMPFC), inferior parietal lobule (IPL), and middle temporal gyrus (MTG), all of which were reported across many studies in a very high degree of reliability; the hippocampus is often reported as well but was observed as relatively less robust than the specific regions (Andrews-Hanna, Reidler, Sepulcre, Poulin, & Buckner, 2010; Buckner, Andrews-Hanna, & Schacter, 2008; Greicius, Krasnow, Reiss, & Menon, 2003; Heuvel, Mandl, Kahn, & Pol, 2009; Heuvel & Pol, 2010; Long et al., 2008; Raichle et al., 2001). Although deactivated during task performance, the DMN is active in the resting brain with a high degree of functional connectivity (FC) between these component regions (Greicius, Krasnow, Reiss, & Menon, 2003; Greicius, Supekar, Menon, & Dougherty, 2009; Long et al., 2008; Raichle, 2011; Raichle & Snyder, 2007).

This resting state activity in the brain has been termed the default-mode brain activity to denote a high-energy expenditure state in which an individual is awake and alert, but not actively involved in an attention demanding or goal directed externally driven task (Fransson, 2006; Raichle et al., 2001; Raichle, 2011). In other words, the DMN is engaged when individuals are left to think to themselves undisturbed (e.g., resting quietly but awake with eyes closed or open or passively viewing a particular visual image) (Raichle et al., 2001; Raichle & Snyder, 2007). The term ‘deactivation’ was often used because analyses and image visualization of brain scans were referenced to a target, experimental task. Within this context, regions relatively more active in a target condition (e.g., reading or classifying pictures) compared to the control task (e.g., passive fixation of an image, rest with eyes open or closed) were labelled ‘activation’. Thus,

reduced activity when target condition was compared to the control condition was labelled 'deactivation' (Buckner et al., 2008).

Many studies have confirmed that other kinds of situations, beyond passive viewing of an image or rest, can engage the default mode network in similar ways. For example, remembering the past (autobiographical memory), envisioning future events (prospection), considering the thoughts and perspectives of other people (theory of mind), and moral decision making all activate multiple regions within the DMN (Andrews-Hanna, 2012; Andrews-Hanna et al., 2010; Spreng & Grady, 2010; Buckner et al., 2008).

The two most clearly defined regions within the DMN that play a role in these situations are the PCC and MPFC (Andrews-Hanna et al., 2010; Broyd et al., 2010) The PCC has been shown to be the only DMN region that directly interacts with all other DMN regions during working memory tasks, which suggests that it may play a pivotal role in how intrinsic activity is mediated throughout the DMN. The PCC is also a key region in cognitive tasks that touch upon various aspects of self-processing (Andrews-Hanna et al., 2010; Fransson & Marrelec, 2008; Leech, Braga, & Sharp, 2013; Leech & Sharp, 2013). The MPFC has been associated with social cognition involving the monitoring of the psychological state of oneself, as well as mentalising about the psychological state of others (Andrews-Hanna et al., 2010; Broyd et al., 2009; Mars et al., 2012).

At present, the majority of RS fMRI assessment has been focused primarily on the DMN. Analysis of RS fMRI data, however, has suggested the existence of three other networks that play a significant role in other cognitive processes as well (Bressler & Menon, 2010; Damoiseaux et al., 2006; Raichle, 2011; Spreng, Sepulchre, Turner, Stevens, & Schacter, 2012).

The first network is the dorsal attention network (DAN), which is comprised of the posterior and anterior intra parietal sulcus (IPS), frontal eye fields (FEF), and extrastriate visual areas such as the middle temporal area (MT+). The DAN appears to be involved in the goal-driven attention orienting (top-down) process and is responsible for the preparation and selection of stimuli for responses (Corbetta & Shulman, 2002; Li et al., 2012). Its activity often increases after presentation of cues associated with the where, when, or to what participants should direct their attention (Fox, Corbetta, Snyder, Vincent, & Raichle, 2005).

The second network is the central executive network (CEN), covering medial and lateral PFC areas such as the dorsolateral prefrontal cortex (dlPFC) and the anterior inferior parietal lobule (aIPL). The CEN is involved in higher-order cognitive control and typically shows activation during performance of higher-level externally-directed cognitive tasks, when the shows decreased deactivation (Bressler & Menon, 2010; Sridharan, Levitin, & Menon, 2008).

The fourth network is the salience network (SN), which is comprised of the insula (INS) and the anterior cingulate cortex (ACC). The SN is believed to play a critical, causal role in switching between the CEN and DMN across cognitive paradigms and stimulus modalities (White, Joseph, Francis, & Liddell, 2010; Sridharan et al., 2008). It is important to recognise the CEN is often paired with SN in some studies, and this combination is often referred to as the fronto-parietal control network (FPCN; Niendam et al., 2012; Spreng et al., 2012; Vincent et al., 2008).

1.4 Default Mode Network and Alzheimer's disease

The exploration of these functional RSN has also provided novel insights into psychiatric and neurological disorders. The most compelling of these is the link between impairment in the DMN and Alzheimer's Disease (AD), where an association between failure to deactivate the DMN when engaging in tasks requiring working memory and attention to exogenous stimuli has been observed in AD patients (Broyd et al., 2009; Buckner et al., 2008; Hafkemeijer, Grond, & Rombouts, 2012). AD is a progressive dementia and is characterised by the formation of neuritic plaques and neurofibrillary tangles in the cortex, with the hallmark symptoms of memory loss, language difficulties, and impairments in executive function (Burns & Iliffe, 2009).

The earliest evidence to suggest the impairment of the DMN in AD was a study by Minoshima et al. (1997), which showed that there is a consistent progressive reduction in glucose metabolism (hypometabolism) in the PCC. This hypometabolism correlated with mental status and dementia severity (Minoshima et al., 1997). Subsequent work showed that the patterns of hypometabolism included PCC as well as other regions of DMN such as the IPL and MPFC (Greicius, Srivastava, Reiss, & Menon, 2004; Buckner et al., 2005).

Structural atrophy in the brain of AD patients also coincides with specific brain regions of the DMN. Buckner et al., (2005) showed that atrophy is present even in patients at the earliest stages of AD, with the PCC and IPL showing prominent atrophy. As dementia progressed, the atrophy rates accelerated across these regions, confirming that the impairment in the DMN is significantly correlated with the severity in dementia.

Functional fMRI changes within the DMN have been explored in various studies which showed that these impairments were consistent with the metabolic and structural changes. Based on the analysis of intrinsic activity correlations and task-induced deactivations, Lustig et al., (2003) showed that deactivation was attenuated significantly in AD patients compared to young adults and cognitively-normal older adults. Rombouts and colleagues (2005) also showed that task-induced deactivation was attenuated in older participants with MCI; signifying altered brain deactivation was already present in patients in the prodromal stage of dementia. Other work has shown that dysfunction in the DMN is also associated with those older people with MCI who then progress to AD (Petrella et al., 2011).

In summary, the DMN seems to be highly disrupted by AD, perhaps related to the high metabolism of DMN regions, particularly the PCC, as these regions appear to be particularly vulnerable to atrophy in AD patients (Buckner, 2008). A recent review by Jacobs, Radua, Luckman, & Sack (2013) also showed that the PCC is a central hub in AD (i.e destabilization of the PCC could cause disruptions in large-scale cognitive networks and lead to structural, functional, and metabolic deficits seen in AD). Brier et al. (2012) concluded that AD does not only affect the DMN, but the DAN and SN as well, with increasing AD severity positively correlating with decreasing FC between all regions of these networks.

1.5 Default Mode Network and Parkinson's disease

As problems in the DMN appear to be tightly linked with AD, it is relevant to ask whether impairments in DMN are also apparent in other types of neurodegenerative disorders. DMN integrity in PD is one such condition of interest. In a recent study, Weintraub et al. (2012) found that the overall pattern of brain atrophy in AD were similar to the progression of cognitive

decline in patients with PD, which indicates that similar brain regions were affected in both disorders.

It is possible then to infer that the PD will also affect the DMN. Several studies that utilize the fMRI support this suggestion. Van Eimeren, Monchi, Ballanger, and Strafella (2009) showed that unmedicated patients with mild to moderate PD demonstrated less deactivation of the PCC, as well as decreased functional connectivity (FC) with the vMPFC, relative to controls, indicating a failure to deactivate the frontal part of the DMN for PD patients. Tessitore et al. (2012) also showed cognitively unimpaired patients with PD have decreased FC of the right medial temporal lobe (MTL) and bilateral inferior parietal cortex (IPC) within the DMN, when compared with controls, which could suggest that there is an prodromal functional disruption of the DMN in PD. Another study report decreased FC of the dentate nucleus (DN) to DMN regions, in cognitively unimpaired PD patients, which implies disruptions in RS FC between the cerebellum and the DMN in PD (Liu et al., 2013). Rektorova, Krajcovicova, Marecek, & Mikl (2012) reported significant decreases of FC in the inferior frontal gyrus (IFG) with the PCC for PD participants with dementia (PD-D), as compared to PD and HC.

1.6 Diffusion Tensor Imaging

It is evident that literature on DMN in PD populations is minimal. Therefore, it is a good opportunity to add to that knowledge and bring a unique contribution to the research of DMN in PD. As imaging data using fMRI were not available in patients given brain scans at the New Zealand Brain Research Institute (NZBRI), where the current study was conducted, diffusion tensor imaging (DTI) was utilized to evaluate the microstructural integrity of the nodal regions within the DMN and other RSNs in the current study, looking at PD patients who through

detailed neuropsychological testing and evaluation of everyday activities had been carefully classified as showing relatively normal cognition (PD-N), mild cognitive impairment (PD-MCI), or with dementia (PD-D). Structural integrity is often examined using grey matter concentration in T1 images, which only provides a crude analogue of structural changes.

DTI is a powerful form of magnetic resonance imaging (MRI) contrast that enables quantification of the direction of diffusing water molecules within the entire brain volume to study microstructural white and grey matter integrity in neurodegenerative diseases and to visualize brain fiber connections via tractography (Le Bihan et al., 2001; Scherfler et al., 2011; Schuff, 2009). Multiple MRI images are taken that measure the ability of water to diffuse along different gradient directions. These measurements allow calculation of the diffusion tensor (angulate variation of diffusion), to derive fractional anisotropy (FA) that represent the local directional 'strength' of white matter, especially nerve bundles, and Mean Diffusivity (MD) that reflect the total magnitude of diffusion and hence, information of alterations in the cellular integrity of grey matter regions (Scherfler et al., 2011; Skudlarski et al., 2008). Generally, FA value decreases when there is microstructural pathology that reflect decreased coherence such as myelination defects in the fiber tract and MD value increases when there is an increase in extracellular space as a result of fiber loss (Chua et al., 2009 Meijer, Bloem, Mahlknecht, Seppi, & Goraj, 2013).

An example of the utilization of DTI in evaluating the DMN is a study by Teipel et al. (2010) that investigated the structural basis of the FC pattern for the DMN. White matter microstructure underlying default mode connectivity was evaluated by deriving FA values of fibre tract integrity DTI and RS-fMRI data from twenty healthy elderly participants (50 – 83 years of age). The results of this study revealed that the functional connectivity between the PCC

and hippocampus from the RS- fMRI data was associated with the FA values of the white matter network connecting the regions of the DMN.

A hypothesis-driven approach based on the functional connectivity of PCC and a data-driven Independent Component Analysis (ICA) approach without a priori selection of correlated regions was shown to include the key regions of the DMN in the RS- fMRI data. When the functional connectivity data between PCC and hippocampus were regressed on the FA maps of white matter microstructure, distinctive subcortical white matter areas were found to match the distribution of DMN components. These structural problems of connectivity coincided with fMRI functional connectivity, supporting the value of using structured integrity to evaluate this network, and by extension, other RSN (Teipel et al., 2010). The findings of this study suggests that DTI is a useful and powerful tool that can be utilized to provide unique information about the microstructural changes that can occur in neurodegenerative disease such as Parkinson's disease (Meijer et al., 2013; Schuff, 2009).

Several studies on PD have shown that DTI is effective at imaging other brain correlates of PD, but not RSNs. However, it has been instructive in showing that DTI is sensitive to changes in PD. Matsui et al. (2007) showed that PD patients possess significant FA reduction in frontal, temporal and occipital white matter compared to controls. Moreover, patients with PD-D showed a significant reduction in bilateral posterior cingulate bundles compared to PD patients who are cognitively normal, which is consistent with the hypotheses in the current project. Another study by Chan et al. (2007) showed that the thalamus, globus pallidus, putamen, and caudate are relatively spared in PD patients who are cognitively normal, with unaltered MD and FA values in these regions. However, the FA value in the substantia nigra of these patients was lower compared to HC. The clinical severity of PD was also found to be correlated inversely

with the FA value in the substantia nigra of these patients. A subsequent study by Gattellaro et al. (2009) reported similar findings with decreased FA and increased MD in the substantial nigra, genu of the corpus callosum, and the superior longitudinal fasciculus, indicating degeneration in temporal and parietal areas of the brain in patients with PD who are cognitively normal.

1.7 The Current Study

The current study investigated the microstructural integrity of the DMN, as well as three other key cognitive RSNs, the DAN, SN, and CEN, based on DTI obtained in three separate groups of patients with PD. One group of patients (PD-N) were cognitively normal, while the second group of patients (PD-MCI) reflect the transitional phase of mild cognitive impairment prior to dementia, and the third group of patients (PD-D) possessed a clear diagnosis of dementia. A comparison group of healthy controls (HC) were included, matched across the three patient groups. The diffusion tensor images used in this study were previously discussed in a PhD study, 'Magnetic resonance imaging of cognition in Parkinson's disease', by Melzer (2011). That thesis focused on whole-brain analysis in patients with PD and did not include evaluation of the RSN in the brain.

The current study made a novel contribution by examining the microstructural integrity of the ROIs within each RSN, by evaluating the FA and MD values for the grey matter voxels in key nodes of the ROIs of these 4 RSNs. One important contribution of the current study was to assess the wider literature to identify the consistent coordinates of the key nodes within each RSN. The RSNs from the relevant past studies were evaluated to derive the coordinates of the ROIs in Montreal Neurological Institute (MNI) space (Friston et al., 1999) or Talairach space

(Turkeltaub et al. 2002) and these coordinates used to derive DTI metrics in nodes within the unique subject space for each individual.

It was expected that there would be minor if any changes in structural integrity of the RSNs for the PD-N group, relative to HC group. Changes in the structural integrity in the PD-MCI group across the RSNs were expected to be similar to approach the structural integrity of the PD-D group, relative to HC and PD-N. The structural integrity of the PD-D group across the RSNs was expected to show loss of integrity, especially for the DMN.

2. METHOD

2.1 Participants

A convenience sample of 118 patients meeting the United Kingdom Parkinson's Disease Society's criteria for idiopathic PD (Hughes, Daniel, Kilford, & Lees, 1992) were recruited from the Movement Disorders Clinic at the New Zealand Brain Research Institute, formerly known as the Van Der Veer Institute for Parkinson's and Brain Research, Christchurch, New Zealand, from May 2007 to March 2010. Patients were diagnosed with probable PD by a neurologist who specialized in movement disorders. The Unified Parkinson's Disease Rating Scale (UPDRS; part III, motor, Gancher, 2006), with Hoehn and Yahr staging (Hoehn & Yahr, 1967) was used to assess disease severity in terms of motor function for participants with PD. Individuals who represented the full spectrum of cognitive status in PD were invited to participate. The control group comprised of 38 healthy volunteers responding to community advertisements, who

reported no subjective cognitive problems on interview, matched to the entire PD sample in terms of the mean age, years of education, and sex ratio.

General exclusion criteria included atypical parkinsonian disorders, history of other neurological or central nervous system disorders (e.g. moderate to severe head injury, stroke, vascular dementia), and major psychiatric or medical illness in the last 6 months. Neuroradiological screening after an MRI brain scan excluded four patients with PD and one control due to moderate-severe white matter disease, one patient with PD due to extensive cerebral atrophy, and one healthy control with severe cerebellar infarct. A further four PD patients and one control were excluded because of excessive motion (due to tremors while in the MRI scanner) or extreme susceptibility artifacts (which produce inconsistent and blurry MRI images). Four controls met the criteria for MCI and were excluded. Analyses were then conducted on the remaining 110 PD patients and 31 control subjects (Table 1).

All participants gave informed consent, with additional consent from a significant other for dementia patients when required. The Upper South Regional Ethics Committee of the New Zealand Ministry of Health approved the study.

Table 1

Demographic and clinical details for each group

	Controls	**PD-N**	**PD-MCI**	**PD-D**	**N-K Analysis (adjacent pairwise)**
n	31	64	28	18	
Age*	69.4 (8.9)	64.4 (8.6)	70.4 (7.6)	74 (6.8)	HC = PD-N = PD-MCI <PD-D
Sex (male : female)	(23 : 8)	(42 : 22)	(19 : 9)	(16 : 2)	NS
Education (years)	13.3 (2.9)	13.3 (2.9)	13.2 (3.4)	12.4 (2.5)	NS
MMSE*	28.4 (1.6)	28.3 (1.6)	26.1 (2.0)	22.9 (3.1)	(HC = PD-N) <PD-MCI <PD-D
MoCA*	27.0 (2.0)	26.7 (2.2)	22.9 (2.4)	16.4 (4.0)	(HC = PD-N) <PD-MCI <PD-D
Global Cognitive Z Score*	0.54 (0.38)	0.16 (0.42)	-0.83 (0.39)	-1.88 (0.51)	HC <PD-N <PD-MCI <PD-D
Domain Z Score[1]					
Executive Function*	0.60 (0.53)	0.37 (0.61)	-0.90 (0.79)	-2.06 (0.5)	(HC = PD-N) <PD-MCI <PD-D
Attention*	0.43 (0.46)	0.11 (0.48)	-0.82 (0.57)	-1.95 (0.60)	HC <PD-N <PD-MCI <PD-D
Learning and Memory*	0.91 (0.77)	0.30 (0.81)	-0.73 (0.63)	-1.7 (0.67)	HC <PD-N <PD-MCI <PD-D
Visuospatial/Visuoperceptual*	0.21 (0.48)	-0.14 (0.45)	-0.87 (0.65)	-1.87 (0.67)	HC <PD-N <PD-MCI <PD-D

Values are Mean (SD); group main effect, *p<.001; MMSE, Mini Mental State Examination; MoCA, Montreal Neurological Assessment; N-K, Newman-Keuls; HC, Healthy Controls; PD-N, cognitively unimpaired PD patients; PD-MCI, PD patients with Mild Cognitive Impairment; PD-D, PD patients with Dementia; NS, Not Significant.

[1]Language measures also contributed to a PD-MCI diagnosis, by using two scores of "fail" to indicate impairment within that domain because two of the three measures (Boston Naming Test; Similarities in the Dementia Rating Scale-2; language score in the ADAS-Cog) had strong ceiling effects in the controls that precluded the use of normative scores.

2.2 Neuropsychological and Neuropsychiatric Assessments

Participants underwent comprehensive neuropsychological testing, that covered five cognitive domains, over two sessions. These cognitive domains were executive function, attention and working memory, learning and memory, visuospatial/visuoperceptual skills and language, consistent with the Movement Disorder Society (MDS) Task Force criteria for diagnosis of dementia (Dubois et al., 2007) or MCI (Litvan et al, 2012).

Executive function was assessed using Action (verb) Fluency (Piatt, Fields, Paolo & Troster, 1999), Trails-Making Test Part B (TMT-B; Reitan, 1958; Arbuthnott & Frank, 2000), and the Delis-Kaplan Executive Function System (D-KEFS; Delis, Kaplan, & Kramer, 2001) Letter Fluency, Category Fluency, Category Switching, and Stroop Interference Test.

Attention, working memory, and processing speed were evaluated using the Stroop Word and Colour Test in the D-KEFS (Delis et al., 2001), Digit Span Test-Forward/Backword (Wechsler, 1997), Adaptive Digit Ordering Test (Werheid et al., 2002), Test Everyday Attention-Map Search (TEA-Map Search; Robertson, Ward, Ridgeway, & Nimmo-Smith, 1996), and Trails-Making Test Part A (TMT-A; Reitan, 1958).

Learning and memory were measured using the free recall, short and long delay recall components of the California Verbal Learning Test-2 Short Form (CVLT-II SF; Delis, Kramer, Kaplan, & Ober, 2000) and the short and long delay recall of the Rey-Osterrieth Complex Figure (ROCF; Meyers & Meyers, 1995). Either short or long delay, but not both could indicate problems for each memory test.

Visuospatial and visuoperceptual skills were assessed using the copy of the ROCF (Meyers & Meyers, 1995), Judgement of Line Orientation (JOL; Benton, Harnay, & Varney

(1975), and the fragmented letter task of the Visual Object and Space Perception Battery (VOS; Warrington & James, 1991).

Language was assessed using the Lansing Boston Naming Test (LBNT, short-form of the Boston Naming Task; Kaplan, Goodglass, & Weintraub, 1983; Lansing, Ivnik, Cullum, & Randolph, 1999), the Similarities subtest, identify which three items is different of the Conceptualization section of the Dementia Rating Scale-2 (DRS-2; Jurica, Leitten, & Mattis, 2001), and the language items, 'naming objects and fingers, verbal language/comprehension of spoken language, and word-finding', of the Alzheimer Disease Assessment Scale – Cognitive subscale (ADAS-COG; Rosen, Mohs, & Davis, 1984; Lezak, 2004),.

The Montreal Cognitive Assessment, Standardized Mini-Mental State Examination, Scales for Outcomes in Parkinson's Disease-Cognition, and the Wechsler Test of Adult Reading (MoCA; Nasreddine, et al., 2005; SMMSE; Molloy & Standish, 1997; SCOPA-Cog; Marinus et al., 2003; WTAR; Holdnack, 2001) were also administered to assess their global cognitive abilities. The MoCA is a brief cognitive screening tool that has been shown to be sensitive to subtle cognitive deficits in PD (Dalrymple-Alford et al., 2010; Chou et al., 2010). The SMMSE is a modified version of the MMSE (Folstein, Folstein, & McHugh, 1975) that has been found to be more reliable in screening elderly patients for cognitive impairment than the MMSE (Molloy, Alemayehu, & Roberts, 1991; Pangman, Sloan, & Guse, 2000; Vertesi et al., 2001). The SCOPA-Cog was developed as a PD-specific scale that focused on the cognitive deficits typically found in PD patients and recent studies have shown that it is a robust and reliable measure of cognitive function in PD, as well as possessing high validity in detecting MCI in PD populations (Forjaz, Frades-Payo, Rodriguez-Blazquez, Ayala, & Martinez-Martin, 2010; Isella et al., 2013, Kulisevsky & Pagonabarraga, 2009). The WTAR was normally used to assess premorbid intelligence, which assess reading irregular words that

are associated with intellectual functions thought to be resistant to cognitive decline as a result of the neurological damage in neurodegenerative disorders (Green et al., 2008).

Neuropsychiatric status for all PD participants was evaluated with the Neuropsychiatric Inventory (NPI; Cummings et al., 1994), and the Geriatric Depression Scale (GDS; Yesavage et al., 1982). PD participants were also assessed for everyday functional activities relevant to dementia with the Functional Assessment Staging Tool, (FAST; Reisberg, 1988), the Activities of Daily Living - International Scale (ADL-IS ; Reisberg et al., 2001), and the Global Deterioration Scale (GDS; Reisberg, Ferris, de Leon, & Crook, 1982).

The diagnosis of PD dementia (PD-D) was based on the criteria established by the MDS Task Force (Dubois et al., 2007), which states impairment (in research, 2 SD below normative data) in at least one measure in two or more cognitive domains, supported by evidence from the neuropsychological tests battery mentioned earlier (DRS-2 and ADAS-COG; Jurica et al., 2001; Rosen et al., 1984) and the Clinical Dementia Rating (CDR; Morris, 1993), along with evidence that the cognitive impairment is severe enough to affect everyday function as reported by a caregiver.

The diagnosis of PD-MCI was based on criteria used at the NZBRI (Dalrymple-Alford et al., 2011), 1.5SD:2 in a single domain (1.5SD below normative data for two measures in at least one of the cognitive domains). These criteria were consistent with the diagnostic criteria of the MDS Task Force for MCI (Litvan et al., 2012). No PD-MCI participants met the criteria for dementia (i.e. their cognitive impairments did not interfere significantly with everyday activities). No PD-N participants met the relevant criteria for PD-MCI or PD dementia.

2.3 MRI Acquisition

Imaging was conducted on a 3 tesla General Electric HDxt scanner (GE Healthcare, Waukesha, WI) with an 8-channel head coil. A 2-dimensional diffusion-weighted, spin-echo, echo planar imaging sequence was used to measure microstructural integrity, with diffusion weighting in 28 uniformly distributed directions (b = 1,000 s/mm²) and 4 acquisitions without diffusion weighting (b = 0 s/mm²): echo time (TE) / repetition time (TR) = 86.4/13,000 milliseconds, flip angle = 90˚, acquisition matrix = 128 × 128 × 48, reconstruction matrix = 256 × 256 × 48, field of view = 240 mm, slice thickness = 3 mm, and reconstructed voxel size = 1.07 × 1.07 × 3 mm³. Volumes were acquired without cardiac gating. A T1-weighted (spoiled gradient recalled echo; TE/TR = 2.8/6.6 milliseconds, inversion time = 400 milliseconds, flip angle = 15˚, acquisition matrix = 256 × 256 × 170, field of view = 250 mm, slice thickness = 1 mm) and a T2-weighted, fluid-attenuated inversion recovery sequence (TE/TR = 105/9,000 milliseconds, inversion time = 2250 milliseconds, slice thickness 3 mm, gap = 1.5 mm) were also acquired.

2.4 MRI Preprocessing

Image preprocessing was performed using the FSL 4.1.6 (FMRIB Software Library, http://fsl.fmrib.ox.ac.uk/fsl/fslwiki/; Smith et al., 2004) and the SPM5 (Statistical Parametric Mapping version 5; http://www.fil.ion.ucl.ac.uk/spm/software/, Wellcome Department of Cognitive Neurology, University College London, UK) in MATLAB 7.6.0 (R2008a, Mathworks, MA, USA). Diffusion-weighted image were motion- and eddy current distortion-corrected using registration and motion correction software in FSL. The diffusion tensor was calculated at each voxel using DTIFIT in FSL, producing fractional anisotropy (FA) and

mean diffusivity (MD) images. The mean b0 image (a volume without diffusion weighting) and other DTI images were then co-registered to the high-resolution, T1-weighted SPGR image in SPM5. Each T1-weighted image was segmented, modulated, and normalized to create grey matter, white matter, and CSF maps, by employing unified segmentation (Ashburner & Friston, 2005) with tissue priors from a probabilistic elderly brain template (Lemaitre, 2005). Normalization parameters produced during segmentation were then used to warp the FA and MD images into the standardized space of the elderly template.

This study defined regions of interest (ROIs) in standard space ('normalized space' or 'MNI space') that were then localized in subject ('native') space in each participant. The segmentation process produced two sets of parameters: normalization parameters, which are used to warp the image in subject space into normalized/standard space, and inverse normalization parameters, which were used to warp images in normalized/standard space back to subject space. After the ROIs were defined, the inverse normalization parameters were used to warp the 'normalized' ROIs into the subject space of each individual. The mean FA/MD value was then extracted from each ROI for each individual and statistical analyses conducted on these values.

2.5 Search Strategy

Regions of interest (ROIs) in standard space for the four cognitive networks and their corresponding (x, y, z) coordinates were first defined by conducting a selective meta-analysis of all the relevant studies that evaluated one or more cognitive networks by searching the PubMed database. The search was conducted up to September 2012, from references beginning January 2005, as most significant papers on the cognitive networks were published after 2005. The following search terms were used: 'default network', 'default mode network', 'resting-state', 'resting-state network', 'dorsal attention', 'dorsal attention network', 'salience

network', 'central executive network', and 'executive control network'. All papers included are in the English language.

2.6 ROIs/Studies Selection Criteria

Studies were included if they met the following criteria: (1) an original research paper in a peer-reviewed journal, (2) only evaluated participants with the age range of between 18 to 100, except for meta-analytic studies that could cover a wider range of ages (3) clear labeling of each ROI and the cognitive brain network to which it belonged, and (4) provided MNI or Talairach coordinates for each ROI in each network. There were two exceptions to these criteria. Manual classification of the ROIs as belonging to a particular network in some studies were performed as the cognitive networks are often labeled under different names with the same underlying definitions (i.e. labelling the DMN as Task Negative Networks, with the other cognitive networks as Task Positive Networks, and the labeling of the SN and CEN are often classified as part of the same cognitive network in some studies) (Fox et al., 2007; Gao & Lin, 2012). The second exception was the exclusion of the hippocampus as part of the DMN, as the hippocampus has been inconsistently associated with the DMN.

The ROIs for each network and their coordinates were then extracted from the selected studies based on three criteria: (1) ROIs that were consistently reported across studies for a particular cognitive network were included as part of the network, (2) MNI or Talairach coordinates for each ROI were either generated from a healthy control group or mixed group (with healthy control group always present and another experimental group), (3) MNI or Talairach coordinates for each ROI were either similar to the coordinates for the same ROI in the same network in other studies.

All Talairach coordinates for the ROIs that were selected in the final analysis were converted to MNI, for the convenience of having a consistent measure for further coordinate

analysis, using a sub-function of the GingerALE software package (Ginger Activation Likelihood Estimation version 2.1.1; Eickhoff et al., 2009; http://www.brainmap.org/ale/), called the 'tal2icbm' transform function, an algorithm which has the ability to transform coordinates between MNI space and Talairach space. It is based on the Lancaster transform, an improved algorithm that substantially reduces Talairach to MNI conversion bias (Laird et al., 2007).

2.7 Derivation of ROIs

Thirty-two studies that assessed one or more cognitive networks met the inclusion criteria. The recorded variables for each selected articles were: health status and mean age of participants, participant instructions (e.g. eyes closed/open or fixating on visual stimuli), how ROIs were derived (e.g. Functional Connectivity or Independent Component Analysis), ROIs of healthy control or mixed group, and the MNI coordinates for each ROI (Talairach coordinates were converted to MNI if used). Twenty-four studies were evaluated for the derivation of DMN ROI (Table 2), eight studies for DAN ROI (Table 3), and eight studies for SN/CEN ROI (Table 4). Abbreviations for the ROIs in these studies are provided in Table 5.

Table 2

Studies assessed to select the ROIs for DMN

Article	DMN	MNI Coordinates	Original Talairach coordinates if present
	TNN		
Fox et al. (2005)	PCC	(-1, -34, 40)	(-2, -36, 37)
Healthy Participants	Retro-splenial	(5, -52, 9)	(3, -51, 8)
Resting State (eyes closed/eyes open)	lLPC	(-49, -66, 49)	(-47, -67, 36)
Visual Stimuli (eyes fixated on crosshair)	rLPC	(58, -66, 41)	(53, -67, 36)
ROIs derived from FC of 3 seed regions referred as the Task Negative Network (TNN), so any regions that was active at the same time as the seed regions was chosen as DMN ROIs	lMPFC	(-2, 42, -10)	(-3, 39, -2)
Seed regions = MPFC, PCC/PCu, LPC	rMPFC	(2, 60, 14)	(1, 54, 21)
MPFC = (-1, 47, -4)	lSFG	(-14, 46, 50)	(-14, 38, 52)
PCC/PCu = (-5, -49, 40)	rSFG	(20, 45, 50)	(17, 37, 52)
LPC = (-45, -67, 36)	lITC	(-64, -35, -17)	(-61, -33, -15)
	rITC	(71, -18, -20)	(65, -17, -15)
	lPHG	(-23, -28, -19)	(-22, -26, -16)
	rPHG	(28, -27, -18)	(25, -26, -14)
	Cerebellum	(8, -58, -48)	(7, -52, -44)

Table 2 (continued)

Article	DMN	MNI Coordinates	Original Talairach coordinates if present
	TNN		
Zhou et al. (2007)	PCC/PCu	(6 ,-54, 30)	
Healthy Participants / Schizophrenia Patients	ldMPFC	(-3, 54, 6)	
Healthy Controls - (Mean Age ± SD: 24 ± 3.9)	rdMPFC	(3, 51, 21)	
Schizophrenia - (Mean Age ± SD: 24 ± 4.9)	lLP	(-42, -69, 33)	
Resting State (eyes closed)	rLP	(48, -57, 30)	
ROIs derived from FC of seed region, so any regions that was active at the same time as the seed region was chosen as DMN ROIs	lITG	(-60, -6, -24)	
Seed region for Task Negative Network (TNN) - PCC/PCu	rITG	(63, -3, -24)	
	lPHG	(-24, -21, -21)	
	rPHG	(27, -12, -30)	
	lMFG	(-39, 12, 51)	
	ROI selected from Resting State ICA		
Harrison et al. (2008)	MeFG	(-9, 57, 24)	(-9, 56, 19)
Healthy Participants	IPL	(-48, -57, 24)	(-48, -54, 25)
(Mean Age ± SD: 26 ± 3.5)	PCG	(-3, -57, 30)	(-3, -54, 30)
Resting State (eyes closed)	IFG	(45, 27, -21)	(45, 25, -19)
Moral Dilemma Task	Cerebellum	(-33, -78, -37)	(-33, -77, -27)
Stroop Task	ITG	(-57, -9, -24)	(-56, -10, -20)

ROIs derived from ICA with ICs spatially correlated to a-priori constructed DMN template	IFG	(-40, 33, -14)	(-40, 31, -13)
ICs which have the highest correlation to the ROIs in the template was selected as DMN ROIs	PHG	(-37, -7, -19)	(-37, -8, -16)

Article	**DMN**	**MNI Coordinates**	**Original Talairach coordinates if present**
	MPFC	(-6, 20, -14)	
Scheeringa et al. (2008)	lIFG	(-48, 30, -14)	
Healthy Participants	rIFG	(38, 44, -18)	
Young Adult / Adult (18 -28)	lMTG	(-62, -2, -24)	
Visual Stimuli (eyes fixated on crosshair)	lCerebellum	(-28, -88, -34)	
ROIs derived from negative correlation with EEG frontal theta value	lIPL/AG	(-42, -68, 28)	
EEG frontal theta activity = EEG index for DMN	rIPL/AG	(46, -64, 36)	
	rCerebellum	(26, -90, -32)	
	rMTG	(70, -32, -8)	
	rMTG	(64, -16, -18)	
	rPCu/ACC	(2, -60, 38)	
	ROI from ICA of HC group		
Mohammadi et al. (2009)	vACC/MPFC/OFC	(-2, 41, 29)	(-3, 35, 33)
Healthy Participants	PCC	(-4, -53, 24)	(-5, -53, 21)
Amyotrophic lateral sclerosis (ALS) Patients	rIPC	(50, -57, 28)	(45, -57, 25)
Middle Age / Elderly (48 - 69)	lIPC	(-46, -60, 31)	(-44, -60, 26)
Resting State (eyes closed)	rTG	(54, 2, -22)	(50, 2, -15)
ROI derived from ICA	lTG	(-53, 1, -17)	(-50, 1, -12)
Self-developed DMN template			

ROIs determined with visual inspection based on their anatomical distribution and comparisons with prior literature.	rPHG	(24, -18, -16)	(21, -17, -12)
	lPHG	(-21, -17, -14)	(-21, -16, -10)

Article	DMN	MNI Coordinates	Original Talairach coordinates if present
	ROI from FC of HC group		
Bluhm et al. (2009)	PCC/PCu	(0, -56, 0)	
Healthy Participants	MPFG	(-2, 68, 12)	
Depressed Patients	lAG	(-50, -60, 30)	
Young Adult / Adult (17 - 35)	lMFG	(-24, 32, 48)	
Resting State (eyes closed)	rCH	(12, 12, 4)	
ROIs derived from FC of seed region, so any regions that was active at the same time as the seed region was chosen as DMN ROIs	rSFG	(26, 38, 46)	
Seed region = PCC/PCu (0, -56, 20)	lCB	(-12, 4, 16)	
	lThalamus	(-20, -16, 10)	
	rMeFG	(6, 38, 24)	
	ROI from FC of HC group		
Boly et al. (2009)	PCC/PCu	(2, -56, 30)	
Healthy Participants	MPFC/STS	(2, 62, -2)	
Vegetative State / Brain Dead Patients	lTPJ	(-48, -66, 48)	
(Mean Age ± SD: 41 ± 11, Range: 26 - 54 yrs.)	rTPJ	(62, -58, 28)	
Resting State (eyes closed)	lPHG	(-24, -34, -28)	
ROIs derived from FC of seed region, so any regions that was active at the same time as the seed region was chosen as DMN ROIs	Temporal Cortex	(54, -10, -30)	

Seed region = PCC (-5, -49, 40)	Medial Thalamus	(-8, -16, 10)	
Schöpf et al. (2010)	lPCu	(-2, -56, 28)	
Healthy Participants	rAG	(50, -70, 34)	
(Mean Age ± SD: 27.3 ± 7.1)	lAG	(-48, -60, 36)	
Resting State (eyes closed)	lMTG	(-60, -14, -22)	
ROIs derived from FENICA	rIFG	(42, 20, 14)	
FENICA - new method of ICA analysis that does not require a priori template or visual inspection			
Article	**DMN**	**MNI Coordinates**	**Original Talairach coordinates if present**
	Mean of 3 test-retest sessions		
Meindl et al. (2010)	ACC	(0, 54, 7)	
Healthy Participants	PCC	(-1, -54, 27)	
Young Adult / Adult (23 - 36)	rIPL	(48, -60, 29)	
Resting State (eyes closed)	lIPL	(-42, -67, 31)	
ROIs derived from ICA	rSFG	(24, 38, 44)	
ROIs derived from ICA with ICs confirmed as DMN components if co-activations of PCC, ACC, IPL were found	lSFG	(-22, 37, 45)	
	ROI from ICA of HC group		
Wu et al. (2011)	PCC	(3, -53, 16)	(3, -51, 17)
Healthy	lIPC	(-49, -60, 31)	(-48, -57, 31)
Alzheimer's Disease (AD)	MPFC	(3, 46, 16)	(3, 45, 12)
Middle-age / Elderly (53 - 79)	rIPC	(54, -60, 28)	(53, -57, 29)
Resting State (eyes closed)	rITC	(63, -6, -19)	(62, -7, -16)
ROIs derived from ICA with ICs spatially correlated to a-priori constructed DMN template	lITC	(-60, -12, -16)	(-59, -12, -13)

Article	DMN	MNI Coordinates	Original Talairach coordinates if present
ICs which have the highest correlation to the ROIs in the template was selected as DMN ROIs	lHC	(-30, -34, -8)	(-30, -33, -5)
Template from previous studies	rHC	(24, -22, -12)	(24, -22, -9)
	ROI from ICA of HC group		
Liao et al. (2011)	PCC/PCu	(-6, -54, 36)	
Healthy Participants	lIPL	(-42, -66, 33)	
Mesial Temporal Lobe Epilepsy Patients	rIPL	(54, - 63, 36)	
Young Adult / Adult / Middle Age (18 -51)	lMesTL	(-21, -15, -27)	
Resting State (eyes closed)	rMesTL	(24, -9, -21)	
ROIs derived from ICA with ICs spatially correlated to a-priori constructed DMN template	lITG	(-60, -12, -21)	
ICs which have the highest correlation to the ROIs in the template was selected as DMN ROIs	rITG	(60, -3, -27)	
Template from previous studies	MPFC	(0, 54, -6)	
	PCu	(1, -64, 43)	
Allen et al. (2011)	PCC	(0, -52, 22)	
Healthy Participants	lAG	(-43, -69, 33)	
Participants from meta-analysis of 34 studies so age varies from adolescence to elderly (Mean Age ± SD: 23.4 ± 9.2, Range: 12 - 71 yrs.)	rAG	(47, -66, 32)	
Visual Stimuli (eyes fixated on crosshair)	MeFG	(-1, 45, -9)	
ROIs derived from ICA	ACC	(0, 41, 4)	
	MCC	(1, -30, 41)	
	rIFG	(32, 22, -15)	
	rMFG	(40, 43, 8)	
	lMFG	(-26, 26, 42)	
	rMFG	(26, 33, 41)	

	MCC	(0, 21, 40)	
Article	**DMN**	**MNI Coordinates**	**Original Talairach coordinates if present**
Camchong et al. (2011)	PCC/PCu	(1, -57, 31)	
Healthy Participants	PCC/CG	(1, -18, 36)	
Schizophrenia Patients	ACG	(1, 38, 12)	
Healthy Controls - (Mean Age ± SD: 41.1 ± 10.6)	rPL	(42, -54, 36)	
Schizophrenia - (Mean Age ± SD: 41.3 ± 9.8)	lPL	(-34, -62, 36)	
Resting State (eyes closed)	rCG	(2, 14, 36)	
ROIs derived from ICA with ICs spatially correlated to a-priori constructed DMN template	lIFG	(-42, 14, 28)	
ICs which have the highest correlation to the ROIs in the template was selected as DMN ROIs	rMFG	(22, 58, -4)	
Template based on previous studies.	lMFG	(-26, 54, 0)	
	rMTG	(50, -50, 16)	
	lMTG	(-50, -50, 16)	
	rThalamus	(10, -18, 8)	
	lThalamus	(-6, -14, 4)	
Li et al. (2011)	PCC	(6, -49, 25)	
Healthy Participants	MPFC	(-12, 62, 8)	
(Mean Age ± SD: 21 ± 3.4)	lIPC	(-43, -67, 33)	
Resting State (eyes closed)	rIPC	(45, -60, 29)	
ROIs derived from ICA with ICs spatially correlated to a-priori constructed DMN template	lInferoTC	(-59, -15, -16)	
ICs which have the highest correlation to the ROIs in the template was selected as DMN ROIs	rInferoTC	(59, -12, -20)	

Template based on literature review of DMN in article	lHippocampus	(-22, -15, -22)	
	rHippocampus	(25, -15, -23)	
Article	**DMN**	**MNI Coordinates**	**Original Talairach coordinates if present**
	PC-VP	(6, -51, 33)	(4, -52, 29)
	lPHG	(-24, -24, -21	(-23, -22, -17)
	rPHG	(24, -22, -21)	(21, -20, -16)
	rAG	(51, -61, 30)	(46, -61, 26)
	lAG	(-51, -63, 31)	(-49, -63, 25)
Tomasi & Volkow (2011)	MeFG	(0, 57, 16)	(-1, 50, 23)
Healthy Participants - meta-analysis of various studies	SFG	(24, 36, 51)	(21, 27, 53)
Young Adult / Adult / Middle Age / Elderly (18 - 71)	ACG	(0, 54, -5)	(-1, 49, 4)
Resting State	MTG	(60, -10, -22)	(55, -9, -15)
ROIs derived from FC of hub region : PC-VP, so any regions that was active at the same time as the seed region was chosen as DMN ROIs	MTG	(63, -33, -6)	(57, -32, 3)
	rIFG	(33, 18, -24)	(30, 17, -15)
	lIFG	(-30, 12, -24)	(-28, 12, -17)
	ITG	(-60, -12, -21)	(-56, -11, -17)
	STG	(-39, 18, -33)	(-37, 18, -24)
	Cerebellum (Semilunar lobule)	(-31, -81, -36)	(-29, -74, -36)
	Brainstem (Medulla)	(-6, -54, -45)	(-6, -48, -41)
	Brainstem (Medulla)	(6, -51, -48)	(5, -45, -43)
	Cerebellum	(24, -85, -30)	(21, -78, -30)
	Cerebellum (Semilunar lobule)	(39, -75, -39)	(35, -68, -37)
	IFG	(42, 33, -18)	(38, 30, 8)
	Brainstem (Midbrain)	(0, -15, -18)	(-1, -14, -13)

	Brainstem (Pons)	(0, -21, -27)	(-1, -19, -22)
Article	**DMN**	**MNI Coordinates**	**Original Talairach coordinates if present**
	aMPFC	(-3, 57, 21)	
Song et al. (2011)	lSFC	(-12, 45, 48)	
Healthy Participants	rSFC	(21, 42, 48)	
Generalized Tonic-Clonic Seizures Epilepsy Patients	vACC	(-3, 36, -6)	
Control - (Mean Age ± SD: 27.1 ± 4.5)	lITC	(-54, -3, -30)	
GTCS Patients - (Mean Age ± SD: 26.1 ± 6.1)	rITC	(54, 0, -30)	
Pre-defined ROIs selected from previous studies	lPHG	(-24, -18, -27)	
	rPHG	(24, -12, -27)	
	PCC	(-3, -45, 33)	
	Rsp	(-15, -54, -6)	
	lLPC	(-54, -69, 36)	
	rLPC	(54, -63, 33)	
	CT	(9, -51, -45)	
Yeo et al. (2011)	MFG	(-27, 23, 48)	
Healthy Participants	lAG	(-41, -60, 29)	
Young Adult / Adult (18 - 35)	lMTG	(-64, -20, -9)	
Resting State (eyes closed)	dMPFC	(-7, 49, 18)	
Resting State (eyes open)	lPHG	(-25, -32, -18)	
Visual Stimuli (eyes fixated on crosshair)	PCu	(-7, -52, 26)	
ROIs derived from FC of seed regions to the right, so any regions that was active at the same time as the seed regions was chosen as DMN ROIs			

Article	DMN	MNI Coordinates	Original Talairach coordinates if present
Koch et al. (2012)	ACC	(1, 50, 11)	(0, 45, 17)
Healthy Participants	PCC	(0, -53, 25)	(-2, - 53, 22)
Mild Cognitive Impairment (MCI) Patients	lLPC	(-44, -67, 24)	(-43, -66, 20)
Alzheimer's Disease (AD) Patients	rLPC	(50, -62, 19)	(45, -61, 17)
Elderly (57 - 100)	lSFG	(-20, 26, 52)	(-20, 19, 52)
Resting State (eyes closed)	rSFG	(28, 24, 51)	(25, 17, 51)
ROIs derived from visually analyzing the ICA data and selecting the regions which has DMN co-activation patterns	lMTC	(-60, -12, -12)	(-57, -11, -9)
	rMTC	(58, -7, -16)***)***	(53, -7, -11)
	lHippocampus	(-21, -15, -13)	(-21, -16, -14)
	rHippocampus	(24, -20, -16)	(21, -19, -12)
Gao & Lin (2012)	lHF	(-21, -15, -14)	
Healthy Participants	rHF	(24, -19, -21)	
Adult (25 - 33)	vMPFC	(0, 51, -7)	
RS (eyes closed)	PCC	(1, -55, 17)	
FT (finger tapping)	lpIPL	(-47, -71, 29)	
MW (movie watching)	rpIPL	(50, -64, 27)	
Pre-defined ROIs selected from Vincent et al. 2008			

Article	DMN	MNI Coordinates	Original Talairach coordinates if present
Qi et al. (2012)			
Healthy Participants			
Minimal Hepatic Encephalopathy (mHE) Patients	lAG	(-33, -76, 40)	
Control - (Mean Age ± SD: 55 ± 9.5)	rAG	(51, -70, 43)	
mHE Patients - (Mean Age ± SD: 56.6 ± 9.1)	rACC	(6, 41, 19)	
Resting State (eyes closed)	lPHG	(-30, -40, -13)	
ROIs derived from ICA with ICs spatially correlated to a-priori constructed DMN template	rPHG	(27, -34, -13)	
ICs which have the highest correlation to the ROIs in the template was selected as DMN ROIs	PCC/PCu	(0, -43, 40)	
Template based on previous studies			
Wang et al. (2012)			
Healthy Participants	MPFC	(12, 54, 0)	
Generalized tonic-clonic seizures (GTCS) Patients	vACC	(0, 27, 18)	
Healthy - (Mean Age ± SD: 27.9 ± 8.4)	PCu	(-9, -51, 51)	
GTCS - (Mean Age ± SD: 27.4 ± 4.5)	rAG	(48, -72, 33)	
Resting State (eyes closed)	PCC/Rsp	(-9, -42, 3)	
ROIs derived from ICA with ICs spatially correlated to a-priori constructed DMN template	lLTC	(-57, -3, -24)	
ICs which have the highest correlation to the ROIs in the template was selected as DMN ROIs			
DMN template from previous studies			

Article	DMN	MNI Coordinates	Original Talairach coordinates if present
Liu et al. (2012)	***ROI from ICA of HC group***		
Healthy Participants	AG	(-51, -68, 40)	(-49, -68, 33)
Alzheimer's Disease (AD)Patients	CG	(-7, -43, 39)	(-8, -45, 35)
Control - Adult / Elderly (49 - 78)	IPL	(-50, -61, 45)	(-48, -62, 38)
AD patients - Adult / Elderly (43 - 76)	MTG	(-51, -63, 35)	(-49, -63, 29)
Resting State (eyes closed)	PCC/PCu	(0, -50, 44)	(-2, -52, 39)
ROIs derived from ICA with ICs spatially correlated to a-priori constructed DMN template	SPL	(-39, -66, 52)	(-38, -68, 44)
ICs which have the highest correlation to the ROIs in the template was selected as DMN ROIs	STG	(-53, 58, 35)	(-51, -59, 29)
Template based on previous studies	Supramarginal	(65, -52, 27)	(59, -53, 25)

Table 2 (continued)

Article	DMN	MNI Coordinates	Original Talairach coordinates if present
	Precuneus	(6, -63, 24)	
De Vogelaere et al. (2012)	lAG	(-51, -69, 24)	
Healthy Participants	rAG	(51, -66, 24)	
Mild Cognitive Impairment (MCI) Patients	lMTG	(-63, -15, -15)	
Healthy - (Mean Age ± SD: 62.1 ± 7.8)	rMTG	(66, -12, -9)	
MCI - (Mean Age ± SD: 67.2 ± 7.9)	ACG	(-6, 42, 18)	
Resting State (eyes closed)	Thalamus	(6, -18, 12)	
ROIs derived from ICA with ICs spatially correlated to a-priori constructed DMN template	lRO	(-45, -12, 18)	
ICs which have the highest correlation to the ROIs in the template was selected as DMN ROIs	lHippocampus	(-24, -15, -12)	
DMN template from GIFT (Group ICA of fMRI Toolbox, available at http://mialab.mrn.org/software/gift/)	rHippocampus	(27, -12, -18)	
	lPostcentral Gyrus	(-30, -33, 51)	
	lIFG	(-51, 15, 33)	
	rSTG	(42, -33, 18)	

Table 2 (continued)

Article	DMN	MNI Coordinates	Original Talairach coordinates if present
Jin et al. (2012)	lLPFC	(-26, 18, 60)	
Healthy	rLPFC	(26, 30, 26)	
amnestic Mild Cognitive Impairment (aMCI)	lHC	(-30, -12, -22)	
Healthy - (Mean Age ± SD: 60.63 ± 8.3)	lPHG	(-30, -26, -20)	
aMCI - (Mean Age ± SD: 60.88 ± 3.22)	lFG	(-32, -26, -18)	
RS (eyes closed)	PCC/Rsp/Precuneus	(-6, -60, 22)	
ROIs derived from ICA with ICs spatially correlated to a-priori constructed DMN template	lMTG	(-54, 4, -12)	
ICs which have the highest correlation to the ROIs in the template was selected as DMN ROIs	rAG	(48, -72, 30)	
DMN template from GIFT (Group ICA of fMRI Toolbox, available at http://mialab.mrn.org/software/gift/)	MPFC	(8, 46, 36)	
	lIPL	(-46, -42, 54)	
	lMCC	(-20, -30, 26)	
	rMCC	(4, -28, 36)	

Table 3

Studies assessed to select the ROIs for DAN

Article	DAN	MNI Coordinates	Original Talairach coordinates if present
Fox et al. (2005)	lIPS	(-23, -65, 53)	(-23, -66, 46)
Healthy Participants	rIPS	(29, -56, 58)	(25, -58, 52)
Resting State (eyes closed/eyes open)	lIPL	(-43, -41, 55)	(-42, -44, 49)
Visual Stimuli (eyes fixated on crosshair)	rIPL	(52, -33, 56)	(47, -37, 52)
ROIs derived from FC of 3 seed regions referred as the Task Positive Network (TPN), so any regions that was active at the same time as the seed regions was chosen as DAN ROIs	lvIPS	(-26, -81, 32)	(-26, -80, 26)
Seed regions = IPS, FEF, MT+	rvIPS	(39, -82, 35)	(35, -81, 29)
IPS = (-25, -57, -46)	lFEF	(-24, -7, 65)	(-24, -12, 61)
FEF = (25, -13, 50)	rFEF	(32, -1, 56)	(28, -7, 54)
MT+ = (-45, -69, -2)	IPCeS	(59, 5, 34)	(54, 0, 35)
	lMT+	(-49, -72, -1)	(-47, -69, -3)
	rMT+	(59, -69, -2)	(54, -63, -8)

Table 3 (continued)

Article	DAN	MNI Coordinates	Original Talairach coordinates if present
	rFEF	(32, -5, 55)	(28, -10, 53)
Fox et al. (2006)	lFEF	(-25, -7, 58)	(-25, -12, 55)
Healthy Participants	rpIPS	(23, -65, 58)	(20, -67, 51)
Resting State (eyes closed/eyes open)	lpIPS	(-22, -67, 53)	(-22, -68, 46)
Visual Stimuli (eyes fixated on crosshair)	raIPS	(39, -45, 49)	(35, -47, 45)
ROIs derived from FC of 3 seed regions referred as the Task Positive Network (TPN), so any regions that was active at the same time as the seed regions was chosen as DAN ROIs	laIPS	(-43, -39, 46)	(-42, -41, 43)
Seed regions identified through meta-analysis of prior studies	lSMA/pre-SMA	(-3, 5, 55)	(-4, -1, 53)
Seed regions = IPS, FEF	rIFG	(57, 10, 25)	(52, 6, 27)
rIPS = (27, -58, 49)	rMT+	(56, -66, -7)	(51, -63, -7)
rFEF = (24, -13, 51)	lMT+	(-48, -72, -5)***)***	(-46, -68, -7)
	rMFG	(41, 43, 14)***)***	(37, 38, 20)
	rINS	(33, 20, 4)	(30, 17, 9)
Zhou et al. (2007)	***TPN***		
Healthy Participants / Schizophrenia Patients	rIFG	(54, 12, 21)	204
Young Adult (Mean Age ± SD: 24 ± 4.9)	lIFG	(-51, 9, 27)	130
Resting State (eyes closed)	rMT+	(44, -64, -12)	121
ROIs derived from FC of seed region	lMT+	(-51, -57, -12)	175
Seed region for TPN - rDPLFC	lCPL	(-12, -75, -27)	21

Table 3 (continued)

Article	DAN	MNI Coordinates	Original Talairach coordinates if present
	MFG	(40, 36, 20)	
	lINS	(-40, 16, 0)	
Grady et al. (2010)	rINS	(36, 16, -8)	
Healthy Participants	lFEF	(-32, -8, 56)	
Young Adult / Elderly	rFEF	(28, -4, 48)	
Age Range - (20 - 30, 56 - 84)	lPreCG	(-56, 8, 28)	
Visual Stimuli - various visual stimulus	rPreCG	(48, 4, 24)	
Visual Tasks	rSUPPMA	(4, -4, 56)	
ROIs was derived from Visual Tasks	lIPL	(-48, -40, 40)	
Brain regions showing more activity for Visual Stimuli = selected as DAN ROIs	rIPL	(44, -44, 44)	
	lIPS	(-28, -60, 56)	
	rIPS	(28, -60, 48)	
	lIOG	(-48, -72, -4)	
	rMOG	(28, -72, 28)	
	rFusiform Gyrus	(44, -64, -12)	

Table 3 (continued)

Article	DAN	MNI Coordinates	Original Talairach coordinates if present
Li et al. (2012)			
Healthy participants / AD patients	lIPS (ls/ipl)	(-39, -63, 56)	
Middle-age / Elderly (53 - 79)	rIPS (rs/ipl)	(42, -51, 52)	
Resting State (eyes closed)	lFEF (lm/ifg)	(-39, 51, 8)	
ROIs derived from ICA with ICs spatially correlated to a-priori constructed DAN template	rFEF (rmfg)	(33, 18, 56)	
ICs which have the highest correlation to the ROIs in the template was selected as DAN ROIs	lFEF (lm/sfg,cg)	(-6, 24, 44)	
Template based on past studies			

Table 3 (continued)

Article	DAN	MNI Coordinates	Original Talairach coordinates if present
Liu et al. (2012)			
Healthy Participants			
Minimal Hepatic Encephalopathy (mHE) Patients	IPL	(43, -48, 62)	(38, -52, 56)
Elderly (55 - 67)	MOG	(56, -66, -10)	(51, -63, -10)
Resting State (eyes closed)	MTG	(61, -58, -10)	(55, -55, -9)
ROIs derived from ICA with ICs spatially correlated to a-priori constructed DAN template	SOG	(-31, -83, 33)	(-30, -82, 26)
ICs which have the highest correlation to the ROIs in the template was selected as DAN ROIs	SPL	(30, -60, 65)	(26, -63, 57)
Template based on previous studies			
Gao & Lin (2012)			
Healthy Participants	lMT+	(-45, -69, -2)	
Adult (25 - 33)	rMT+	(50, -69, -3)	
Resting State (eyes closed)	lIPS	(-27, -52, 57)	
Finger Tapping Task	rIPS	(24, -56, 55)	
Movie Watching	lFEF	(-25, -8, 50)	
Pre-defined ROI selected from Vincent et al. 2008	rFEF	(27, -8, 50)	

Table 3 (continued)

Article	DAN	MNI Coordinates	Original Talairach coordinates if present
Fornito et al. (2012)			
Healthy Participants	lIPS	(-27, -69, 39)	
Adults (19 - 36)	rIPS	(33, -45, 48)	
Memory Task	rpSTS	(51, -42, 15)	
ROIs derived from ICA with ICs spatially correlated to a-priori constructed DAN template	lFEF	(-48, 6, 30)	
ICs which have the highest correlation to the ROIs in the template was selected as DAN ROIs	ldPreCS	(-27, -6, 63)	
ROI determined with visual inspection based on their anatomical distribution and derived from prior literature	lCuneus	(-12, -102, 3)	

Table 4

Studies assessed to select the ROIs for SN/CEN

Article	SN **(bold)**/*CEN(italics)*	MNI Coordinates	Original Talairach coordinates if present
Fox et al. (2005)			
Healthy Participants	**SMA/pre-SMA**	(-1, 7, 52)	(-2, 1, 51)
Resting State (eyes closed/eyes open)	**laINS**	(-47, 7, 5)	(-45, 5, 8)
Visual Stimuli (eyes fixated on crosshair)	**raINS**	(49, 7, 10)	(45, 4, 14)
ROIs derived from FC of 3 seed regions referred as the Task Negative Network (TPN), so any regions that was active at the same time as the seed regions was chosen as SN ROIs	*ldlPFC*	(-44, 45, 21)	(-40, 39, 26)
Seed regions = MPF, PCC/PCu, LP	*rdlPFC*	(42, 47, 16)	(38, 41, 22)
MPF = (-1, 47, -4)			
PCC/Pcu = (-5, -49, 40)			
LP = (-45, -67, 36)			

Table 4 (continued)

Article	SN (bold)/*CEN (italics)*	MNI Coordinates	Original Talairach coordinates if present
	rINS	(42, 10, -12)	
	lINS	(-40, 18, -12)	
	rTP	(52, 20, -18)	
	lTP	(-52, 16, -14)	
Seeley et al. (2007)	**CG**	(0,44, 28)	
Healthy Participants	**rdACC**	(6, 22, 30)	
Young Adult (ROI Analysis - Age: 18 -25)	**ldACC**	(-6, 18, 30)	
Young Adult / Adult / Elderly (ICA Analysis - Age: 18 - 70)	**rSMA/PreSMA**	(6, 8, 58)	
Resting State (eyes closed)	**lSMA/PreSMA**	(-4, 14, 48)	
ROIs derived from ICA with ICs spatially correlated to a-priori constructed SN/CEN template	**rSTG**	(64, -38, 6)	
ICs which have the highest correlation to the ROIs in the template was selected as SN/CEN ROIs	**lSTG**	(-62, -16, 8)	
.	**rPO**	(58, -40, 30)	
	lPO	(-60, -40, 40)	
	lFP	(-24, 56, 10)	
	rvlPFC	(42, 46, 0)	
	rdlPFC	(30, 48, 22)	
	ldlPFC	(-38, 52, 10)	
	lINS	(-36, 24, -10)	

rdlPFC	(46, 46, 14)	
ldlPFC	(-34, 46, 6)	
rvlPFC	(34, 56, -6)	
lvlPFC	(-32, 54, -4)	
FO	(56, 14, 14)	
rdlPFC/FEF	(30, 12, 60)	
ldlPFC/FEF	(-32, 18, 50)	
dMPFC	(0, 36, 46)	
rLPC	(38, -56, 44)	
lLPC	(-48, -48, 48)	
IT	(58, -54, -16)	

Article	**SN (bold)/***CEN (italics)*	**MNI Coordinates**	**Original Talairach coordinates if present**
Zhou et al. (2007)	*ldlPFC*	(-48, 39, 12)	
Healthy Participants / Schizophrenia Patients	*rdlPFC*	(48, 42, 21)	
Young Adult (Mean Age ± SD: 24 ± 4.9)	**rINS**	(36, 21, 3)	
Resting State (eyes closed)	**lINS**	(-33, 21, 3)	
ROIs derived from FC of seed region, so any regions that was active at the same time as the seed region was chosen as SN ROIs	*rIPL/PostCG*	(63, -30, 33)	
Seed for SN/CEN - rDPLFC	*lIPL/PostCG*	(-51, -36, 45)	

Sridharan et al. (2008)	**rFIC**	(37, 25, -4)
Healthy	**lFIC**	(-32, 24, -6)
Young Adult / Adult (19 - 29)	**ACC**	(4, 30, 30)
Resting State (eyes closed)	*rdlPLFC*	(45, 16, 45)
Auditory Task (listening to Baroque music)	*rPPC*	(54, -50, 50)
Visual Oddball Task	*lPPC*	(-38, -53, 45)
ROI derived from ICA of Auditory Task only		

Article	**SN (bold)**/*CEN (italics)*	**MNI Coordinates**	**Original Talairach coordinates if present**
	lINS	(-43, -10, 7)	(-41, -11, 9)
	rINS	(46, 2, -6)	(42, 0, 0)
White et al. (2010)	**lSTG**	(-53, -30, 16)	(-50, -31, 15)
Healthy Participants / Schizophrenia Patients	**rSTG**	(59, -28, 8)	(53, -29, 10)
Young Adult / Adult (20 - 37)	**lPcG**	(-66, 5, 5)	(-62, 3, 8)
Visual Stimuli (eyes fixated on crosshair)	**rPcG**	(61, 4, 10)	(55, 1, 14)
Somatosensory Stimuli (vibratory stimuli to right index fingertip)	**lACG**	(-5, 35, 28)	(-6, 22, 40)
ROI derived from ICA	**rACG**	(5, 29, 37)	(3, 28, 32)
ROI determined with visual inspection based on their spatial distribution from previous studies	**rMeFG**	(5, 15, 47)	(3, 8, 47)
	lSFG	(-31, 58, 15)	(-30, 51, 22)
	rSFG	(34, 20, 10)	(30, 16, 15)
	lMFG	(-50, 24, 40)	(-48, 17, 41)
	rMFG	(53, 27, 40)	(48, 20, 43)
	lIPL	(-57, -45, 51)	(-54, -48, 45)
	rIPL	(62, -35, 49)	(56, -39, 46)

	rAG	(50,-65, 41)	(45, -70, 35)

Article	SN/*CEN*	MNI Coordinates	Original Talairach coordinates if present
Liu et al. (2012)	**ACC**	(-1, 29, 18)	(-2, 24, 23)
Healthy Participants	**CG**	(-1, 31, 24)	(-2, 25, 28)
Alzheimer's Disease (AD)	**AI**	(-44, 15, -8)	(-42, 13, -2)
Healthy Control - (49 - 78)	**MFG**	(-29, 59, 14)	(-28, 52, 21)
AD patients - (43 - 76)	**STG**	(-51, 17, -13)	(-48, 15, -7)
Resting State (eyes closed)	*ACC*	(5, 37, -20	(4, 34, -10)
ROI derived from ICA with ICs spatially correlated to a template	*Caudate*	(-6, 15, -13)	(-6, 13, -6)
ICs which have the highest correlation to template was selected as DMN	*IFG*	(-23, 24, -23)	(-22, 23, -15)
Template based on previous studies	*MFG*	(-23, 26, -24)	(-22, 25, -15)
	MeFG	(3, 59, -14)	(2, 54, -3)
	SFG	(9, 61, -12)	(8, 56, -1)

Article	SN (bold)/*CEN* (italics)	MNI Coordinates	Original Talairach coordinates if present
Fornito et al. (2012) *Healthy* *Adults (19 - 36)* *Memory Task (MT)* ***ROI derived from ICA with ICs spatially correlated to a template ICs which have the highest correlation to template was selected as SN/CEN ROIs*** ***ROI determined with visual inspection based on their anatomical distribution and comparisons from prior literature***	*lIPL* *rIPL* *lIFG* *rIFG* *ldMPFC* *lFO* **lMTG** **rMTG** **rMFG** **rAI** **lSPL**	(-45, -66, 39) (54, -45, 45) (-48, 18, 24) (54, 21, 15) (-6, 36, 42) (-36, 18, -18) (-60, -45, -6) (-36, -6, 21) (21, 57, 24) (39, 24, -6) (-39, -51, 48)	
Gao & Lin (2012) *Healthy Participants* *Adult (25 - 33)* *Resting State (eyes closed)* *Finger Tapping Task* *Movie Watching* ***Pre-selected ROI from Vincent et al. 2008 (labelled as FPCN)***	*laPFC* *raPFC* **ACC** *laIPL* *raIPL* *ldIPFC* *rdlPFC* **lINS** **rINS**	(-36, 57, 9) (34, 52, 10) (3, 31, 27) (-52, -49, 47) (52, -46, 46) (-50, 20, 34) (46, 14, 43) (-31, 21, -1) (31, 22, -2)	

Table 5

List of ROI Abbreviations

Abbreviations	Regions
l	left
r	right
AC	Anterior Cingulate
ACC	Anterior Cingulate Cortex
ACG	Anterior Cingulate Gyrus
AG	Angular Gyrus
AI	Anterior Insula
aINS	anterior Insula
aIPL	anterior Inferior Parietal Lobule
aIPS	anterior Intraparietal Suclus
aMPFC	anterior Medial Prefrontal Cortex
aPFC	anterior Prefrontal Cortex
CB	Caudate Body
CG	Cingulate Gyrus
CH	Caudate Head
CPL	Cerebellar Posterior Lobe
CT	Cerebellar Tonsils
dACC	dorsal Anterior Cingulate Cortex
dlPFC	dorsolateral Prefrontal Cortex
dMPFC	dorsomedial Prefrontal Cortex
dPreCS	dorsal Precentral Sulcus
FEF	Frontal Eye Fields
FIC	Fronto-Insular Cortex
FG	Fusiform Gyrus
FO	Frontal Operculum
FP	Frontal Pole
HC	Hippocampus
HF	Hippocampal Formation
IFG	Inferior Frontal Gyrus
INS	Insula
IOG	Inferior Occipital Gyrus
IPC	Inferior Parietal Cortex
IPL	Inferior Parietal Lobule
IPS	Intraparietal Sulcus
IT	Inferior Temporal
ITC	Inferior Temporal Cortex
InferoTC	Inferolateral Temporal Cortex
ITG	Inferior Temporal Gyrus

LP	Lateral Parietal Region
LPC	Lateral Parietal Cortex
LPFC	Lateral Prefrontal Cortex
LTC	Lateral Temporal Cortex
MCC	Middle Cingulate Cortex
MeFG	Medial Frontal Gyrus
MeTG	Medial Temporal Gyrus
MesTL	Mesial Temporal Lobe
MiCG	Mid Cingulate Gyrus
MFG	Middle Frontal Gyrus
MOG	Middle Occipital Gyrus
MPFC	Medial Prefrontal Cortex
MPFG	Medial PreFrontal Gyrus
MTC	Medial Temporal Cortex
MTG	Middle Temporal Gyrus
MT+	Middle Temporal Area
OFC	Orbital Frontal Cortex
OFG	Orbital Frontal Gyrus
PC	Posterior Cingulate
PCC	Posterior Cingulate Cortex
PcG	Precentral Gyrus
PCG	Posterior Cingulate Gyrus
PCeS	Precentral Sulcus
PCu	Precuneus
PHG	Parahippocampal Gyrus
pIPL	posterior Inferior Parietal Lobule
pIPS	posterior Intraparietal Sulcus
PL	Parietal Lobule
PO	Parietal Operculum
PPC	Posterior Parietal Cortex
PreCG	Precentral Gyrus
pSTS	posterior Superior Temporal Sulcus
rAG	Angular Gyrus
RO	Rolandic Operculum
Rsp	Restrosplenial
SFC	Superior Frontal Cortex
SFG	Superior Frontal Gyrus
SMA	Supplementary Motor Area
SOG	Superior Occipital Gyrus
SPL	Superior Parietal Lobule
STG	Superior Temporal Gyrus
STS	Superior Frontal Sulcus
TG	Temporal Gyrus

TP	Temporal Pole
TPJ	Temporo-Parietal Junction
vACC	ventral Anterior Cingulate Cortex
vlPFC	ventrolateral Prefrontal Cortex
vIPS	ventral Intraparietal Sulcus
vMPFC	Ventral Medial Prefrontal Cortex
VP	Ventral Precuneus

2.8 Definition of DMN ROIs

The DMN included the posterior cingulate cortex (PCC), dorsal medial prefrontal cortex (dMPFC), ventral medial prefrontal cortex (vMPFC), left posterior inferior parietal lobule (lpIPL), right posterior inferior parietal lobule (rpIPL), left middle temporal region (lMTG), and right middle temporal region (rMTG). The location of these ROIs in the brain is presented from Figure 1 to Figure 5.

The PCC, dMPFC, and vMPFC, were divided into the left and right region, by deleting the single midline brain voxels and then adjusting the ROIs to minimise the inclusion of cerebrospinal fluid (CSF) or white matter tracts. These modifications to the ROI were done in standard space with Magnetic Resonance Image conversion v4 (MRIcron version 4, April 2011; Rorden & Brett, 2000, http://www.mccauslandcenter.sc.edu/mricro/mricron/), a standalone program that allows efficient viewing and exporting of brain images, as well as aiding in the drawing and editing of anatomical ROIs, after the ROIs were constructed (refer to *ROI Analysis* below). The newly modified left and right PCC, dMPFC, and vMPFC in the brain are presented from Figure 1 to Figure 3.

Figure 1

PCC in the DMN (location derived from mean coordinate analysis in current study)

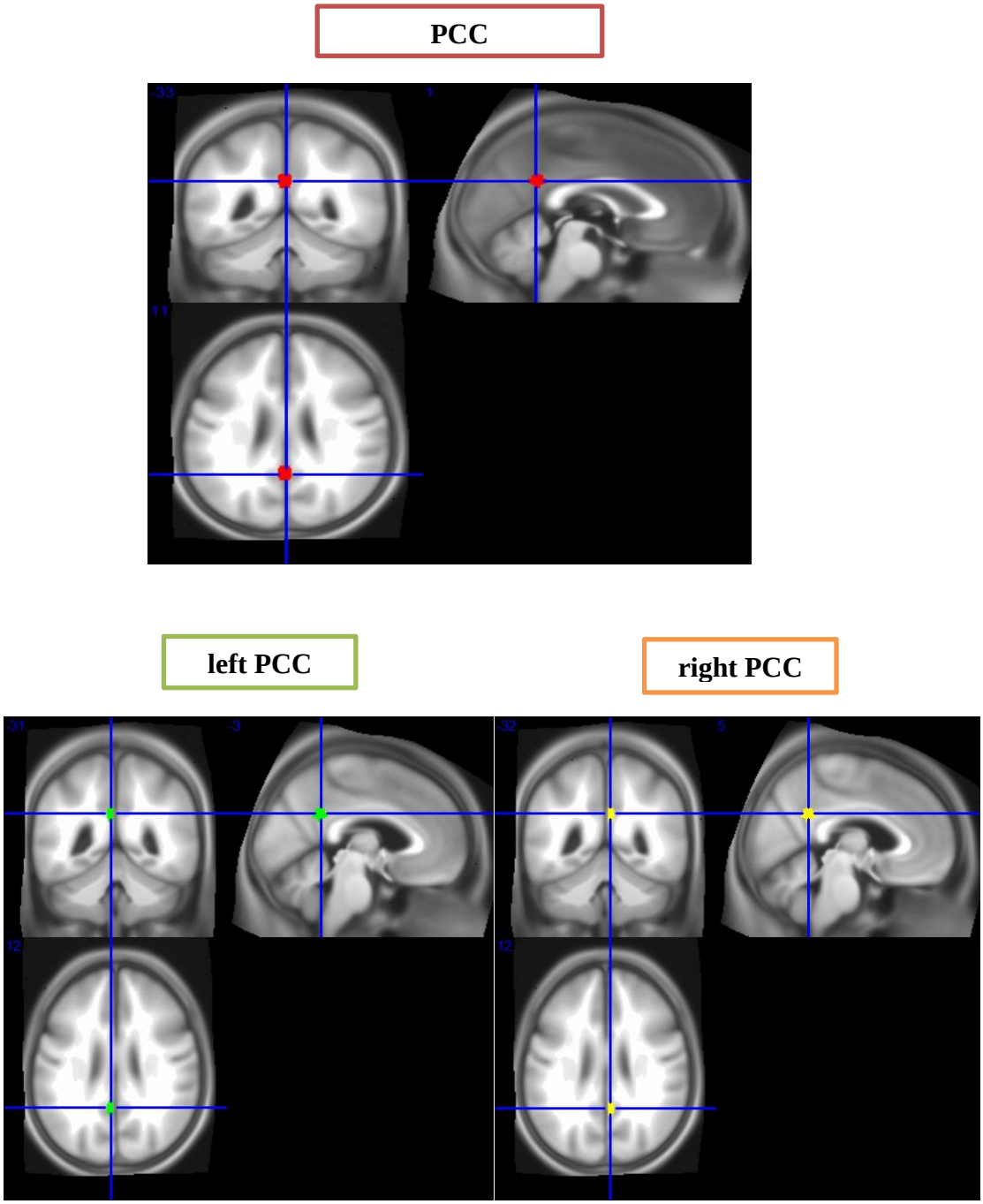

Figure 2

dMPFC in the DMN (location derived from mean coordinate analysis in current study)

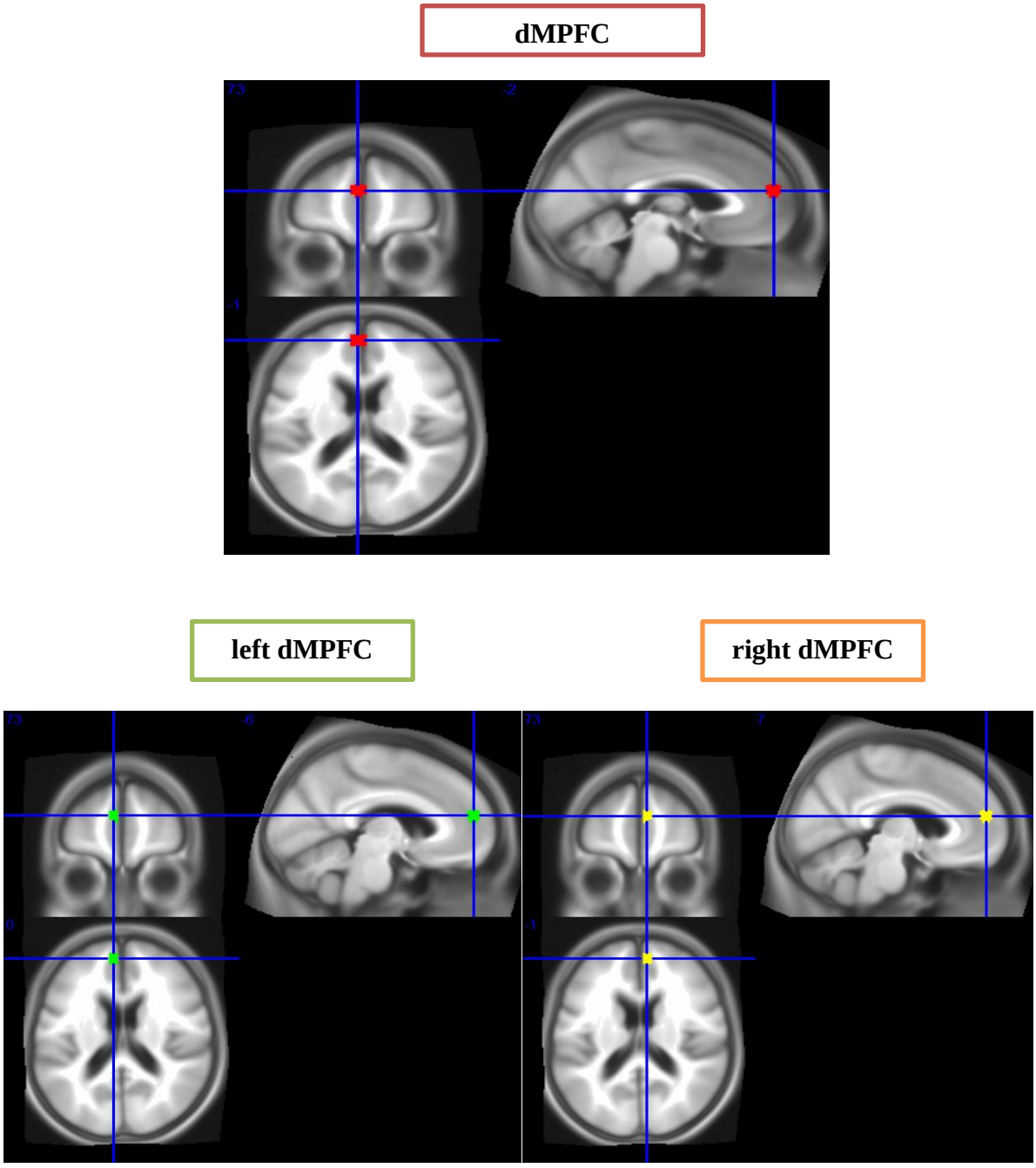

Figure 3

vMPFC in the DMN (location derived from mean coordinate analysis in current study)

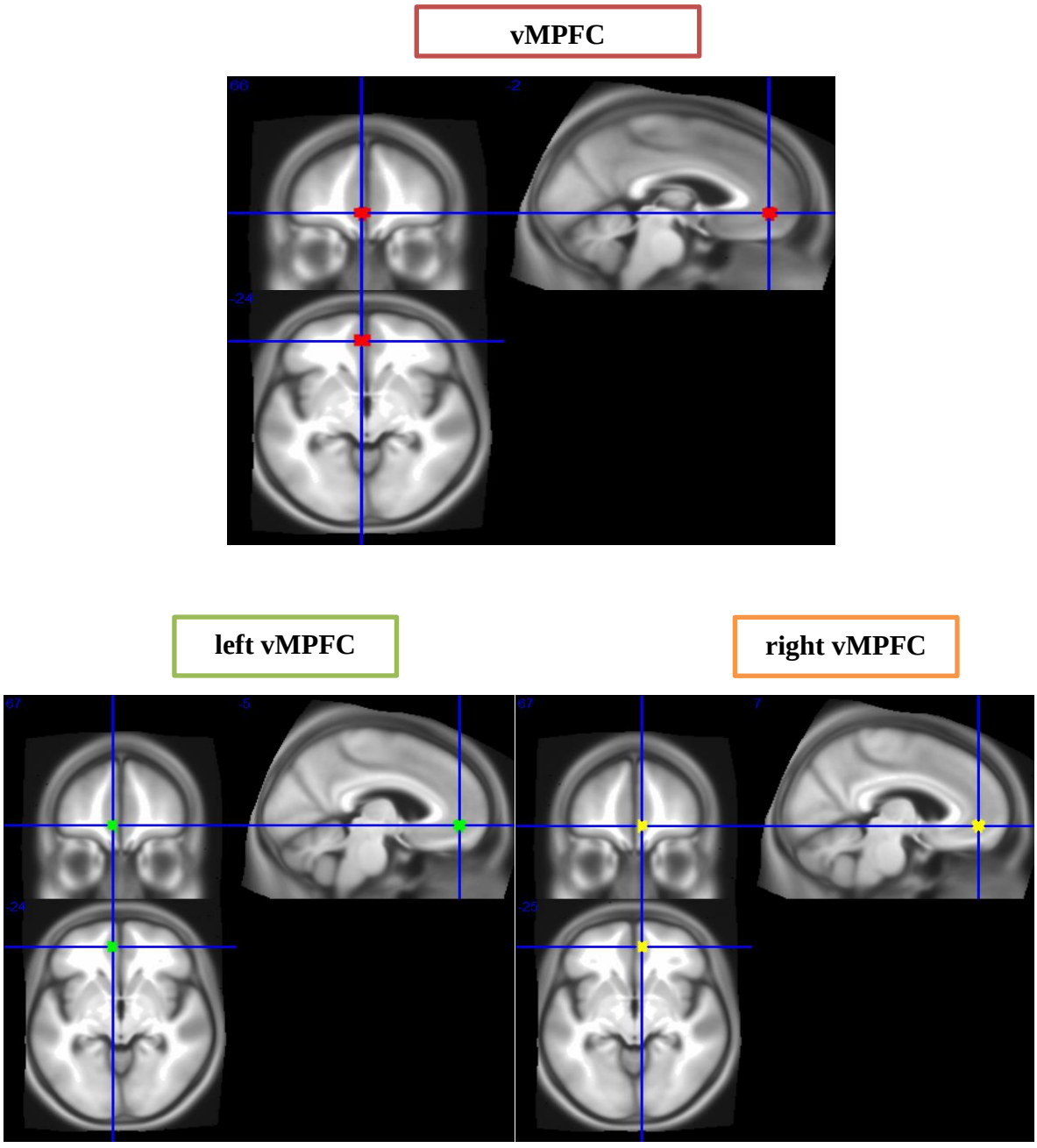

Figure 4

pIPL in the DMN (6mm sphere, location derived from mean coordinate analysis in current study)

left pIPL

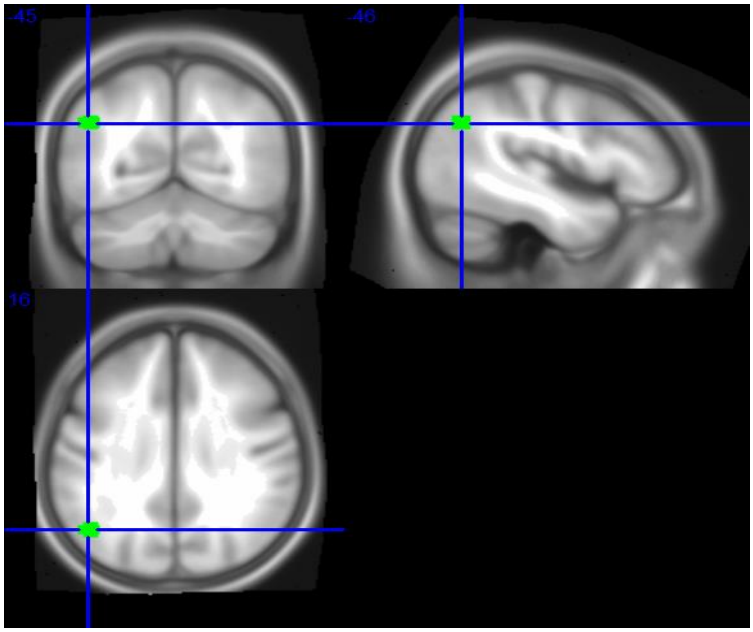

right pIPL

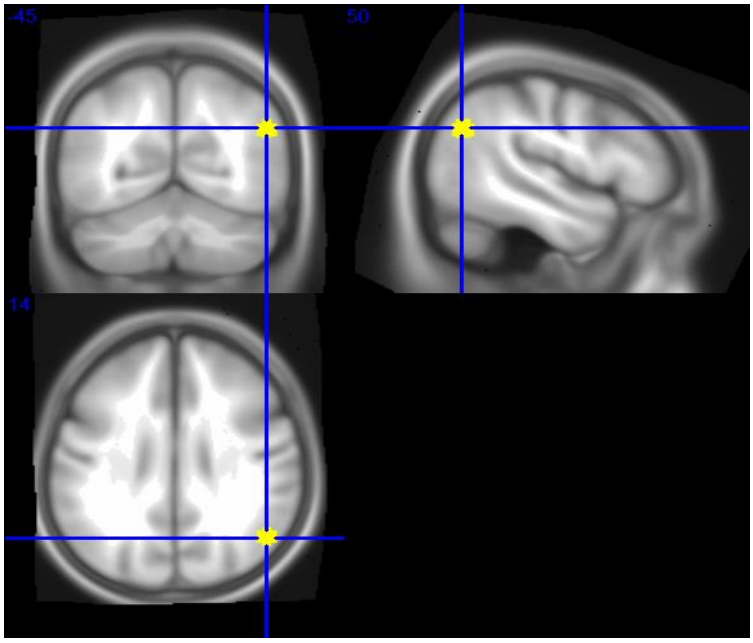

Figure 5

MTG in the DMN (location derived from mean coordinate analysis in current study)

left MTG

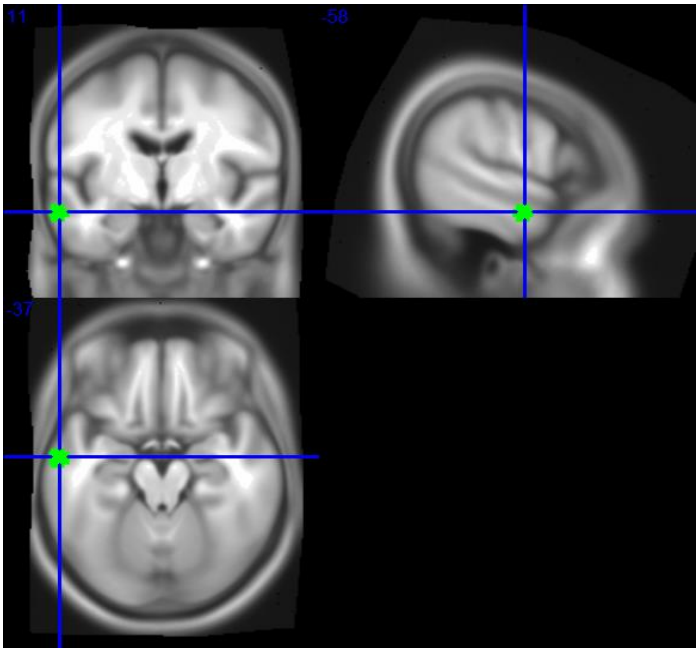

right MTG

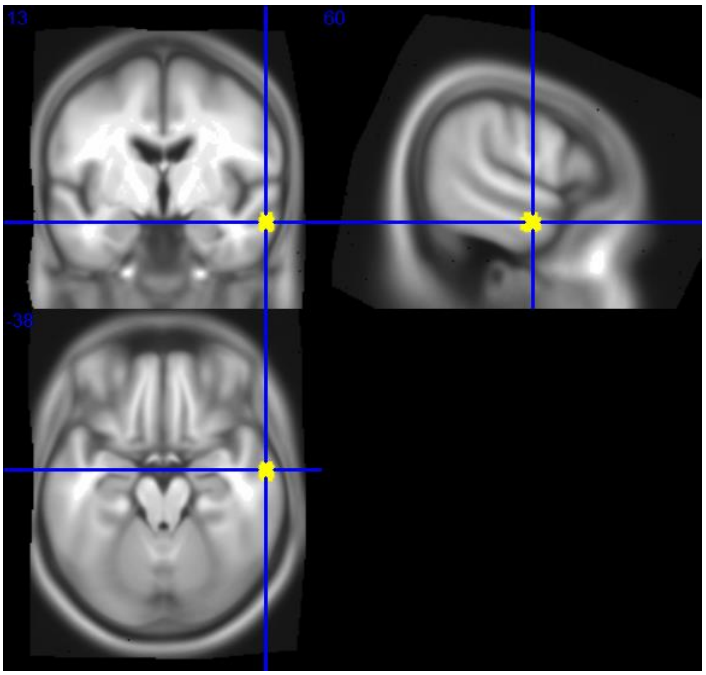

2.9 Definition of DAN ROIs

The left frontal eye fields (lFEF), right frontal eye fields (rFEF), left posterior intra parietal sulcus (lpIPS), right posterior intra parietal sulcus (rpIPS), left anterior intra parietal sulcus (laIPS), right anterior intra parietal sulcus (raIPS), left middle temporal area (lMT+), and right middle temporal area (rMT+) are the ROIs that were selected as part of the DAN. The location of these ROIs in the brain is presented from Figure 6 to Figure 9.

2.10 Definition of SN/CEN ROIs

The SN ROIs comprised of the left anterior cingulate cortex (lACC), right anterior cingulate cortex (rACC), left insula (lINS), and the right insula (rINS). The location of these ROIs in the brain is presented in Figure 10 and Figure 11.

The CEN ROIs included the left dorsal lateral prefrontal cortex (ldlPFC), right dorsal lateral prefrontal cortex (rdlPFC), left anterior inferior parietal lobule (laIPL), and right anterior inferior parietal lobule (raIPL). The location of these ROIs in the brain is presented in Figure 12 and Figure 13.

Figure 6

FEF in the DAN (location derived from mean coordinate analysis in current study)

left FEF

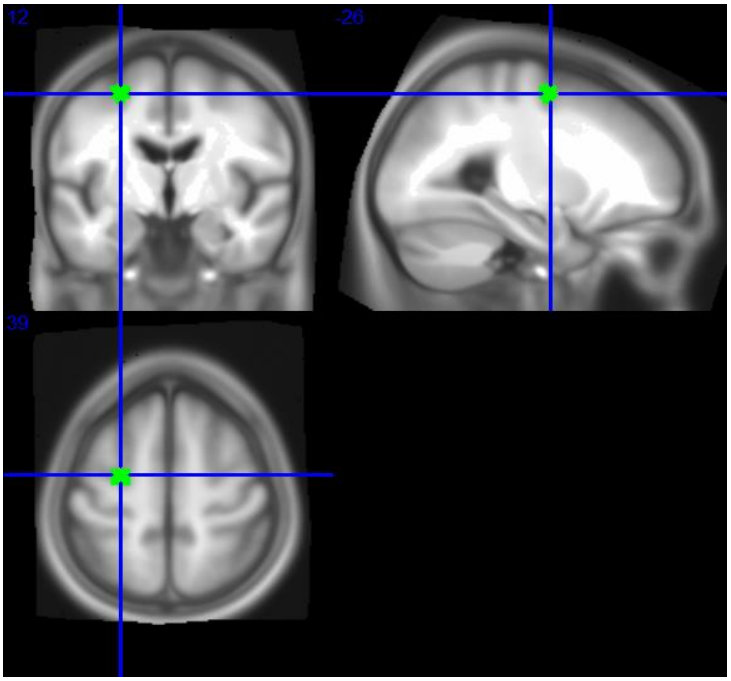

right FEF

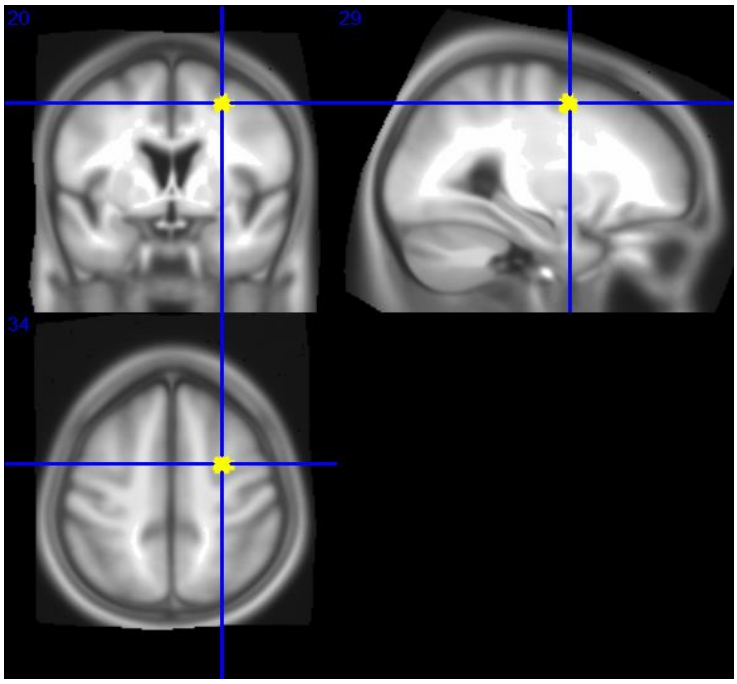

Figure 7

pIPS in the DAN (location derived from mean coordinate analysis in current study)

left pIPS

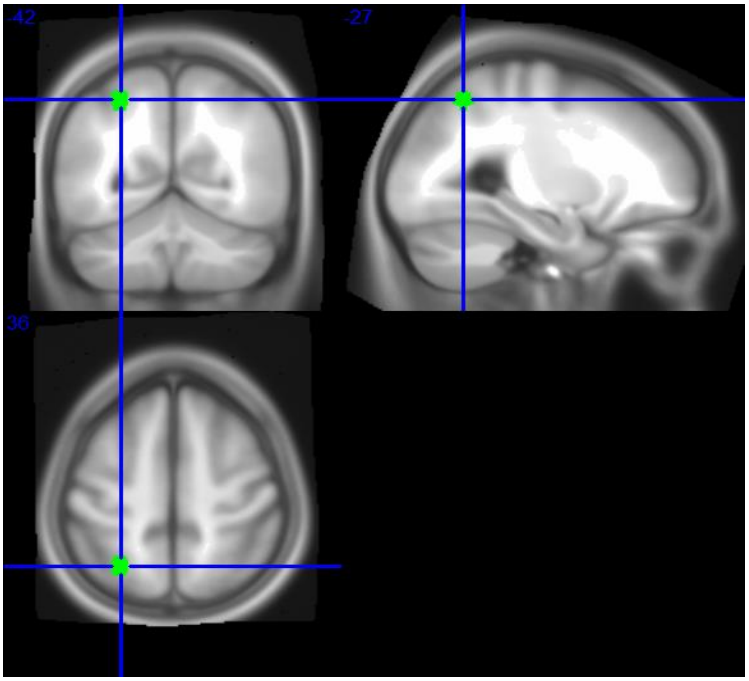

right pIPS

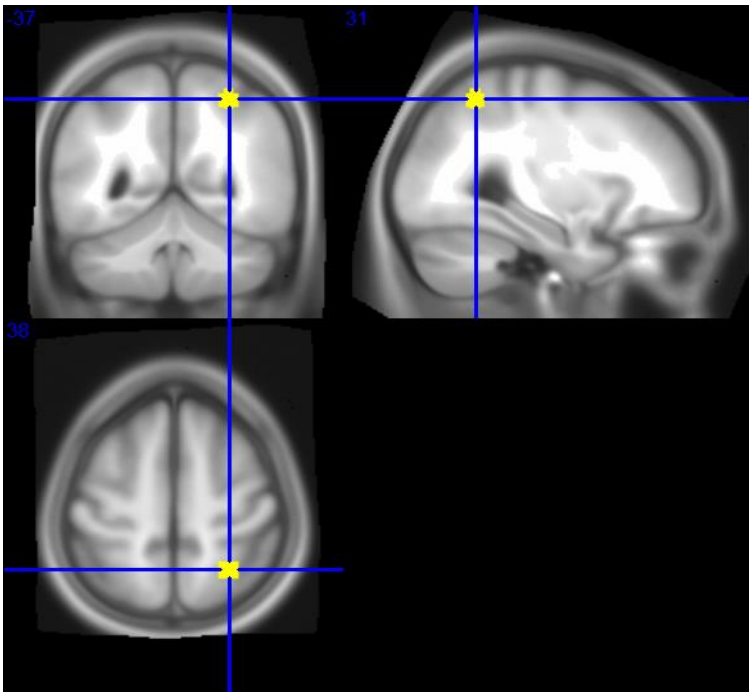

Figure 8

aIPS in the DAN (location derived from mean coordinate analysis in current study)

left aIPS

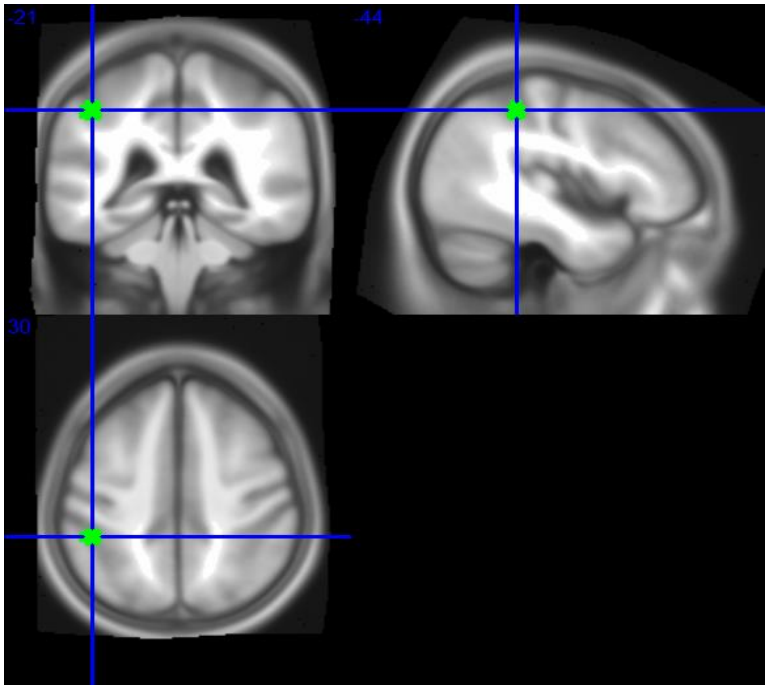

right aIPS

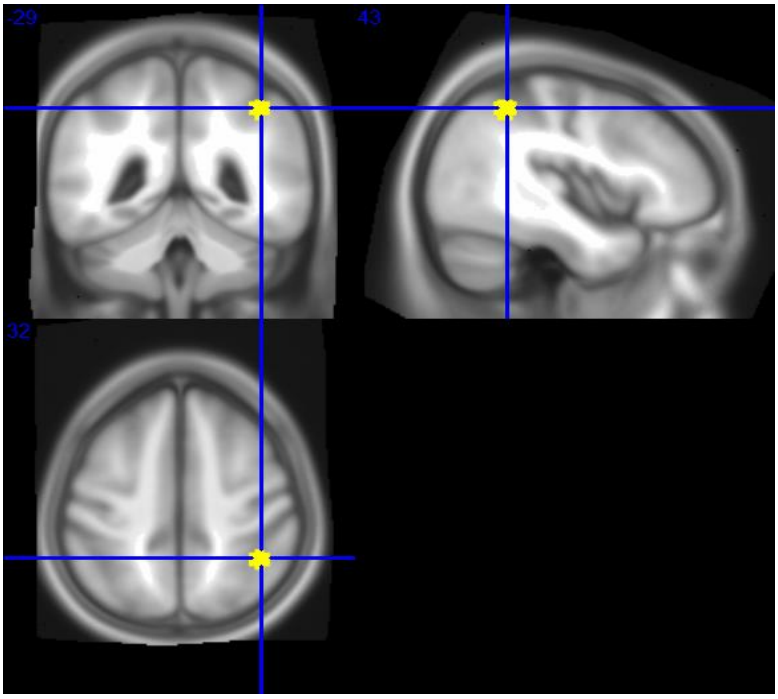

Figure 9

MT+ in the DAN (location derived from mean coordinate analysis in current study)

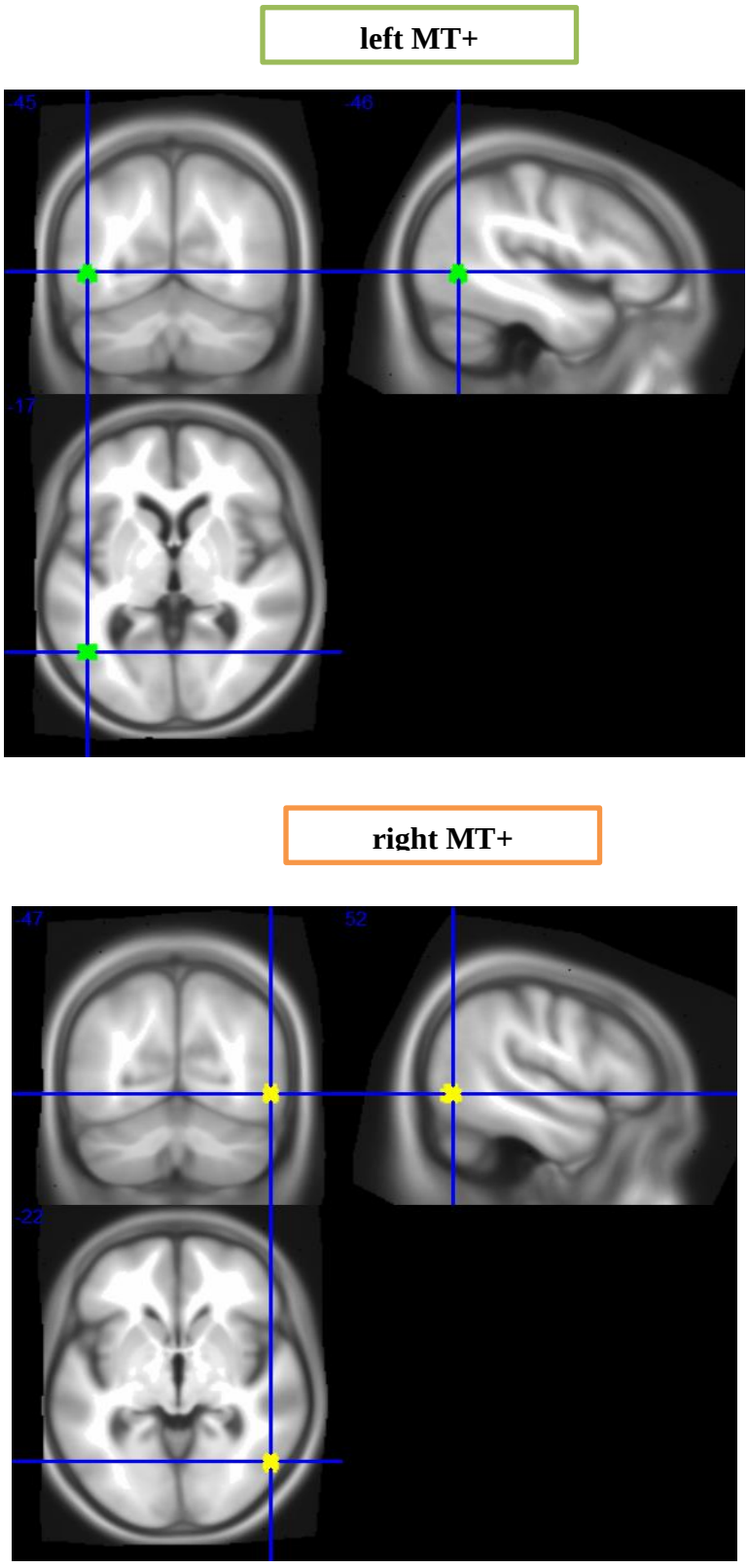

Figure 10

ACC in the SN (location derived from mean coordinate analysis in current study)

left ACC

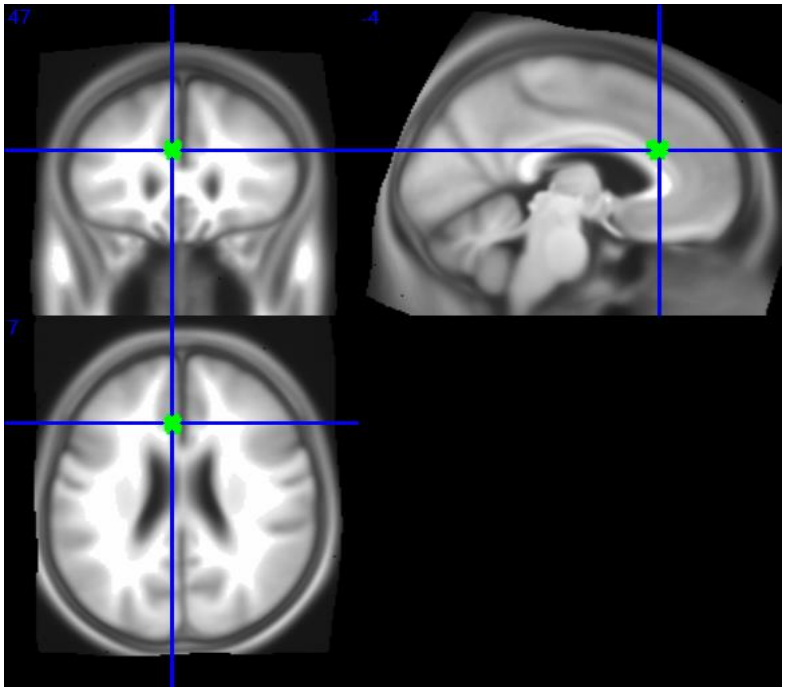

right ACC

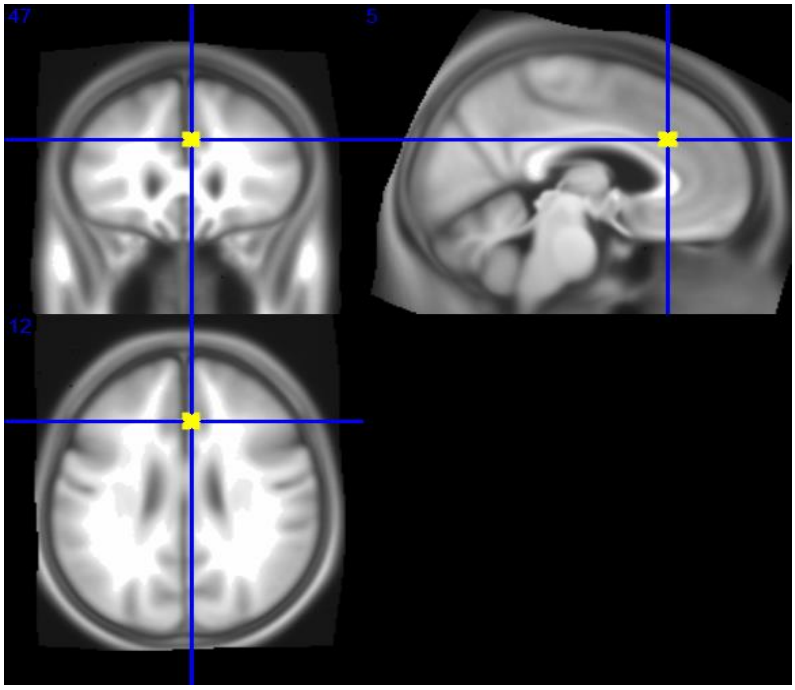

Figure 11

INS in the SN (location derived from mean coordinate analysis in current study)

left INS

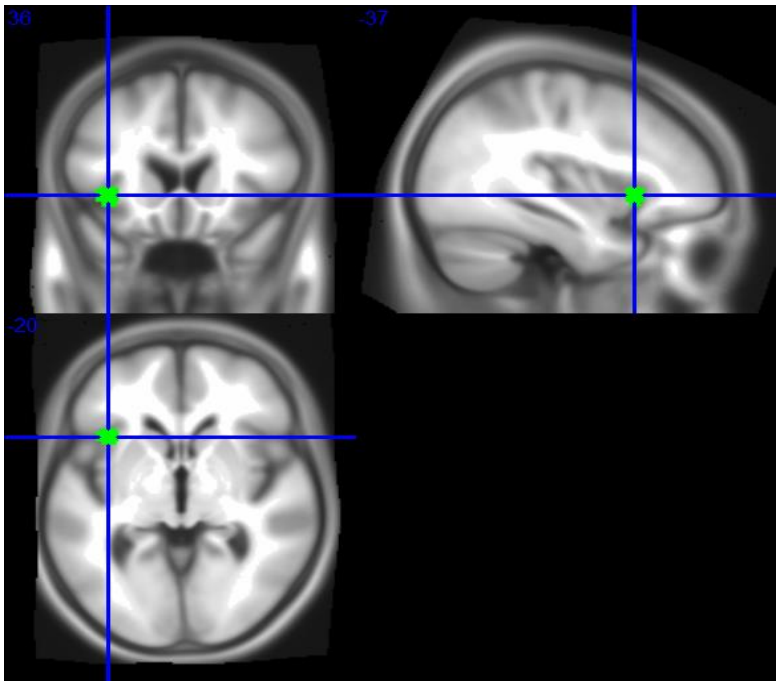

right INS

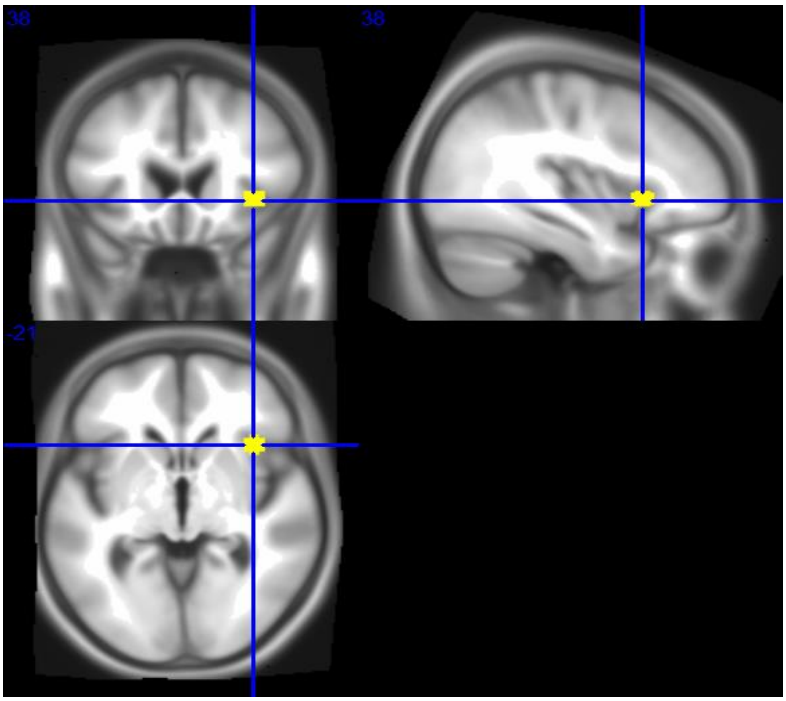

\

Figure 12

dlPFC in the CEN (location derived from mean coordinate analysis in current study)

left dlPFC

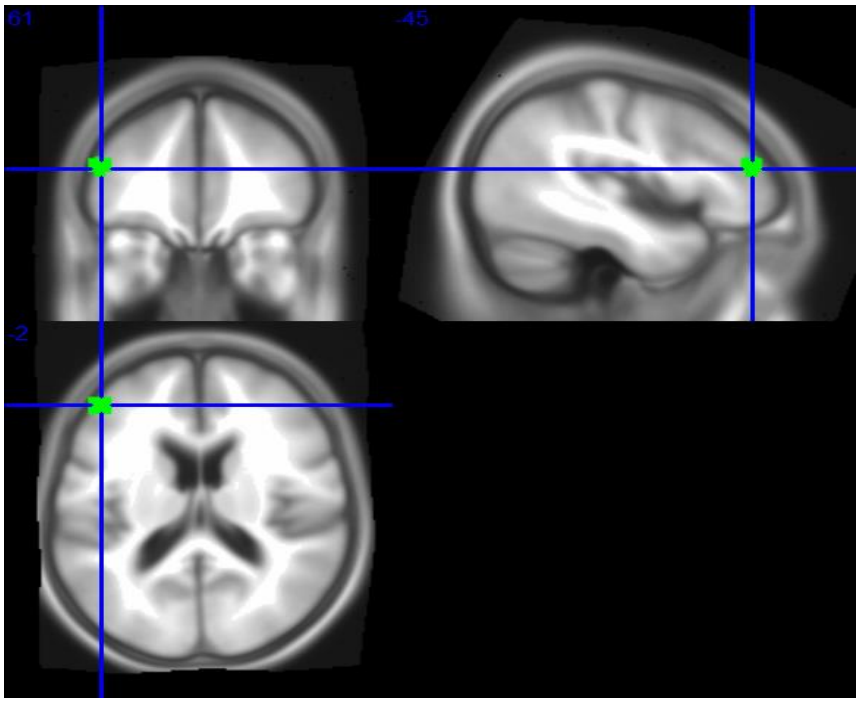

right dlPFC

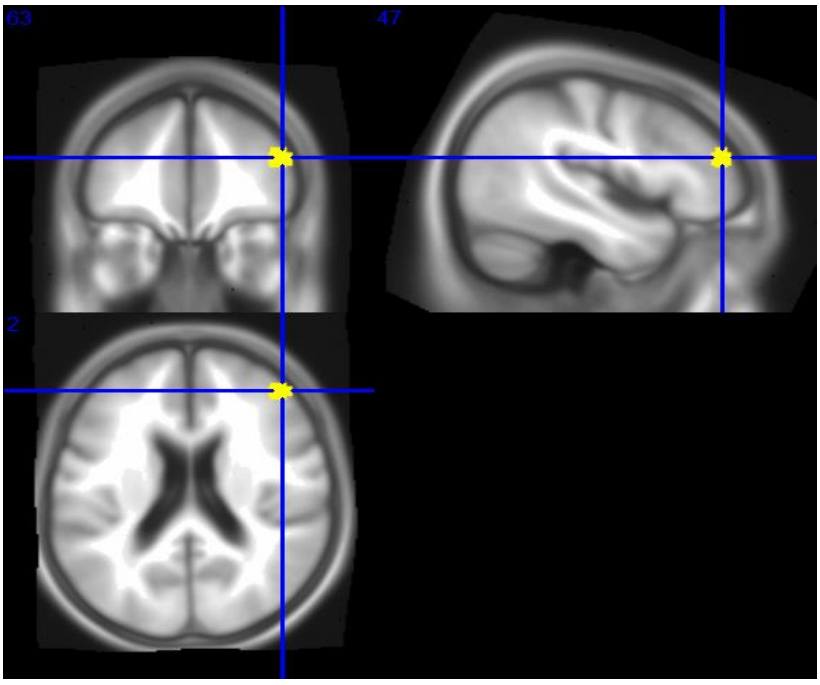

Figure 13

aIPL in the CEN (location derived from mean coordinate analysis in current study)

left aIPL

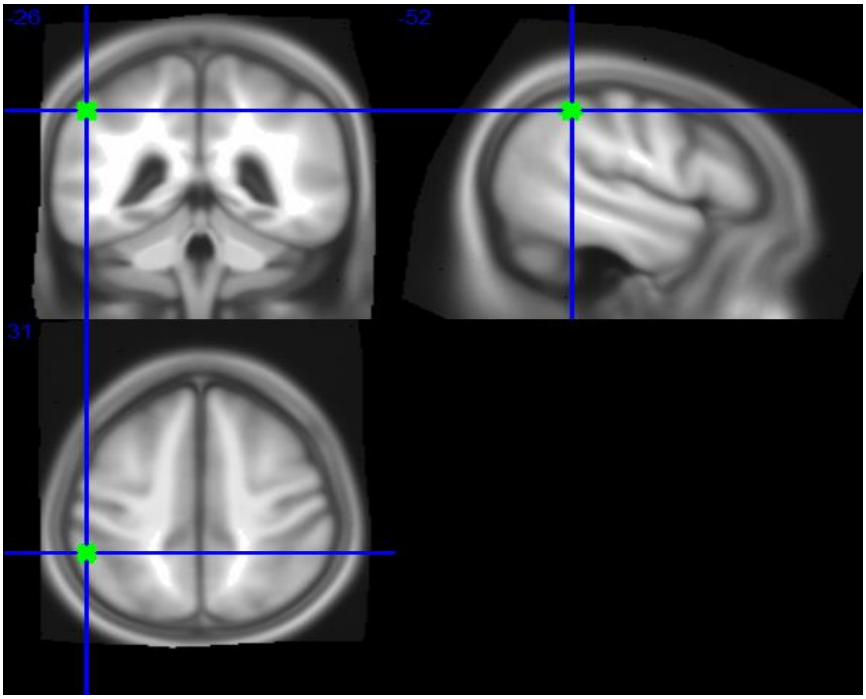

right aIPL

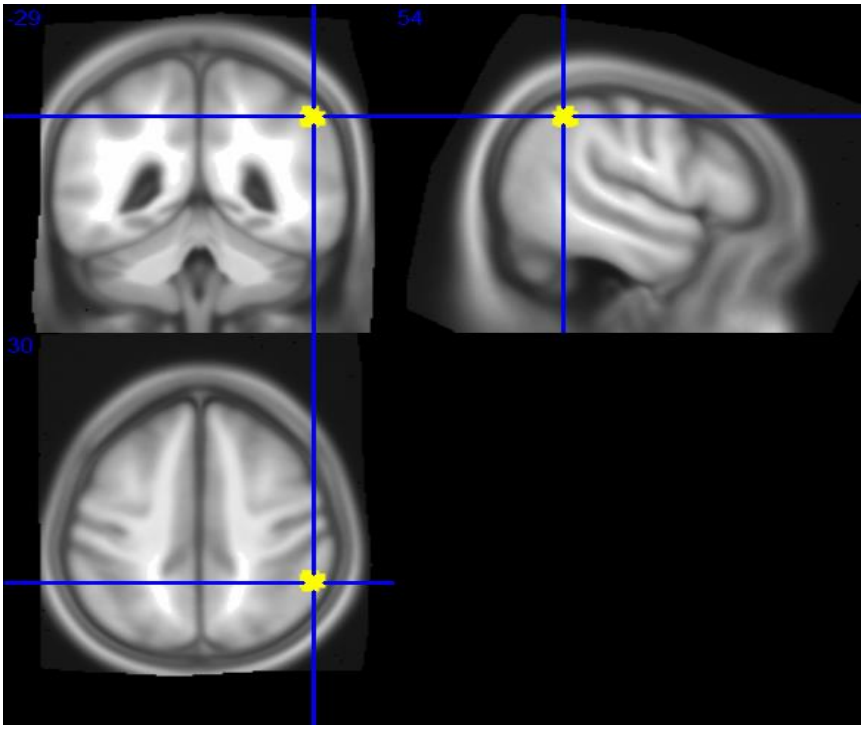

2.11 Formation of Mean ROI Coordinate

The ROIs and their corresponding (x, y, z) coordinates were then organized based on their label (e.g. the dMPFC and its coordinates from different studies were considered together). The total number of coordinates for a particular ROI averaged across the selected studies, generated the mean coordinate that were used to define the location of the ROI in a particular network:

$$\frac{\sum_{i=1}^{n}(x_i, y_i, z_i)}{n}$$

where n is the number of studies that contain the particular ROI and its corresponding coordinate, x_i is the x coordinate from study i, y_i is the y coordinate from study i, and z_i is the z coordinate from study i.

The complete list of ROIs, their corresponding coordinates, the particular cognitive network a ROI belongs to, and the health status, age and number of participants from selected studies for each ROI is summarised in the following tables: Table 6 to Table 12 show the studies assessed to derive the mean coordinates for the ROIs in DMN, Table 13 to Table 20 for DAN, Table 21 to Table 24 for SN, and Table 25 to Table 28 for CEN. Table 29 presents the final derived mean MNI coordinate for each ROI in each network. Figure 1 to Figure 13 (see above) show the location of these ROIs in the brain, based on the coordinates provided in Table 29.

Table 6

Studies assessed for the formation of the mean coordinate for PCC in the DMN

Studies	PCC Coordinate
Fox et al. (2005) Healthy (N = 10)	(-1, -34, 40)
Zhou et al. (2007) Healthy / Schizophrenia Young Adult (Mean Age ± SD: 24 ± 4.9) (N = 18)	(6 , -54, 30)
Harrison et al. (2008) Healthy Young Adult (Mean Age ± SD: 26 ± 3.5) (N =22)	(-3, -57, 30)
Mohammadi et al. (2009) Healthy / Amyotrophic Lateral Sclerosis Middle Age / Elderly (45 - 68) (N = 20)	(-4, -53, 24)
Boly et al. (2009) Healthy / Vegetative State / Brain Dead Middle Age (Mean Age ± SD: 41 ± 11) (N = 6)	(2, -56, 30)
Meindl et al. (2010) Healthy Young Adult / Adult (23 - 36) (N = 18)	(-1, -54, 27)
Wu et al. (2011) Healthy Middle Age / Elderly (53 - 79) (N = 15)	(3, -53, 16)

Liao et al. (2011) Healthy / Mesial Temporal Lobe Epilepsy Young Adult / Middle Age (18 -51) (N = 20)	(-6, -54, 36)
Allen et al. (2011) Healthy Age Varies (Mean Age ± SD: 23.4 ± 9.2) (N = 603)	(0, -52, 22)
Camchong et al. (2011) Healthy / Schizophrenia Middle Age (Mean Age = 41) (N = 58)	(1, -57, 31)
Song et al. (2011) Healthy / Generalized Tonic-Clonic Seizures Control - (Mean Age ± SD: 27.1 ± 4.5) GTCS Patients - (Mean Age ± SD: 26.1 ± 6.1) (N = 43)	(-3, -45, 33)
Li et al. (2011) Healthy Young Adult (Mean Age ± SD: 21 ± 3.4) (N = 12)	(6, -49, 25)
Tomasi & Volkow (2011) Healthy Young Adult / Adult / Elderly (N = 969)	(6, -51, 33)
Koch et al. (2012) Healthy / Mild Cognitive Impairment / Alzheimer's disease Elderly (57 - 100) (N = 53)	(0, -53, 25)
Gao & Lin (2012) Healthy Adult (25 - 33) (N = 19)	(1, -55, 17)

Qi et al. (2012) Healthy / minimal Hepatic Encephalopathy Control - (Mean Age ± SD: 55 ± 9.5) mHE Patients - (Mean Age ± SD: 56.6 ± 9.1) (N = 19)	(0, -43, 40)
Liu et al. (2012) Healthy / Alzheimer's Disease Control - (49 - 78) AD patients - (43 - 76) (N = 36)	(0, -50, 44)
Jin et al. (2012) Healthy / amnesic Mild Cognitive Impairment Elderly (Healthy - Mean Age ± SD: 60.63 ± 8.3) Elderly (aMCI - Mean Age ± SD: 60.88 ± 3.22) (N = 18)	(-6, -60, 22)

Table 7

Studies assessed for the formation of the mean coordinate for dMPFC in the DMN

Studies	dMPFC Coordinates
Fox et al. (2005) Healthy (N = 10)	(0, 51, 2)
Zhou et al. (2007) Healthy / Schizophrenia Young Adult (Mean Age ± SD: 24 ± 4.9) (N = 18)	(0, 53, 14)
Harrison et al. (2008) Healthy (Mean Age ± SD: 26 ± 3.5) (N =22)	(-9, 57, 24)
Mohammadi et al. (2009) Healthy / Amyotrophic Lateral Sclerosis Middle Age / Elderly (45 - 68) (N = 20)	(-2, 41, 29)
Bluhm et al. (2009) Healthy / Depression Young Adults / Adults (17 - 35) (N = 15)	(-2, 68, 12)
Meindl et al. (2010) Healthy Young Adult / Adult (23 - 36) (N = 18)	(0, 54, 7)
Tomasi & Volkow (2011) Healthy Young Adult / Adult / Elderly (N = 969)	(0, 57, 16)

Wu et al. (2011) Healthy / Alzheimer's Disease Middle Age / Elderly (53 - 79) (N = 15)	(3, 46, 16)
Song et al. (2011) Healthy / Epilepsy Control - (Mean Age ± SD: 27.1 ± 4.5) Epilepsy Patients - (Mean Age ± SD: 26.1 ± 6.1) (N = 43)	(-3, 57, 21)
Li et al. (2011) Healthy Young Adult (Mean Age ± SD: 21 ± 3.4) (N = 12)	(-12, 62, 8)
Yeo et al. (2011) Healthy Young Adult / Adult (18 - 35) (N = 1000)	(-7, 49, 18)
Tomasi & Volkow (2011) Healthy Young Adult / Adult / Elderly (N = 969)	(0, 57, 16)
Jin et al. (2012) Healthy / amnesic Mild Cognitive Impairment Elderly (Healthy - Mean Age ± SD: 60.63 ± 8.3) Elderly (aMCI - Mean Age ± SD: 60.88 ± 3.22) (N = 18)	(8, 46, 36)

Table 8

Studies assessed for the formation of the mean coordinate for vMPFC in the DMN

Studies	vMPFC Coordinates
Scheeringa et al. (2008) Healthy Young Adult (18 -28) (N = 20)	(-6, 20, -14)
Boly et al. (2009) Healthy / Vegetative State / Brain Dead Middle Age (Mean Age ± SD: 41 ± 11) (N = 6)	(2, 62, -2)
Liao et al. (2011) Healthy / Mesial Temporal Lobe Epilepsy Young Adult / Middle Age (18 -51) (N = 20)	(0, 54, -6)
Allen et al. (2011) Healthy Age Varies (Mean Age ± SD: 23.4 ± 9.2) (N = 603)	(-1, 45, -9)
Camchong et al. (2011) Healthy / Schizophrenia Middle Age (Mean Age = 41) (N = 58)	(-2, 56, -2)
Gao & Lin (2012) Healthy Adult (25 - 33) (N = 19)	(0, 51, -7)

Table 9

Studies assessed for the formation of the mean coordinate for left pIPL in the DMN

Studies	lpIPL Coordinates
Fox et al. (2005) Healthy (N = 10)	(-49, -67, 49)
Zhou et al. (2007) Healthy / Schizophrenia Young Adult (Mean Age ± SD: 24 ± 4.9) (N = 18)	(-42, -69, 33)
Harrison et al. (2008) Healthy (Mean Age ± SD: 26 ± 3.5) (N =22)	(-48, -57, 24)
Scheeringa et al. (2008) Healthy Young Adult (18 -28) (N = 20)	(-42, -68, 28)
Mohammadi et al. (2009) Healthy / Amyotrophic Lateral Sclerosis Middle Age / Elderly (45 - 68) (N = 20)	(-46, -60, 31)
Bluhm et al. (2009) Healthy / Depression Young Adults / Adults (17 - 35) (N = 15)	(-50, -60, 30)
Boly et al. (2009) Healthy / Vegetative State / Brain Dead Middle Age (Mean Age ± SD: 41 ± 11) (N = 6)	(-48, -66, 48)

Schöpf et al. (2010) Healthy Age varies (Mean Age ± SD: 27.3 ± 7.1) (N = 28)	(-48, -60, 36)
Meindl et al. (2010) Healthy Young Adult / Adult (23 - 36) (N = 18)	(-42, -67, 31)
Wu et al. (2011) Healthy / Alzheimer's Disease Middle Age / Elderly (53 - 79) (N = 15)	(-49, -60, 31)
Liao et al. (2011) Healthy / Mesial Temporal Lobe Epilepsy Young Adult / Middle Age (18 -51) (N = 20)	(-42, -66, 33)
Allen et al. (2011) Healthy Age Varies (Mean Age ± SD: 23.4 ± 9.2) (N = 603)	(-43, -69, 33)
Camchong et al. (2011) Healthy / Schizophrenia Middle Age (Mean Age = 41) (N = 58)	(-34, -62, 36)
Song et al. (2011) Healthy / Epilepsy Control - (Mean Age ± SD: 27.1 ± 4.5) Epilepsy Patients - (Mean Age ± SD: 26.1 ± 6.1) (N = 43)	(-54, -69, 36)
Li et al. (2011) Healthy Young Adult (Mean Age ± SD: 21 ± 3.4) (N = 12)	(-43, -67, 33)

Yeo et al. (2011) Healthy Young Adult / Adult (18 - 35) (N = 1000)	(-41, -60, 29)
Tomasi & Volkow (2011) Healthy Young Adult / Adult / Elderly (N = 969)	(-51, -63, 31)
Koch et al. (2012) Healthy / Mild Cognitive Impairment / Alzheimer's disease Elderly (57 - 100) (N = 53)	(-44, -67, 24)
Gao & Lin (2012) Healthy Adult (25 - 33) (N = 19)	(-47, -71, 29)
Qi et al. (2012) Healthy / minimal Hepatic Encephalopathy Control - (Mean Age ± SD: 55 ± 9.5) mHE Patients - (Mean Age ± SD: 56.6 ± 9.1) (N = 19)	(-33, -76, 40)
Liu et al. (2012) Healthy / Alzheimer's Disease Control - (49 - 78) AD patients - (43 - 76) (N = 36)	(-50, -61, 45)
De Vogelaere et al. (2012) Healthy / Mild Cognitive Impairment Adults (19 - 36) (N = 32)	(-51, -69, 24)
Jin et al. (2012) Healthy / amnesic Mild Cognitive Impairment Elderly (Healthy - Mean Age ± SD: 60.63 ± 8.3)	(-46, -42, 54)

Elderly (aMCI - Mean Age ± SD: 60.88 ± 3.22) (N = 18)	

Table 10

Studies assessed for the formation of the mean coordinate for rpIPL in the DMN

Studies	rpIPL Coordinates
Zhou et al. (2007) Healthy / Schizophrenia Young Adult (Mean Age ± SD: 24 ± 4.9) (N = 18)	(48, -57, 30)
Scheeringa et al. (2008) Healthy Young Adult (18 -28) (N = 20)	(46, -64, 36)
Mohammadi et al. (2009) Healthy / Amyotrophic lateral sclerosis Middle Age / Elderly (45 - 68) (N = 20)	(50, -57, 28)
Boly et al. (2009) Healthy / Vegetative State / Brain Dead Middle Age (Mean Age ± SD: 41 ± 11) (N = 6)	(62, -58, 28)
Schöpf et al. (2010) Healthy Age varies (Mean Age ± SD: 27.3 ± 7.1) (N = 28)	(50, -70, 34)
Meindl et al. (2010) Healthy Young Adult / Adult (23 - 36) (N = 18)	(48, -60, 29)
Wu et al. (2011) Healthy / Alzheimer's Disease Middle Age / Elderly (53 - 79)	(54, -60, 28)

(N = 15)	
Liao et al. (2011) Healthy / Mesial Temporal Lobe Epilepsy Young Adult / Middle Age (18 -51) (N = 20)	(54, - 63, 36)
Allen et al. (2011) Healthy Age Varies (Mean Age ± SD: 23.4 ± 9.2) (N = 603)	(47, -66, 32)
Camchong et al. (2011) Healthy / Schizophrenia Middle Age (Mean Age = 41) (N = 58)	(42, -54, 36)
Song et al. (2011) Healthy / Epilepsy Control - (Mean Age ± SD: 27.1 ± 4.5) Epilepsy Patients - (Mean Age ± SD: 26.1 ± 6.1) (N = 43)	(54, -63, 33)
Li et al. (2011) Healthy Young Adult (Mean Age ± SD: 21 ± 3.4) (N = 12)	(45, -60, 29)
Tomasi & Volkow (2011) Healthy Young Adult / Adult / Elderly (N = 969)	(51, -61, 30)
Koch et al. (2012) Healthy / Mild Cognitive Impairment / Alzheimer's disease Elderly (57 - 100) (N = 53)	(50, -62, 19)
Gao & Lin (2012) Healthy	

Adult (25 - 33) (N = 19)	(50, -64, 27)
Qi et al. (2012) Healthy / minimal Hepatic Encephalopathy Control - (Mean Age ± SD: 55 ± 9.5) mHE Patients - (Mean Age ± SD: 56.6 ± 9.1) (N = 19)	(51, -70, 43)
De Vogelaere et al. (2012) Healthy / Mild Cognitive Impairment Adults (19 - 36) (N = 32)	(51, -66, 24)
Jin et al. (2012) Healthy / amnesic Mild Cognitive Impairment Elderly (Healthy - Mean Age ± SD: 60.63 ± 8.3) Elderly (aMCI - Mean Age ± SD: 60.88 ± 3.22) (N = 18)	(48, -72, 30)

Table 11

Studies assessed for the formation of the mean coordinate for left MTG in the DMN

Studies	lMTG Coordinates
Zhou et al. (2007) Healthy / Schizophrenia Young Adult (Mean Age ± SD: 24 ± 4.9) (N = 18)	(-60, -6, -24)
Harrison et al. (2008) Healthy Young Adult (Mean Age ± SD: 26 ± 3.5) (N =22)	(-57, -9, -24)
Scheeringa et al. (2008) Healthy Young Adult (18 -28) (N = 20)	(-62, -2, -24)
Mohammadi et al. (2009) Healthy / Amyotrophic lateral sclerosis Middle Age / Elderly (45 - 68) (N = 20)	(-53, 1, -17)
Schöpf et al. (2010) Healthy Age varies (Mean Age ± SD: 27.3 ± 7.1) (N = 28)	(-60, -14, -22)
Wu et al. (2011) Healthy / Alzheimer's Disease Middle Age / Elderly (53 - 79) (N = 15)	(-60, -12, -16)
Liao et al. (2011) Healthy / Mesial Temporal Lobe Epilepsy	(-60, -12, -21)

Young Adult / Middle Age (18 -51) (N = 20)	
Li et al. (2011) Healthy Young Adult (Mean Age ± SD: 21 ± 3.4) (N = 12)	(-59, -15, -16)
Yeo et al. (2011) Healthy Young Adult / Adult (18 - 35) (N = 1000)	(-64, -20, -9)
Song et al. (2011) Healthy / Generalized Tonic-Clonic Seizures Control - (Mean Age ± SD: 27.1 ± 4.5) GTCS Patients - (Mean Age ± SD: 26.1 ± 6.1) (N = 43)	(-54, -3, -30)
Koch et al. (2012) AD / MCI / Healthy Elderly (57 - 100) (N = 53)	(-60, -12, -12)
De Vogelaere et al. (2012) Healthy / MCI Adults (19 - 36) (N = 32)	(-63, -15, -15)
Wang et al. (2012) Healthy / Generalized Tonic-Clonic Seizures Adult (Healthy - Mean Age ± SD: 27.93 ± 8.35) Adult (GTCS - Mean Age ± SD: 27.37 ± 4.50) (N = 32)	(-57, -3, -24)

Table 12

Studies assessed for the formation of the mean coordinate for rMTG in the DMN

Studies	rMTG Coordinates
Zhou et al. (2007) Healthy / Schizophrenia Young Adult (Mean Age ± SD: 24 ± 4.9) (N = 18)	(63, -3, -24)
Scheeringa et al. (2008) Healthy Young Adult (18 -28) (N = 20)	(64, -16, -18)
Mohammadi et al. (2009) Healthy / Amyotrophic lateral sclerosis Middle Age / Elderly (45 - 68) (N = 20)	(54, 2, -22)
Wu et al. (2011) Healthy / Alzheimer's Disease Middle Age / Elderly (53 - 79) (N = 15)	(63, -6, -19)
Liao et al. (2011) Healthy / Mesial Temporal Lobe Epilepsy Young Adult / Middle Age (18 -51) (N = 20)	(60, -3, -27)
Song et al. (2011) Healthy / Generalized Tonic-Clonic Seizures Control - (Mean Age ± SD: 27.1 ± 4.5) GTCS Patients - (Mean Age ± SD: 26.1 ± 6.1) (N = 43)	(54, 0, -30)

Table 13

Studies assessed for the formation of the mean coordinate for left FEF in the DAN

Studies	lFEF Coordinates
Fox et al. (2005) Healthy (N = 10)	(-24, -7, 65)
Fox et al. (2006) Healthy (N = 10)	(-25, -7, 58)
Grady et al. (2010) Healthy Young Adult / Elderly (20 - 30, 56 - 84) (N = 47)	(-32, -8, 56)
Gao & Lin (2012) Healthy Adult (25 - 33) (N = 19)	(-25 -8, 50)

Table 14

Studies assessed for the formation of the mean coordinate for right FEF in the DAN

Studies	rFEF Coordinates
Fox et al. (2005) Healthy (N = 10)	(32, -1, 56)
Fox et al. (2006) Healthy (N = 10)	(32, -5, 55)
Grady et al. (2010) Healthy Young Adult / Elderly (20 - 30, 56 - 84) (N = 47)	(28, -4, 48)
Gao & Lin (2012) Healthy Adult (25 - 33) (N = 19)	(27, -8, 50)

Table 15

Studies assessed for the formation of the mean coordinate for left pIPS in the DAN

Studies	lpIPS Coordinates
Fox et al. (2005) Healthy (N = 10)	(-23, -65, 53)
Fox et al. (2006) Healthy (N = 10)	(-22, -67, 53)
Grady et al. (2010) Healthy Young Adult / Elderly (20 - 30, 56 - 84) (N = 47)	(-28, -60, 56)
Gao & Lin (2012) Healthy Adult (25 - 33) (N = 19)	(-27, -52, 57)
Fornito et al. (2012) Healthy Adults (19 - 36) (N = 16)	(-27, -69, 39)
Li et al. (2011) Healthy Young Adult (Mean Age ± SD: 21 ± 3.4) (N = 12)	(-39, -63, 56)

Table 16

Studies assessed for the formation of the mean coordinate for right pIPS in the DAN

Studies	rpIPS Coordinates
Fox et al. (2005) Healthy (N = 10)	(29, -56, 58)
Fox et al. (2006) Healthy (N = 10)	(23, -65, 58)
Grady et al. (2010) Healthy Young Adult / Elderly (20 - 30, 56 - 84) (N = 47)	(28, -60, 48)
Gao & Lin (2012) Healthy Adult (25 - 33) (N = 19)	(24, -56, 55)
Li et al. (2011) Healthy Young Adult (Mean Age ± SD: 21 ± 3.4) (N = 12)	(42, -51, 52)
Liu et al. (2012) Healthy / Alzheimer's disease Control - (49 - 78) AD patients - (43 - 76) (N = 36)	(43, -48, 62)

Table 17

Studies assessed for the formation of the mean coordinate for left aIPS in the DAN

Studies	laIPS Coordinates
Fox et al. (2005) Healthy (N = 10)	(-43, -41, 55)
Fox et al. (2006) Healthy (N = 10)	(-43, -39, 46)
Grady et al. (2010) Healthy Young Adult / Elderly (20 - 30, 56 - 84) (N = 47)	(-48, -40, 40)

Table 18

Studies assessed for the formation of the mean coordinate for right aIPS in the DAN

Studies	raIPS Coordinates
Fox et al. (2005) Healthy (N = 10)	rIPL (52, -33, 56)
Fox et al. (2006) Healthy (N = 10)	raIPS (39, -45, 49)
Grady et al. (2010) Healthy Young Adult / Elderly (20 - 30, 56 - 84) (N = 47)	rIPL (44, -44, 44)
Fornito et al. (2012) Healthy Adults (19 - 36) (N = 16)	rIPS (33, -45, 48)

Table 19

Studies assessed for the formation of the mean coordinate for left MT+ in the DAN

Studies	lMT+ Coordinates
Fox et al. (2005) Healthy (N = 10)	(-49, -72, -1)
Fox et al. (2006) Healthy (N = 10)	(-48, -72, -5)
Zhou et al. (2007) Healthy / Schizophrenia Young Adult (Mean Age ± SD: 24 ± 4.9) (N = 18)	(-51, -57, -12)
Grady et al. (2010) Healthy Young Adult / Elderly (20 - 30, 56 - 84) (N = 47)	(-48, -72, -4)
Gao & Lin (2012) Healthy Adult (25 - 33) (N = 19)	(-45, -69, -2)

Table 20

Studies assessed for the formation of the mean coordinate for right MT+ in the DAN

Studies	rMT+ Coordinates
Fox et al. (2005) Healthy (N = 10)	(59, -69, -2)
Fox et al. (2006) Healthy (N = 10)	(56, -66, -7)
Zhou et al. (2007) Healthy / Schizophrenia Young Adult (Mean Age ± SD: 24 ± 4.9) (N = 18)	(44, -64, -12)
Gao & Lin (2012) Healthy Adult (25 - 33) (N = 19)	(50, -69, -3)

Table 21

Studies assessed for the formation of the mean coordinate for left ACC in the SN

Studies	lACC Coordinates
Seeley et al. (2007) Healthy All Ages (18 - 70) (N = 14)	(-6, 18, 30)
White et al. (2010) Healthy / Schizophrenia Young Adult / Adult (20 - 37) (N = 19)	(-5, 35, 28)
Liu et al. (2012) Healthy / Alzheimer Disease Control - (49 - 78) AD patients - (43 - 76) (N = 36)	(-1, 29, 18)

Table 22

Studies assessed for the formation of the mean coordinate for right ACC in the SN

Studies	rACC Coordinates
Seeley et al. (2007) Healthy All Ages (18 - 70) (N = 14)	(6, 22, 30)
Sridharan et al. (2008) Healthy Young Adult / Adult (19 - 29) (N = 13)	(4, 30, 30)
White et al. (2010) Healthy / Schizophrenia Young Adult / Adult (20 - 37) (N = 19)	(5, 29, 37)
Gao & Lin (2012) Healthy Adult (25 - 33) (N = 19)	(3, 31, 27)

Table 23

Studies assessed for the formation of the mean coordinate for left INS in the SN

Studies	lINS Coordinates
Fox et al. (2005) Healthy (N = 10)	(-47, 7, 5)
Seeley et al. (2007) Healthy All Ages (18 - 70) (N = 14)	(-40, 18, -12)
Zhou et al. (2007) Healthy / Schizophrenia Young Adult (Mean Age ± SD: 24 ± 4.9) (N = 18)	(-33, 21, 3)
Sridharan et al. (2008) Healthy Young Adult / Adult (19 - 29) (N = 13)	(-32, 24, -6)
Gao & Lin (2012) Healthy Adult (25 - 33) (N = 19)	(-31, 21, -1)
Liu et al. (2012) Healthy (AD data not included) Control - (49 - 78)	(-44, 15, -8)

AD patients - (43 - 76) (N = 36)	

Table 24

Studies assessed for the formation of the mean coordinate for right INS in the SN

Studies	**rlINS Coordinates**
Fox et al. (2005) Healthy (N = 10)	(49, 7, 10)
Seeley et al. (2007) Healthy All Ages (18 - 70) (N = 14)	(42, 10, -12)
Zhou et al. (2007) Healthy / Schizophrenia Young Adult (Mean Age ± SD: 24 ± 4.9) (N = 18)	(36, 21, 3)
Sridharan et al. (2008) Healthy Young Adult / Adult (19 - 29) (N = 13)	(37, 25, -4)
Gao & Lin (2012) Healthy Adult (25 - 33) (N = 19)	(31, 22, -2)
Fornito et al. (2012) Healthy	(39, 24, -6)

Adults (19 - 36) (N = 16)	

Table 25

Studies assessed for the formation of the mean coordinate for left dlPFC in the CEN

Studies	**ldlPFC Coordinates**
Fox et al. (2005) Healthy (N = 10)	(-44, 45, 21)
Zhou et al. (2007) Healthy / Schizophrenia Young Adult (Mean Age ± SD: 24 ± 4.9) (N = 18)	(-48, 39, 12)

Table 26

Studies assessed for the formation of the mean coordinate for right dlPFC in the CEN

Studies	**rdlPFC Coordinates**
Fox et al. (2005) Healthy (N = 10)	(42, 47, 16)
Zhou et al. (2007)	

Healthy / Schizophrenia Young Adult (Mean Age ± SD: 24 ± 4.9) (N = 18)	(48, 42, 21)

Table 27

Studies assessed for the formation of the mean coordinate for left laIPL in the CEN

Studies	**laIPL Coordinates**
Seeley et al. (2007) Healthy All Ages (18 - 70) (N = 14)	(-48, -48, 48)
Zhou et al. (2007) Healthy / Schizophrenia Young Adult (Mean Age ± SD: 24 ± 4.9) (N = 18)	(-51, -36, 45)
White et al. (2010) Healthy / Schizophrenia Young Adult / Adult (20 - 37) (N = 19)	(-57, -45, 51)
Gao & Lin (2012) Healthy Adult (25 - 33) (N = 19)	(-52, -49, 47)

Table 28

Studies assessed for the formation of the mean coordinate for right laIPL in the CEN

Studies	raIPL Coordinates
Sridharan et al. (2008) Healthy Young Adult / Adult (19 - 29) (N = 13)	(54, -50, 50)
Gao & Lin (2012) Healthy Adult (25 - 33) (N = 19)	(52, -46, 46)
Fornito et al. (2012) Healthy Adults (19 - 36) (N = 16)	(54, -45, 45)

Table 29

Mean coordinates of ROIs in all network derived from selected studies

Network	Regions of Interest	Mean Coordinate
DMN	PCC	(0, -51, 29)
	dMPFC	(-2, 54, 17)
	vMPFC	(-2, 48, -7)
	lpIPL	(-45, -64, 34)
	rpIPL	(50, -63, 31)
	lMTG	(-59, -9, 20)
	rMTG	(60, -7, -21)
DAN	lFEF	(-26, -8, 57)
	rFEF	(29, 0, 51)
	lpIPS	(-28, -61, 53)
	rpIPS	(30, -56, 55)
	laIPS	(-45, -40, 47)
	raIPS	(42, -42, 49)
	lMT+	(-46, -64, -1)
	rMT+	(52, -67, -5)
SN	lACC	(-4, 27, 25)
	rACC	(4, 28, 30)
	lINS	(-37, 18, -3)
	rINS	(38, 19, -2)
CEN	ldlPFC	(-46, 42, 17)
	rdlPFC	(45, 44, 19)
	laIPL	(-52, -45, 48)
	raIPL	(53, -47, 47)

*refer to Table 5 for abbreviations

2.12 ROI Processing/Analysis

ROIs were first constructed in standard space ('normalized/MNI space'). The ROIs were then warped into subject space for each individual. MarsBar 0.42, a toolbox for SPM5 which allows for the construction and definition of ROIs, (MARSeille Boîte À Région d'Intérêt release 0.42; Brett, Anton, Valabregue, & Poline, 2002), was used to build the ROIs. The process was as follows: (1) MarsBar was accessed in SPM5, (2)'Build' was selected, (3) 'Type of ROI' selected was sphere, (4) 'Centre of sphere' coordinates (x, y, z) for a particular ROI were entered based on meta-analysis findings, (5) A 6mm 'sphere radius' was selected, (6) 'Description of ROI' was used to label a particular ROI, (7) The ROI was saved as *.mat file, (8) The ROIs was then 'exported' as an image, and lastly, (9) The ROI (*.mat file) was converted to a NifTI (*.nii file) image.

A radius of 6-mm was selected because this was estimated as an optimal size to cover all relevant voxels but exclude excessive white matter tracts or CSF in the brain. The .mat file format (MATLAB binary file format) was converted to .nii file format (NifTI data format) as MRIcron, the program that used to draw and edit anatomical ROIs in this study, cannot use the .mat file format.

After all the ROIs for the cognitive networks were constructed in standard space, the next step of analysis involved applying inverse spatial normalization parameters to produce ROIs in the individual subject space of each participant. In other words, the ROIs in standard space were 'customized' to fit the brain of each participant. This process was conducted to reduce anatomical and functional variability, as the location of the subject space ROIs depends on the accuracy of the normalization, which may vary from individual to individual.

To perform this 'reverse engineering' task, inverse normalization parameters were used to warp the ROIs in standard space into the subject space of each participant, by executing several MATLAB scripts (custom-made by Dr. Tracy Melzer to perform this task). Visual checks of the location for each ROI in the brain of every participant were then performed to examine whether ROIs appeared correctly placed or the ROIs covered excessive white matter tracts or CSF. In the event of any such problem, the ROIs were manually re-adjusted using MRIcron.

After the visual checks and modifications were performed, the mean FA and MD value of each ROI in subject space for each participant were extracted. This analysis focused on DTI metrics within grey matter regions. Therefore, FA and MD values from only GM voxels contributed to the mean of a specific ROI. Co-registered GM and WM from the structural segmentation process were used to define voxels within each ROI as grey matter or white matter. To contribute to the mean FA/MD value for a given individual's ROI, each voxel had to have a greater than 10% chance of being GM or WM (to eliminate contribution from CSF) and also have a FA value <0.3, indicative of GM (i.e. not pertaining to a white matter tract). If these conditions were met, the FA/MD value from that voxel was extracted and contributed to the calculation of the ROI's mean FA/MD.

3. Results

3.1 ANCOVA MD

ANCOVA (with age and education as covariates) followed by Newman-Keuls post-hoc comparison tests were performed on the mean MD values for each participant group in a particular ROI for each RSN.

The ANCOVA for the group main effects for MD in the left and right ROIs of the four networks are summarized on Table 30 and the mean values for the four participant groups for each ROI in every RSN are shown in Figure 14 to Figure 26. The Newman-Keuls Test tables are presented in the Appendix.

Table 30

MD: Group main effect for the ANCOVA for each ROI for the four cognitive networks

CEN	dlPFC		aIPL							
	Left	Right	Left	Right						
	F (3,135) = 3.07, p<.03	F (3,135) = 1.73, p=.2	F (3,135) = .73, p=.5	F (3,135) = .48, p=.7						
SN	ACC		INS							
	Left	Right	Left	Right						
	F (3,135) = 5.63, p<.001	**F (3,135) = 6.68, p<.0003**	F (3,135) = 1.86, p=.1	**F (3,135) = 3.94, p<.01**						
DAN	FEF		aIPS		pIPS		MT+			
	Left	Right	Left	Right	Left	Right	Left	Right		
	F (3,135) = .47, p=.7	**F (3,135) = 3.33, p<.02**	**F (3,135) = 4.15, p<.01**	F (3,135) = 2.06, p=.1	F (3,135) = 2.64, p=.05	F (3,135) = 1.25, p=.3	**F (3,135) = 6.03, p<.01**	**F (3,135) = 3.17, p<.03**		
DMN	PCC		dMPFC		vMPFC		pIPL		MTG	
	Left	Right	Left	Right	Left	Right	Left	Right	Left	Right
	F (3,135) = 4.34, p<.01	**F (3,135) = 3.85, p<.01**	**F (3,135) = 5.49, p<.001**	**F (3,135) = 4.3, p<.01**	F (3,135) = 1.57, p=.2	**F (3,135) = 4.82, p<.003**	**F (3,135) = 3.14, p<.03**	F (3,135) = .51, p=.7	**F (3,135) = 3.51, p<.02**	**F (3,135) = 3.89, p<.01**

All bolded F-ratios are significant. Age and education of participants were used as co-variates; age was significant for all ROIs ($p<0.05$), except left ACC of the SN. Education was not significant for any ROI. For abbreviations, see Table 5.

Figure 14

Differences between the means (±sem) of the MD of the PCC for the four groups controlling for age and education.

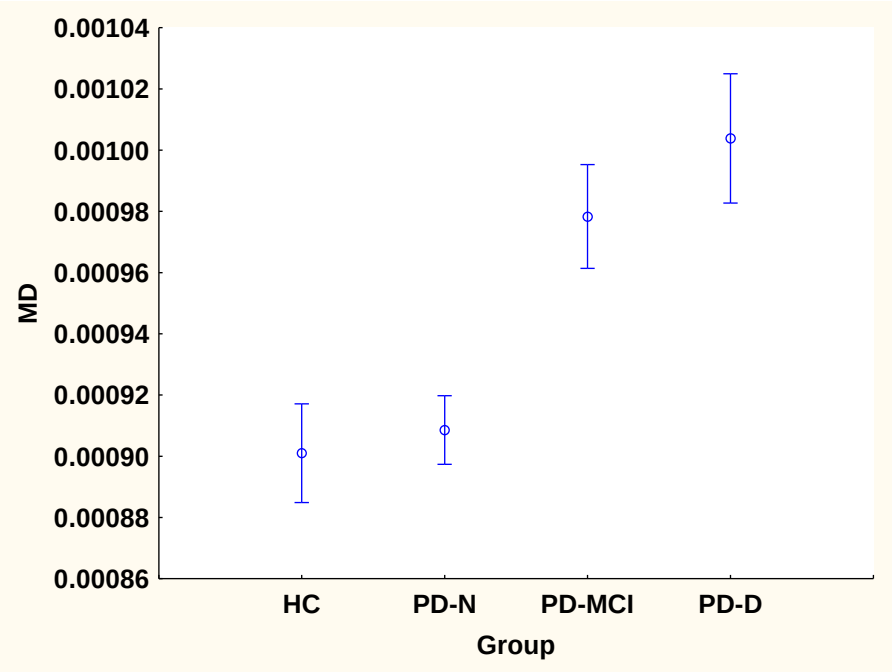

Fig 14A. DMN ANCOVA showing lPCC: Pairwise group differences (N-K): (HC = PD-N) < (PD-MCI = PD-D).

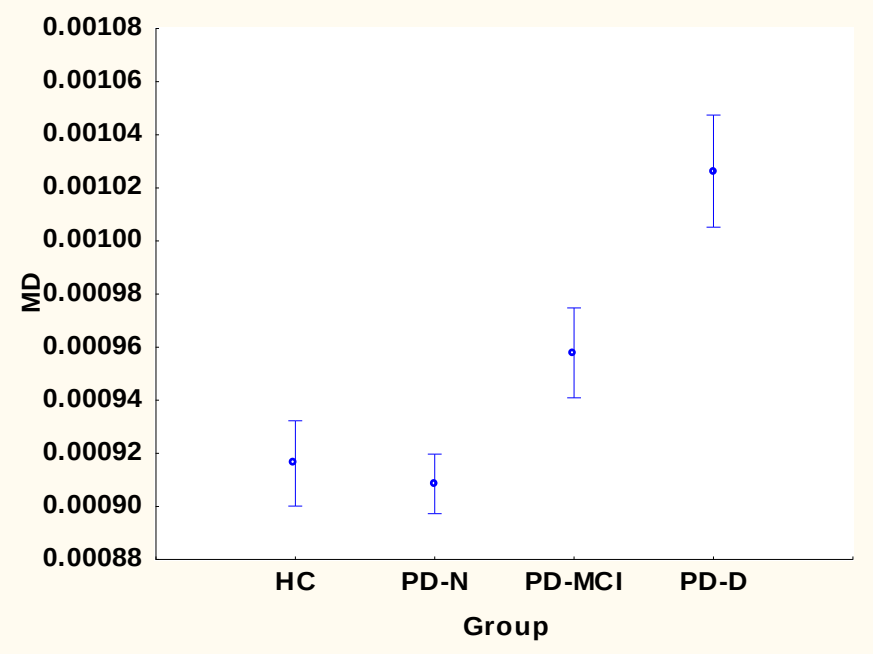

Fig 14B. DMN ANCOVA showing rPCC: Pairwise group differences (N-K): (HC = PD-N = PD-MCI) < PD-D.

Figure 15

Differences between the means (±sem) of the MD of the dMPFC for the four groups controlling for age and education.

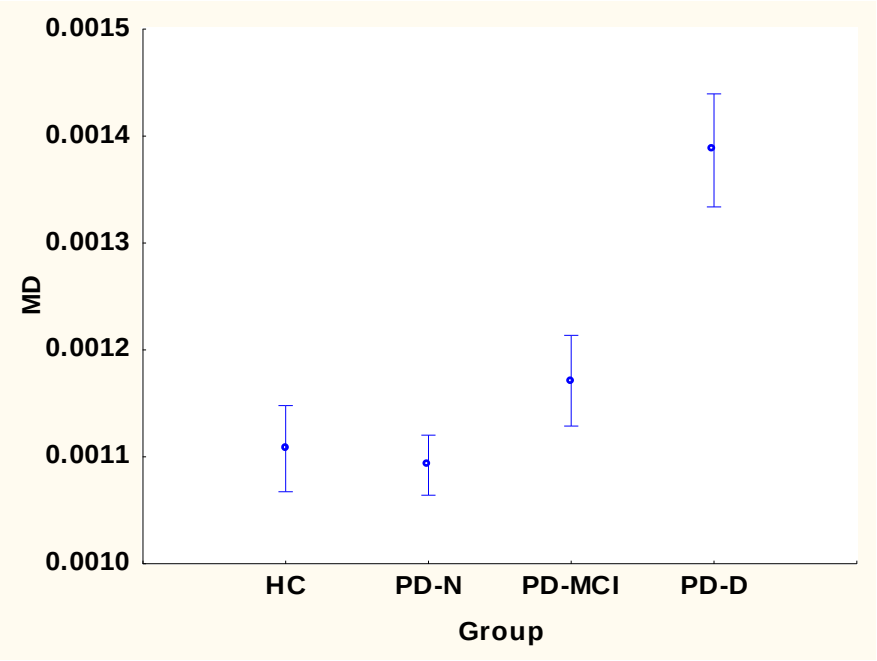

Fig 15A. DMN ANCOVA showing ldMPFC: Pairwise group differences (N-K): (HC = PD-N = PD-MCI) < PD-D.

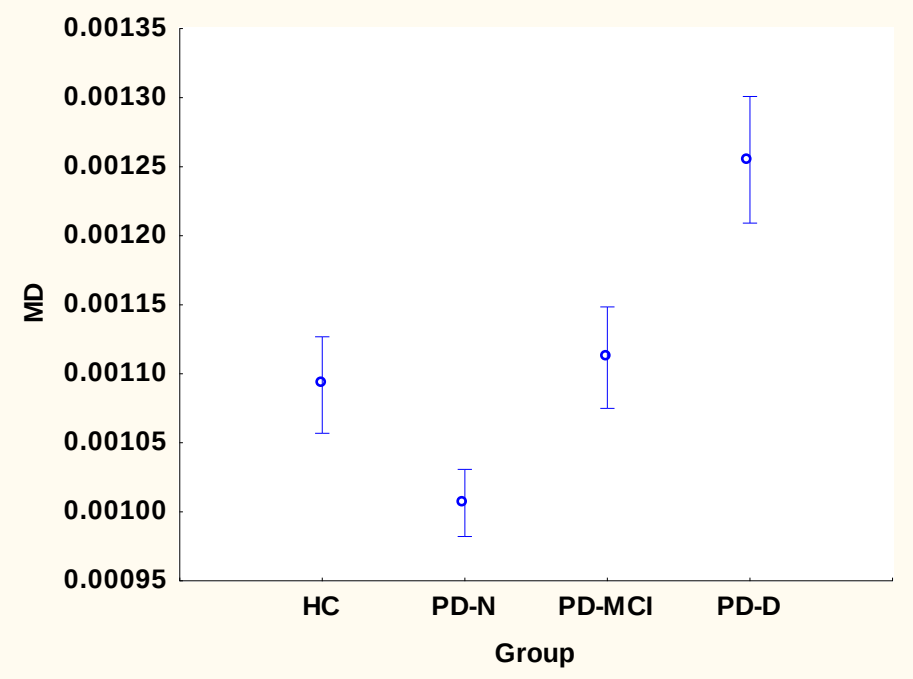

Fig 15B. DMN ANCOVA showing rdMPFC: Pairwise group differences (N-K): (HC = PD-N = PD-MCI) < PD-D.

Figure 16

Differences between the means (±sem) of the MD of the vMPFC for the four groups controlling for age and education.

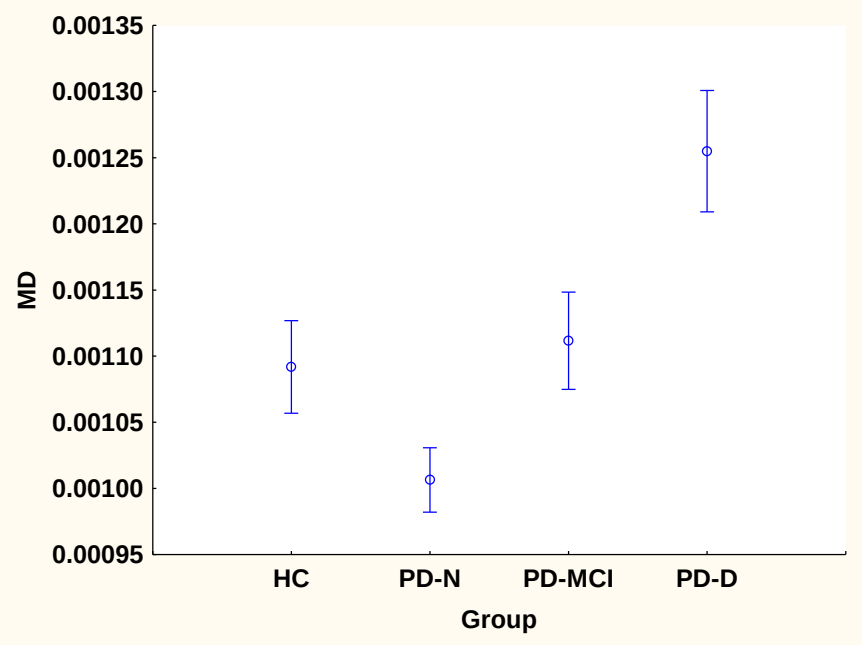

Fig 16A. DMN ANCOVA showing lvMPFC: Pairwise group differences (N-K): (HC = PD-N) < PD-D and PD-MCI not different to any other group.

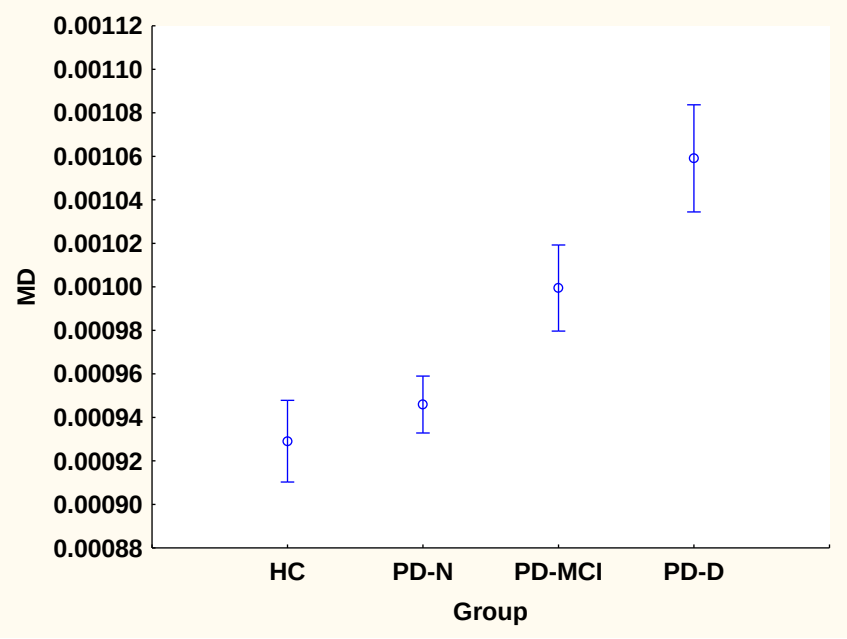

Fig 16B. DMN ANCOVA showing rvMPFC: Pairwise group differences (N-K): (HC = PD-N) and PD-MCI) < PD-D, HC < PD-MCI, and PD-N = PD-MCI.

Figure 17

Differences between the means (±sem) of the MD of the pIPL for the four groups controlling for age and education.

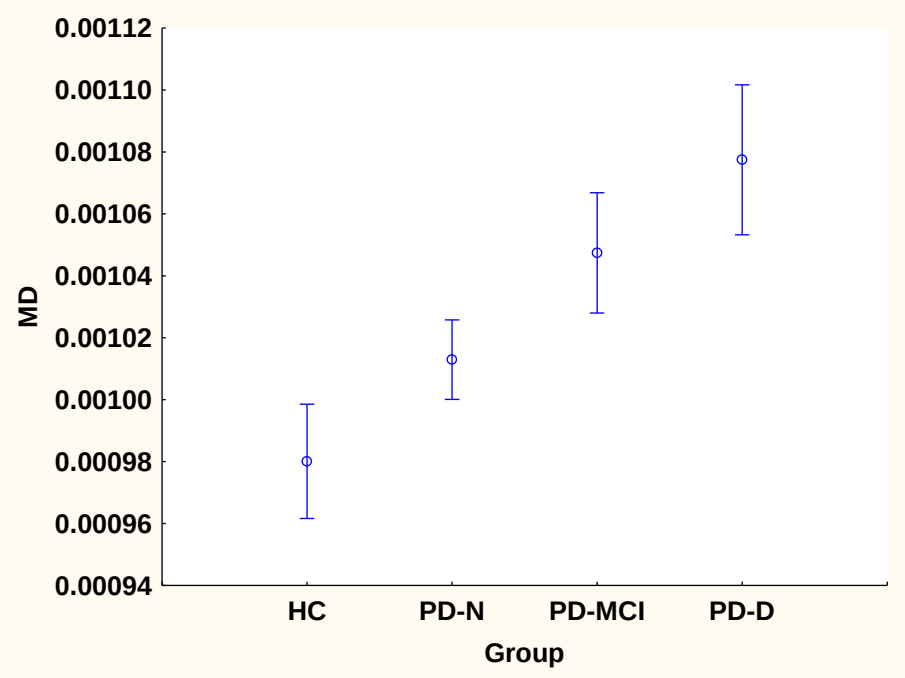

Fig 17A. DMN ANCOVA showing lpIPL: Pairwise group differences (N-K): HC = PD-N, HC < (PD-MCI = PD-D), PD-N = PD-MCI, PD-N < PD-D.

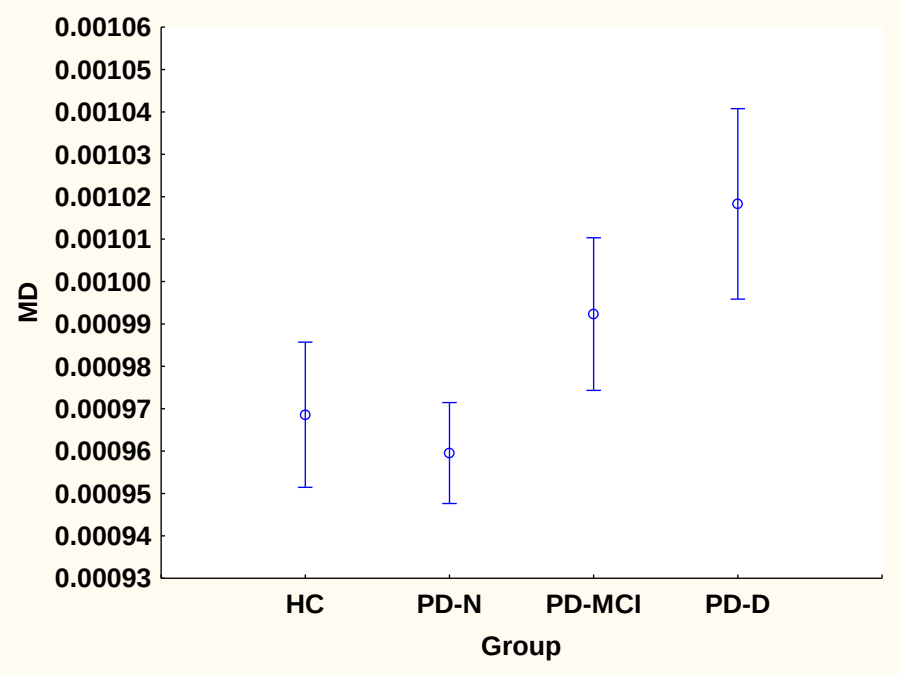

Fig 17B. DMN ANCOVA showing rpIPL: Pairwise group differences (N-K): (HC = PD-N = PD-MCI = PD-D).

Figure 18

Differences between the means (±sem) of the MD of the MTG for the four groups controlling for age and education.

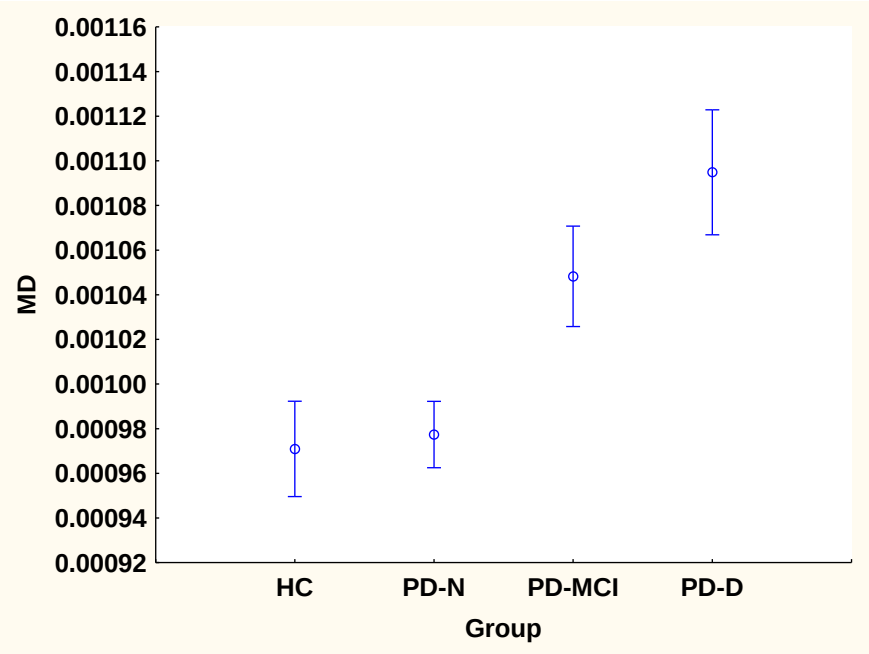

Fig 18A. DMN ANCOVA showing lMTG: Pairwise group differences (N-K): (HC = PD-N) < (PD-MCI = PD-D).

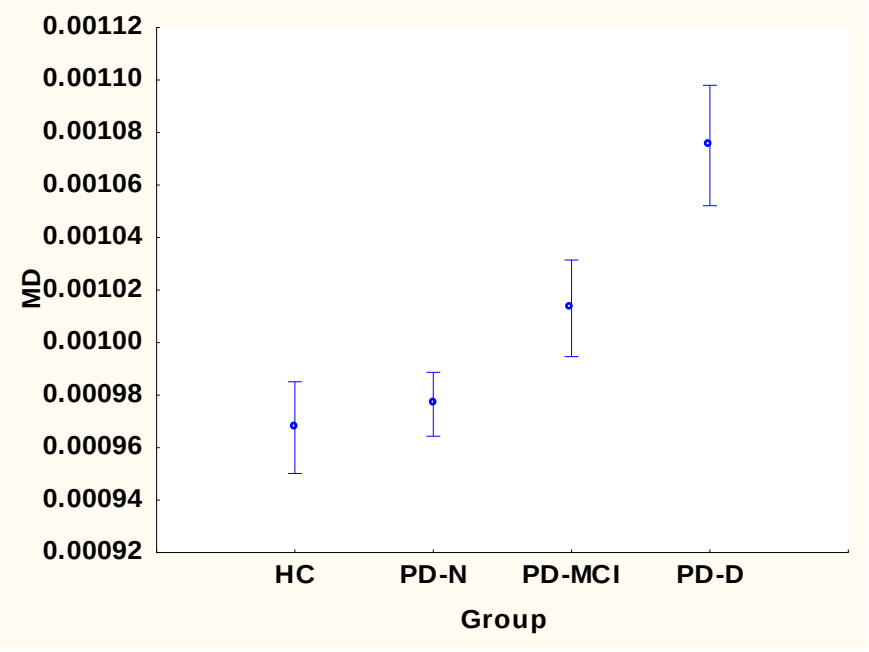

Fig 18B. DMN ANCOVA showing rMTG: Pairwise group differences (N-K): (HC = PD-N = PD-MCI) < PD-D.

Figure 19

Differences between the means (±sem) of the MD of the FEF for the four groups controlling for age and education.

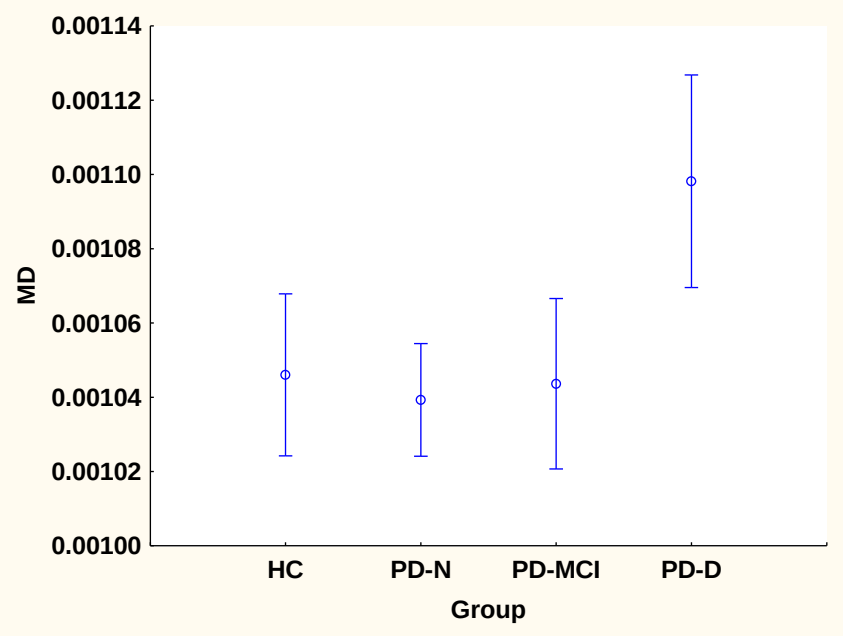

Fig 19A. DAN ANCOVA showing lFEF: Pairwise group differences (N-K): (HC = PD-N = PD-MCI = PD-D).

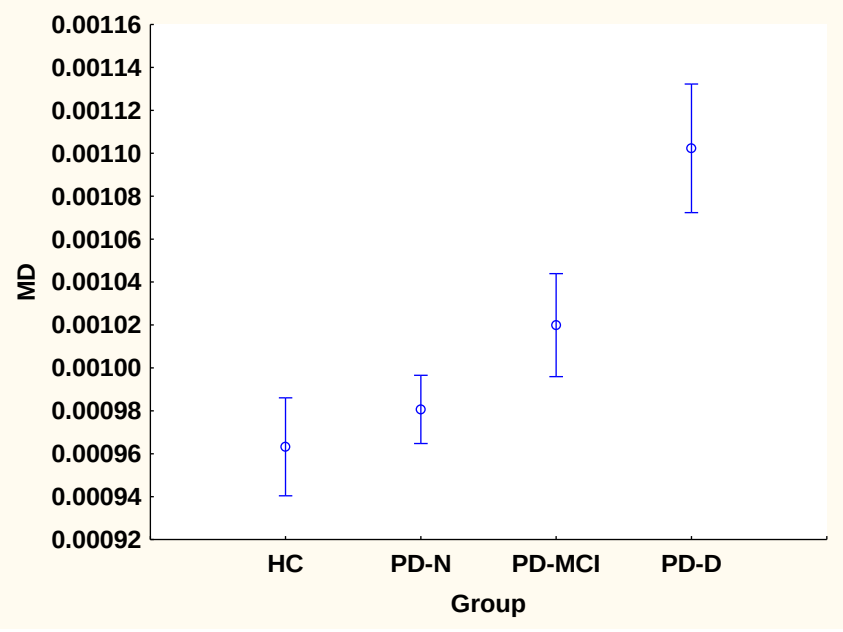

Fig 19B. DAN ANCOVA showing rFEF: Pairwise group differences (N-K): (HC = PD-N = PD-MCI) < PD-D.

Figure 20

Differences between the means (±sem) of the MD of the aIPS for the four groups controlling for age and education.

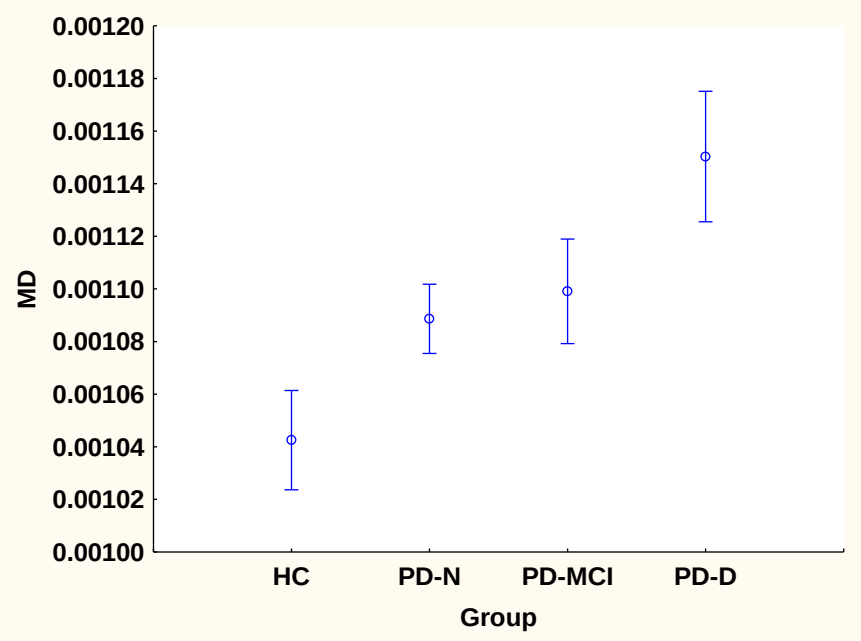

Fig 20A. DAN ANCOVA showing laIPS: Pairwise group differences (N-K): HC = PD-N = PD-MCI, HC < PD-D, (PD-N = PD-MCI = PD-D).

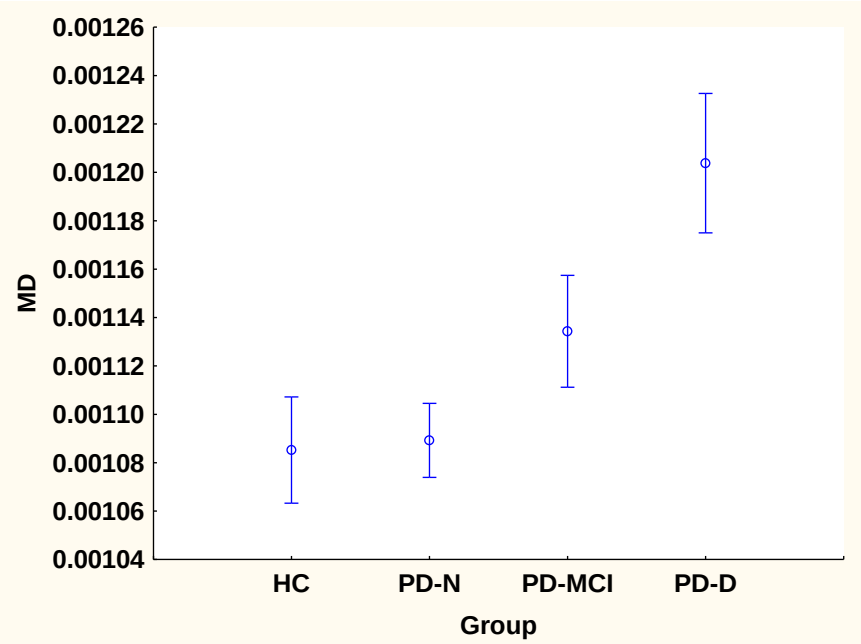

Fig 20B. DAN ANCOVA showing raIPS: Pairwise group differences (N-K): (HC = PD-N = PD-MCI) < PD-D.

Figure 21

Differences between the means (±sem) of the MD of the pIPS for the four groups controlling for age and education.

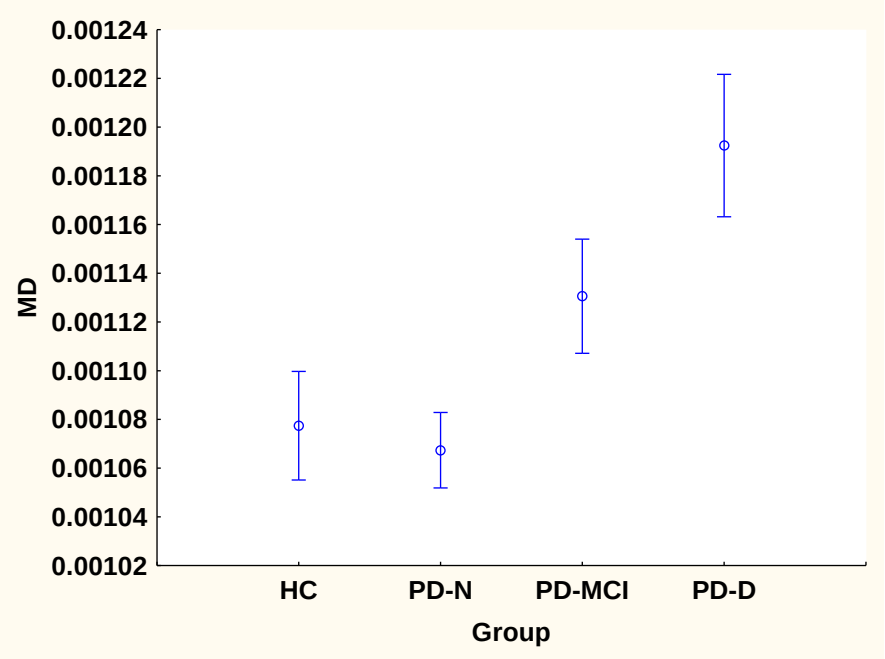

Fig 21A. DAN ANCOVA showing lpIPS: Pairwise group differences (N-K): HC = PD-N = PD-MCI, (HC = PD-N) < PD-D, PD-MCI = PD-D.

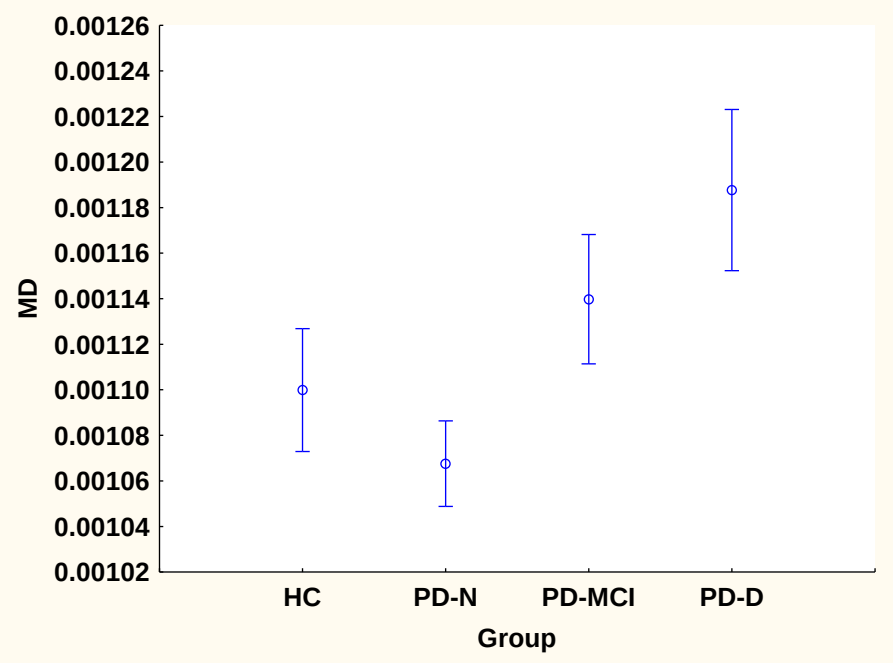

Fig 21B. DAN ANCOVA showing rpIPS: Pairwise group differences (N-K): HC = PD-MCI = PD-D, HC = PD-N, PD-N = PD-MCI, PD-N < PD-D.

Figure 22.

Differences between the means (±sem) of the MD of the MT+ for the four groups controlling for age and education.

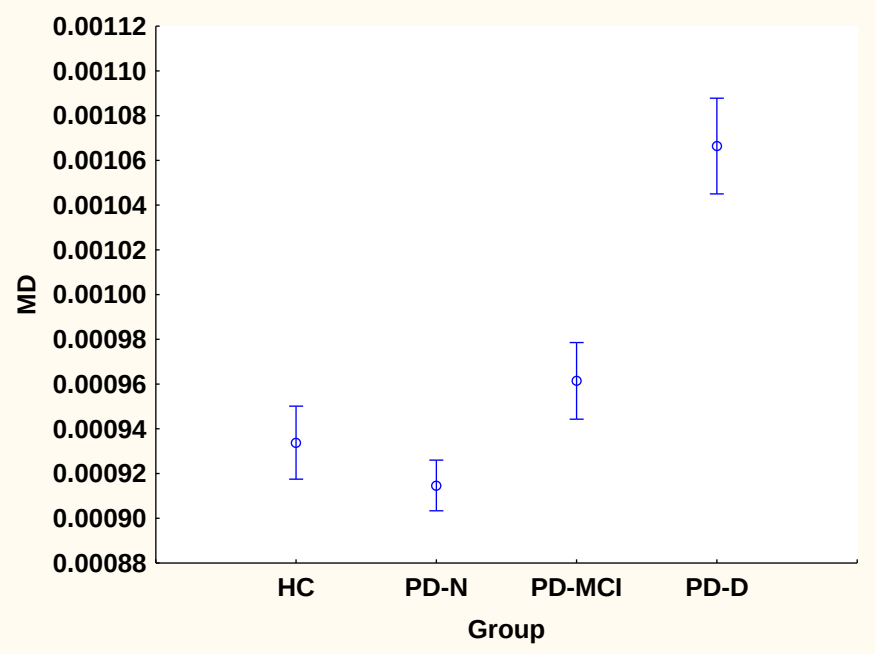

Fig 22A. DAN ANCOVA showing lMT+: Pairwise group differences (N-K): (HC = PD-N = PD-MCI) < PD-D.

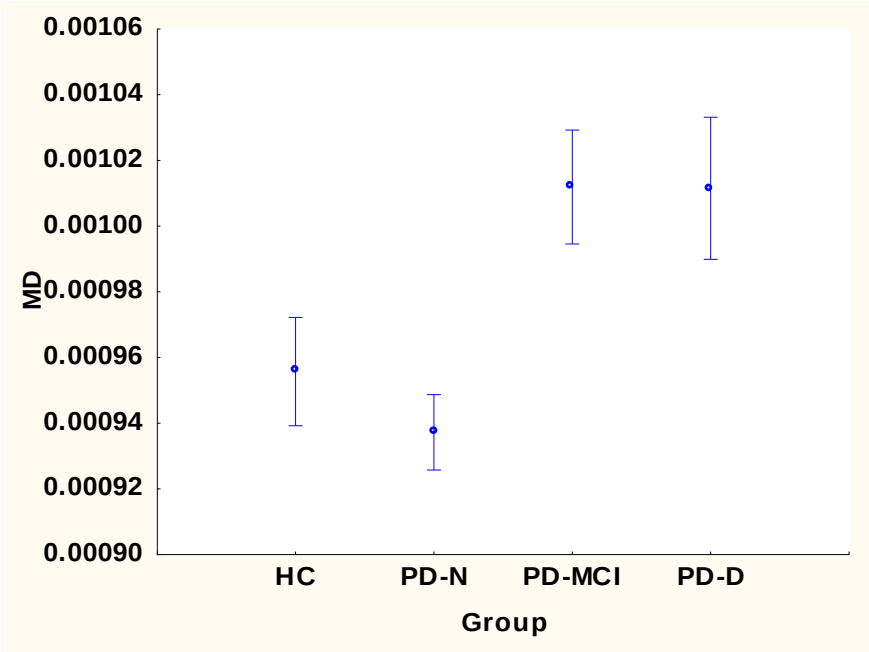

Fig 22B. DAN ANCOVA showing rMT+: Pairwise group differences (N-K): (HC = PD-N) < PD-D, HC = PD-MCI, PD-N <PD-MCI, PD-MCI = PD-D.

Figure 23

Differences between the means (±sem) of the MD of the ACC for the four groups controlling for age and education.

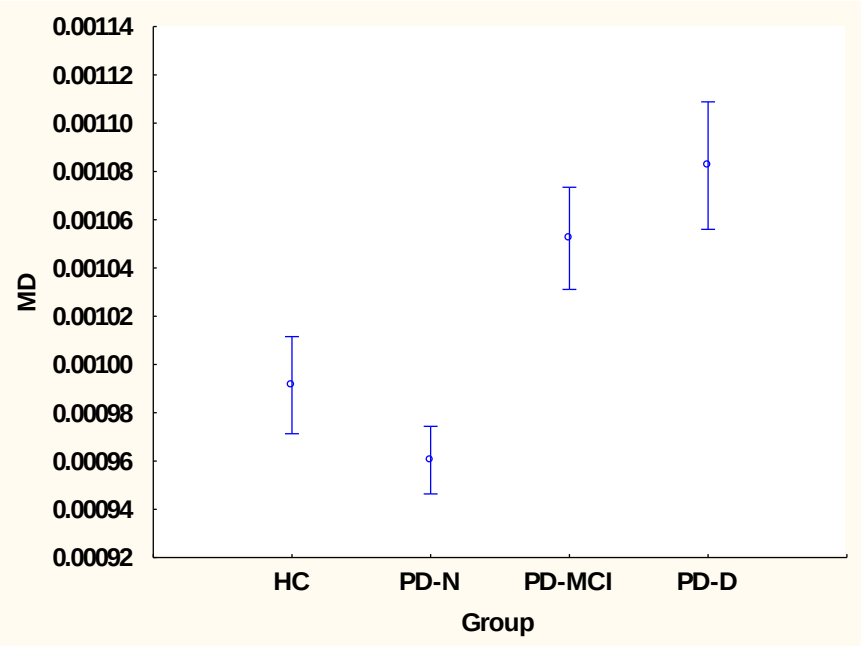

Fig 23A. SN ANCOVA showing lACC: Pairwise group differences (N-K): (HC = PD-N) < (PD-MCI = PD-D)

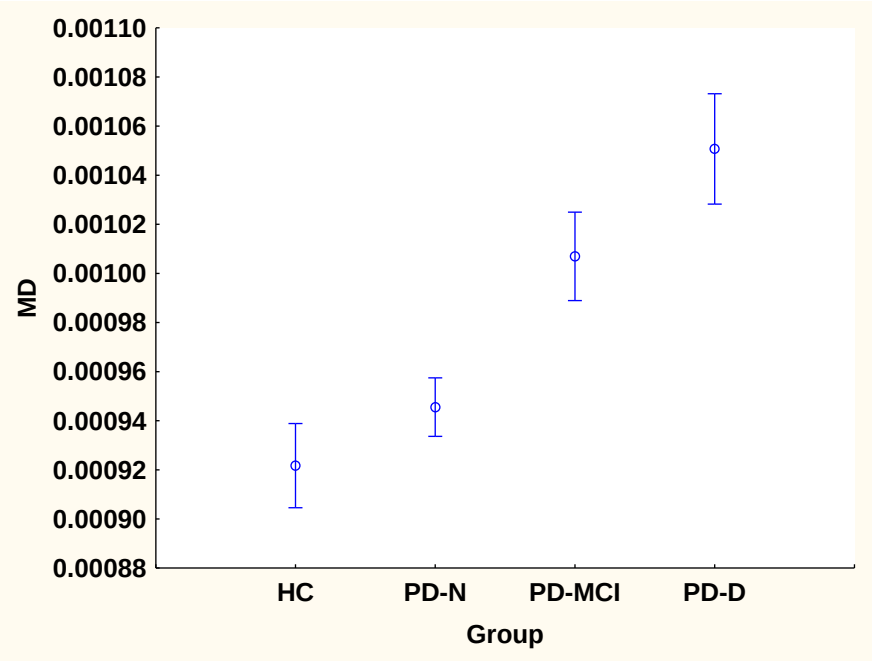

Fig 23B. SN ANCOVA showing rACC: Pairwise group differences (N-K): (HC = PD-N) < (PD-MCI = PD-D).

Figure 24

Differences between the means (±sem) of the MD of the INS for the four groups controlling for age and education.

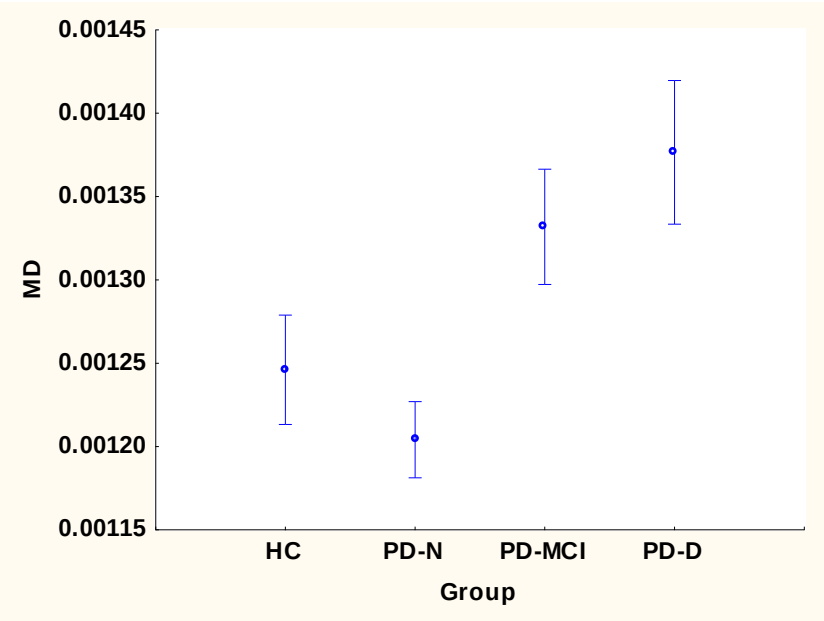

Fig 24A. SN ANCOVA showing lINS: Pairwise group differences (N-K): (HC = PD-N) < PD-D, HC = PD-MCI, PD-N < (PD-MCI = PD-D)

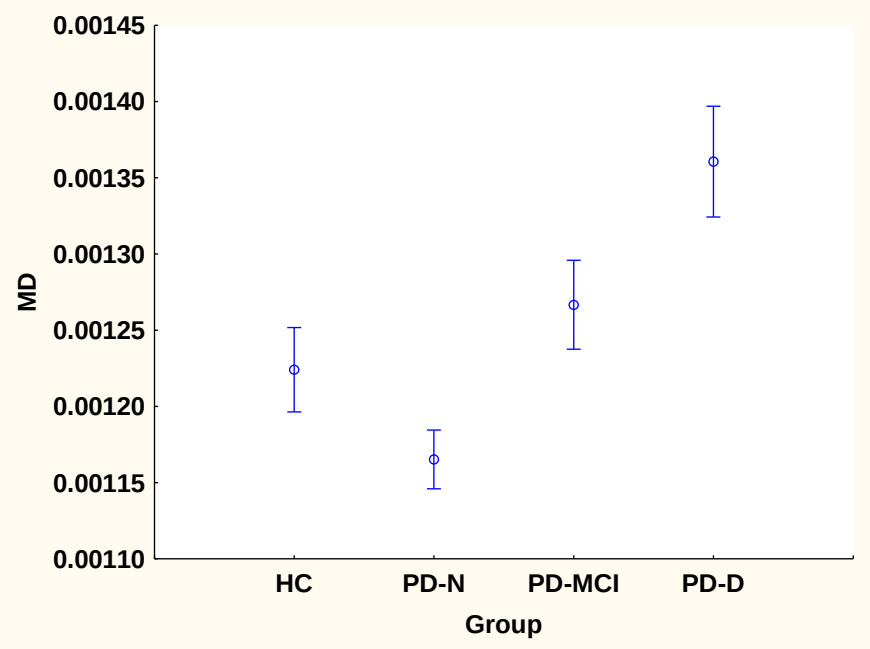

Fig 24B. SN ANCOVA showing rINS: Pairwise group differences (N-K): (HC = PD-N) < PD-D, HC = PD-MCI, PD-N < PD-MCI < PD-D.

Figure 25

Differences between the means (±sem) of the MD of the dlPFC for the four groups controlling for age and education.

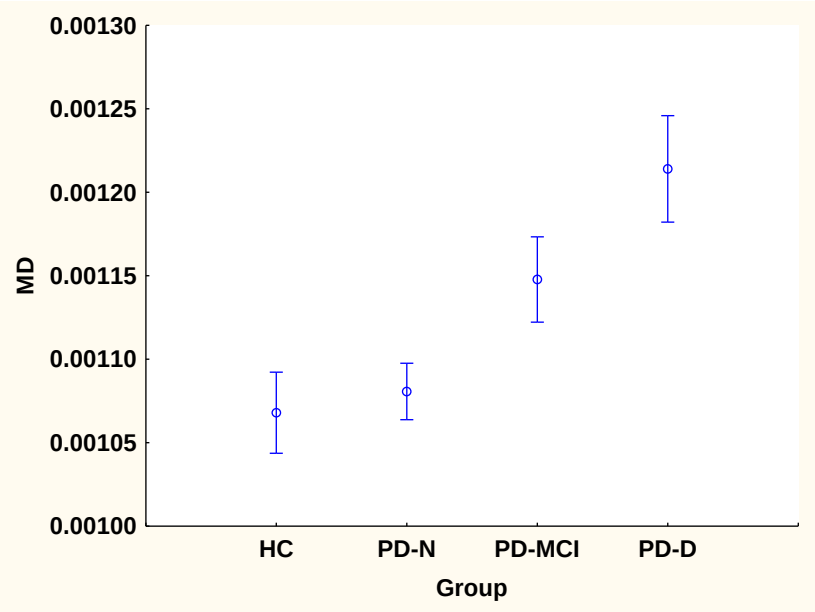

Fig 25A. CEN ANCOVA showing ldlPFC: Pairwise group differences (N-K): (HC = PD-N) < PD-D, HC = PD-N = PD-MCI, PD-MCI = PD-D.

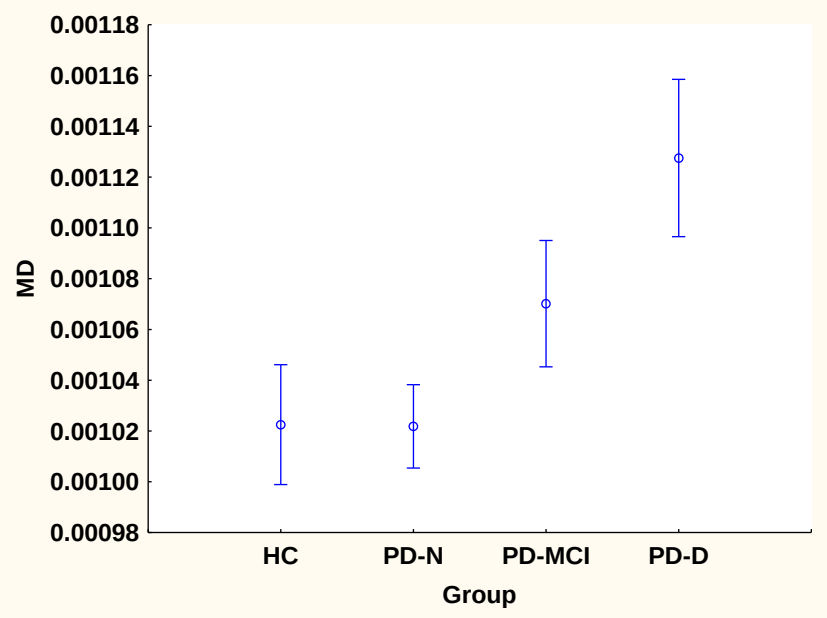

Fig 25B. CEN ANCOVA showing rdlPFC: Pairwise group differences (N-K): (HC = PD-N) < (PD-MCI = PD-D).

Figure 26

Differences between the means (±sem) of the MD of the aIPL for the four groups controlling for age and education.

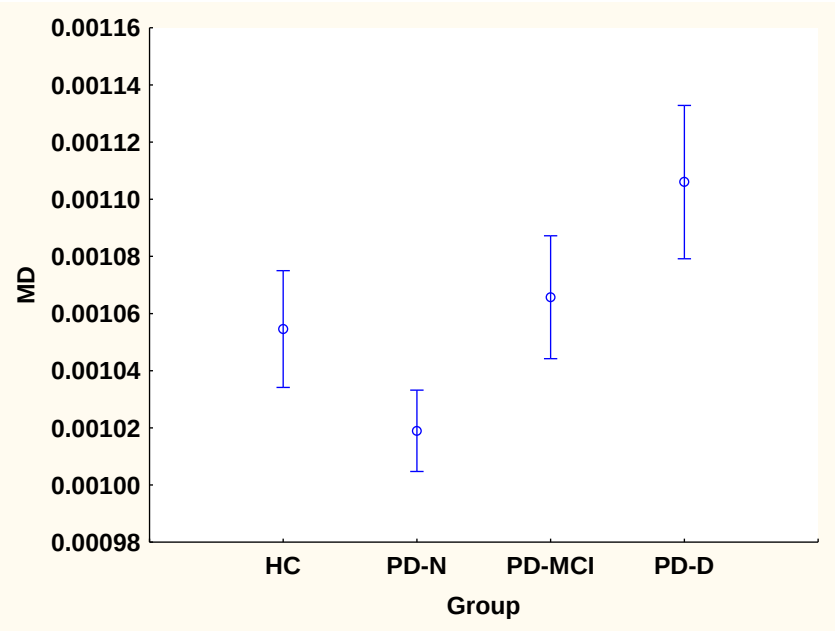

Fig 26A. CEN ANCOVA showing laIPL: Pairwise group differences (N-K): HC = PD-N = PD-MCI, HC < PD-D, PD-N = PD-MCI = PD-D.

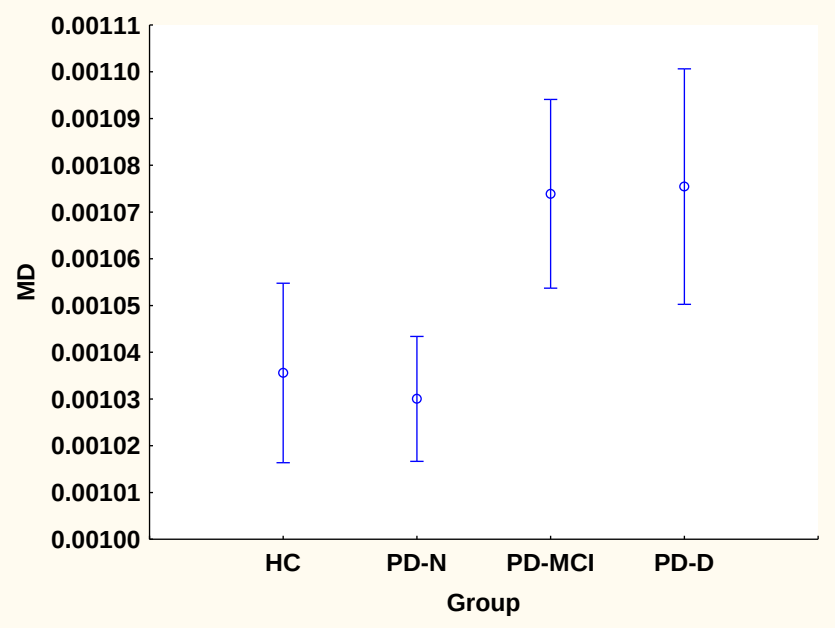

Fig 26B. CEN showing ANCOVA raIPL: Pairwise group differences (N-K): HC = PD-N= PD-MCI = PD-D

As shown in Table 30, age have a significant effect on every ROI except the left ACC of the SN. Education has no effect on any ROI.

In the DMN, significant group main effects were found for both left and right PCC, dMPFC and the MTG, but only for the right vMPFC and left pIPL. Post-hoc Newman-Keuls (N-K) tests showed that the PD-D group had significantly higher MD values than the HC and PD-N groups for each ROI, except the right pIPL. The PD-D group also had significantly higher MD values than the PD-MCI group in most ROIs, except the left vMPFC, left MTG, and both left and right pIPL. The PD-MCI group had significantly higher MD values than the PD-N group in the left PCC and the left MTG, and higher than the HC in the same two regions plus also the right vMPFC and the left pIPL. There were no group differences for right IPL. No significant differences were found for any DMN ROI between the PD-N group and the HC group. To summarise, the PD-D group showed a decline in structural micro-integrity relative to the PD-N and HC groups across all nodes of the DMN, except the right pIPL. The PD-MCI group showed a more selective change, for only a few nodes in the left hemisphere, specifically the left PCC, left vMPFC, left pIPL and left MTG, where they were similar to the PD-D group, although this leftward change was not significantly different to the PD-N and HC group for the left vMPFC and to the PD-N group only for the left pIPL. No differences were found between the PD-N and HC groups for all nodes.

For the DAN, significant group main effects were found for both left and right ROIs for the MT+, right FEF, and left laIPS. Post-hoc N-K tests show that the PD-D group had significantly higher MD values than both the HC and PD-N group for the left and right MT+, right FEF, right aIPS, and left pIPS, higher value than the HC group only for left aIPS, and higher value than the PD-N group only for right pIPS. The PD-D group also had significantly higher MD values than the PD-MCI group for the right FEF, right aIPS, and left MT+. The

PD-MCI group had significantly higher MD values than the PD-N group for the right MT+ only. There were no significant group differences in left FEF. No significant differences were found for any DAN ROI between the PD-MCI group and the HC group or between the PD-N group and HC group. In summary, the PD-D group displayed weaker structural micro-integrity when compared to the PD-N or HC groups across all nodes of the DAN, except the left FEF. The PD-MCI group displayed a more selective change, which was sometimes intermediate between the PD-D group and other groups (left and right pIPS, left aIPS) with a suggestion of change to, right MT+, in particular. There were no deficits in the DAN for the PD-N group compared to the HC group.

In the SN, significant group main effects were found for both left and right ROIs of the ACC and right INS. Post-hoc N-K tests show that the PD-D group had significantly higher MD values than the HC and PD-N group for both left and right ROIs of the ACC and INS. Interestingly, PD-D group and the PD-MCI were similar across three of the four SN nodes, with the PD-MCI group showing better integrity only for the right INS. The PD-MCI group had significantly higher MD values than the HC and PD-N group for both left and right rACC, and higher value than the PD-N group only for both left and right INS. No significant differences were found for between the PD-N group and HC group. To summarise, the PD-D group showed a decline in structural micro-integrity relative to the PD-N and HC groups across all nodes of the SN. The PD-MCI group was generally similar to the PD-D group for the DAN but the right INS showed relative integrity. No differences were found between the HC and PD-N groups for any SN nodes.

For the CEN, significant group main effects were only found for left dlPFC. Post-hoc N-K tests show that the PD-D group had significantly higher MD values than the HC and PD-N group for both left and right dlPFC. The MD values across all nodes for the PD-D group did not significantly differ with the MD values of the nodes for the PD-MCI group. The PD-

MCI group had significantly higher MD values than the HC and PD-N group for the right dlPFC only. There were no group differences in right aIPL. No significant differences were found between the HC and PD-N group. In summary, the PD-D group displayed weaker structural micro-integrity relative to the PD-N or HC groups for the dlPFC of the CEN, but relatively little change in the aIPL. The PD-MCI group showed an intermediate change for the dlPFC. Again, the PD-N and HC groups showed comparable MD values for the CEN.

3.2 ANCOVA FA

ANCOVA (with age and education as covariates) followed by Newman-Keuls post-hoc comparison tests were performed on the mean FA values for each participant group for each ROI in a particular ROI for each RSN.

The ANCOVA for the group main effects for FA in the left and right ROIs of the four networks are summarized on Table 31 and the mean values for the four participant groups for each ROI in every RSN are shown in Figure 27 to Figure 39. The Newman-Keuls Test tables are presented in the Appendix.

Table 31

FA: Group main effect for the ANCOVA for each ROI for the four cognitive networks

	dlPFC		aIPL							
CEN	Left	Right	Left	Right						
	F (3,135) = 1.84, p = .1	F (3,135) = 37, p=.8	F (3,135) = 2.13, p=.1	F (3,135) = 1.3, p=.3						
SN	ACC		INS							
	Left	Right	Left	Right						
	F (3,135) = 2.36, p=.1	F (3,135) = 1.98, p=.1	**F (3,135) = 4.34, p<.01**	F (3,135) = .87, p=.5						
DAN	FEF		aIPS		pIPS		MT+			
	Left	Right	Left	Right	Left	Right	Left	Right		
	F (3,135) = 4.23, p <.01	F (3,135) = .41, p=.8	F (3,135) = 2.05, p=.1	F (3,135) = .89, p=.5	F (3,135) = .67, p=.6	F (3,135) = .93, p=.5	F (3,135) = .62, p=.6	F (3,135) = 1.24, p=.3		
DMN	PCC		dMPFC		vMPFC		pIPL		MTG	
	Left	Right	Left	Right	Left	Right	Left	Right	Left	Right
	F (3,135) = 3.20, p <.03	F (3,135) = 1.52, p=.2	F (3,135) = .24, p=.9	F (3,135) = 1.16, p=.3	F (3,135) = 1.69, p=.2	F (3,135) = 1.73, p=.2	F (3,135) = .85, p=.5	F (3,135) = .1, p=.96	F (3,135) = .2, p=.9	F (3,135) = .13, p=.9

All bolded F-ratios are significant. Age and education of participants were used as co-variates; age was not significant for all ROIs ($p<0.05$), except right pIPL of the DMN; education was not significant for any ROI except right INS of the SN and left pIPS of the DAN. For abbreviations, see Table 5.

Figure 27

Differences between the means (±sem) of the FA of the PCC for the four groups controlling for age and education.

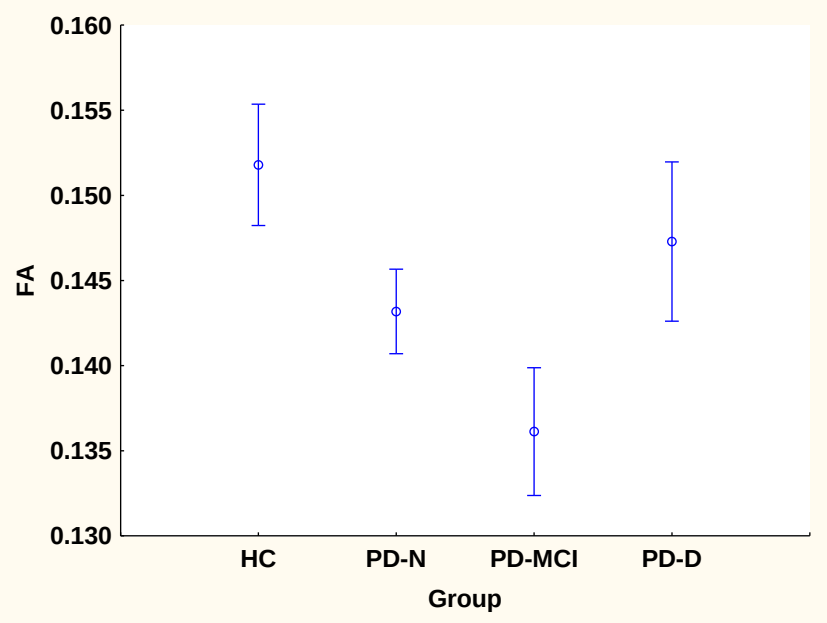

Fig 27A. DMN showing ANCOVA of lPCC: Pairwise group differences (N-K): HC = PD-N = PD-D, HC <PD-MCI, PD-N = PD-MCI = PD-D.

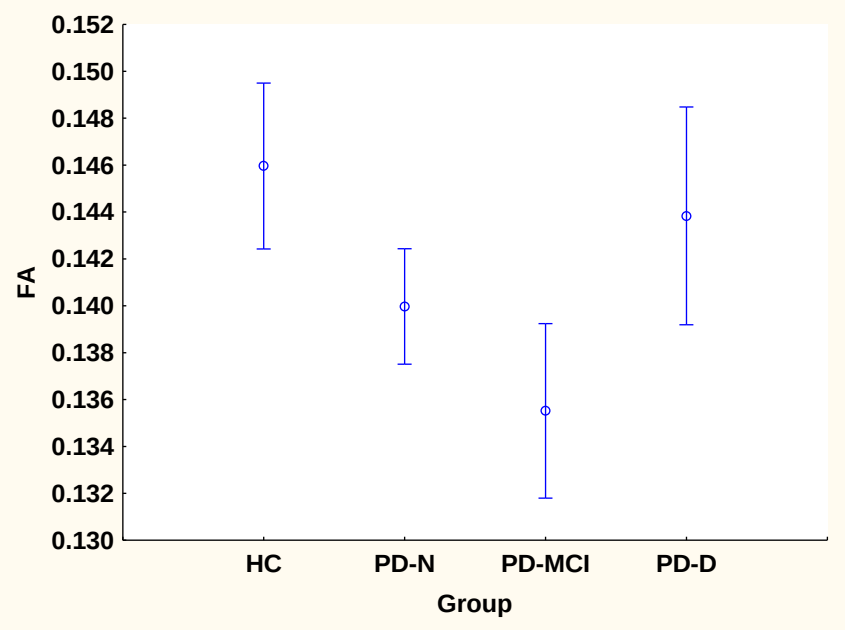

Fig 27B. DMN showing ANCOVA of rPCC: Pairwise group differences (N-K): (HC = PD-N = PD-MCI = PD-D).

Figure 28

Differences between the means (±sem) of the FA of the dMPFC for the four groups controlling for age and education.

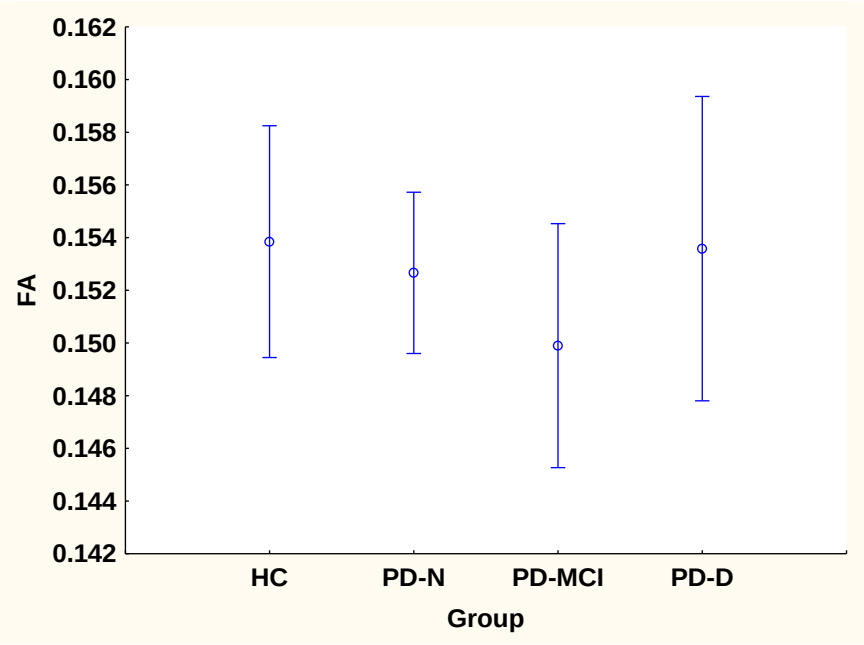

Fig 28A. DMN showing ANCOVA of ldMPFC: Pairwise group differences (N-K): (HC = PD-N = PD-MCI = PD-D).

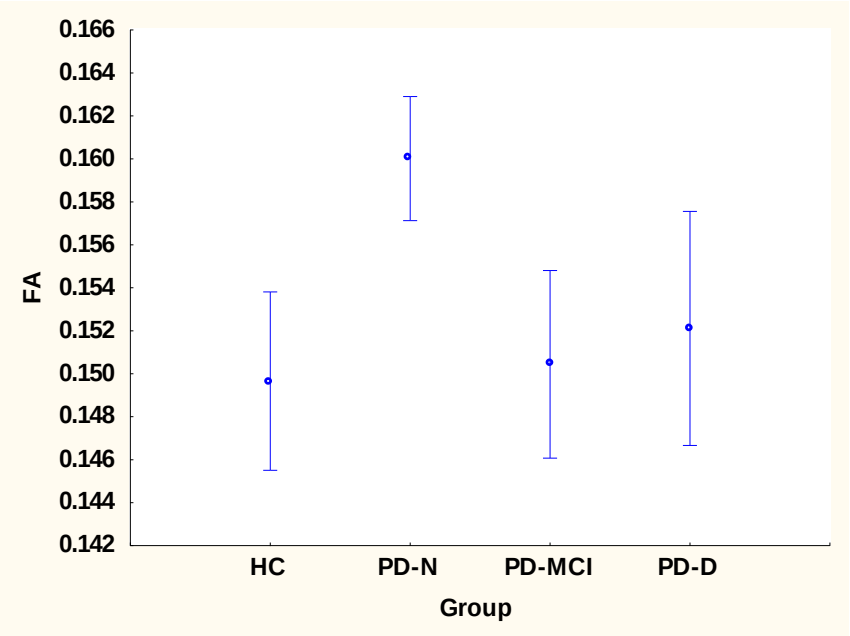

Fig 28B. DMN ANCOVA showing rdMPFC: Pairwise group differences (N-K): (HC = PD-N = PD-MCI = PD-D).

Figure 29

Differences between the means (±sem) of the FA of the vMPFC for the four groups controlling for age and education.

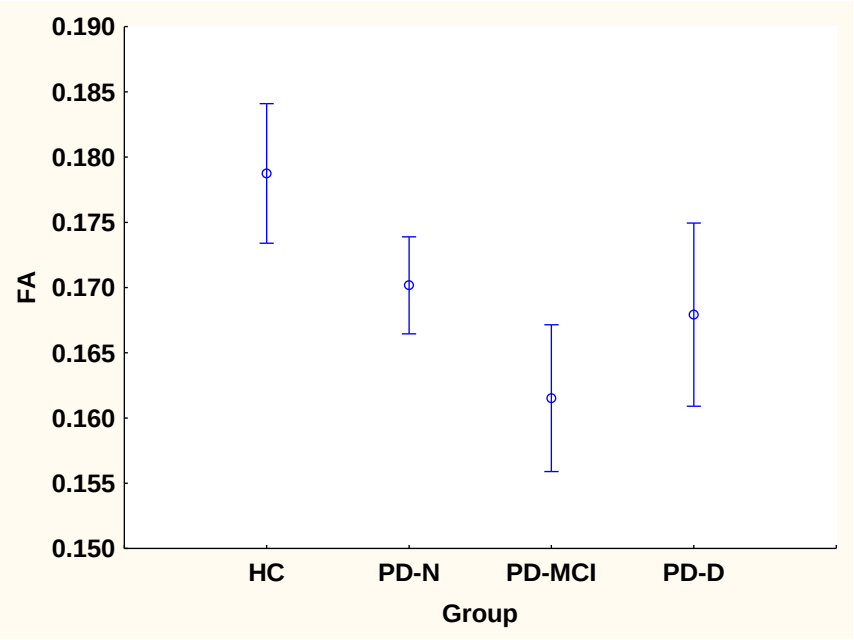

Fig 29A. DMN ANCOVA showing lvMPFC: Pairwise group differences (N-K): (HC = PD-N = PD-MCI = PD-D).

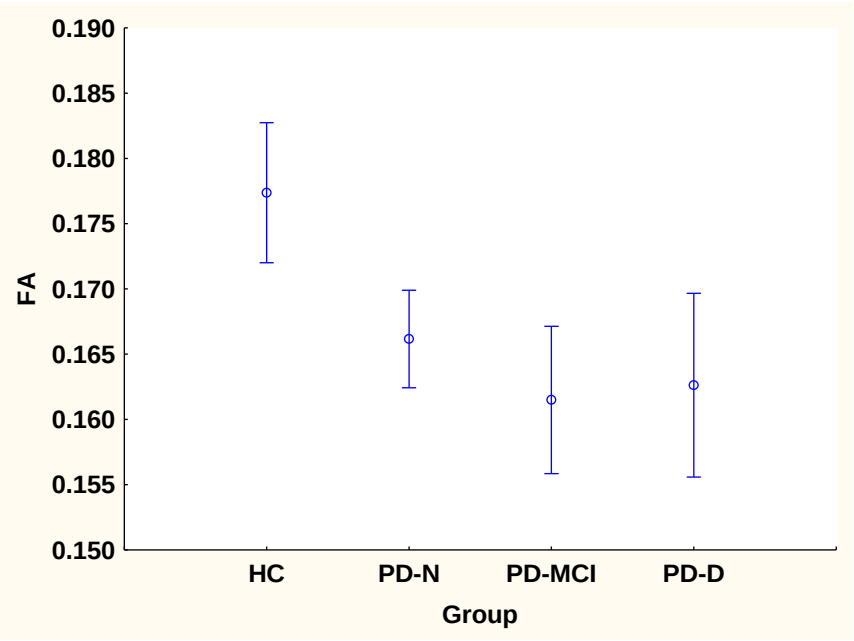

Fig 29B. DMN ANCOVA showing rvMPFC: Pairwise group differences (N-K): (HC = PD-N = PD-MCI = PD-D).

Figure 30

Differences between the means (±sem) of the FA of the pIPL for the four groups controlling for age and education.

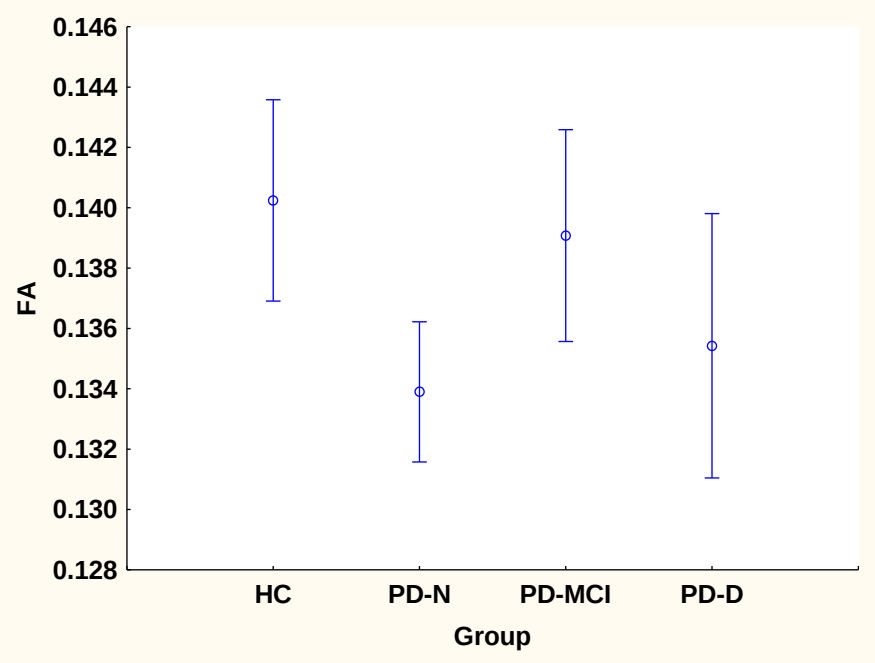

Fig 30A. DMN ANCOVA showing lpIPL: Pairwise group differences (N-K): (HC = PD-N = PD-MCI = PD-D).

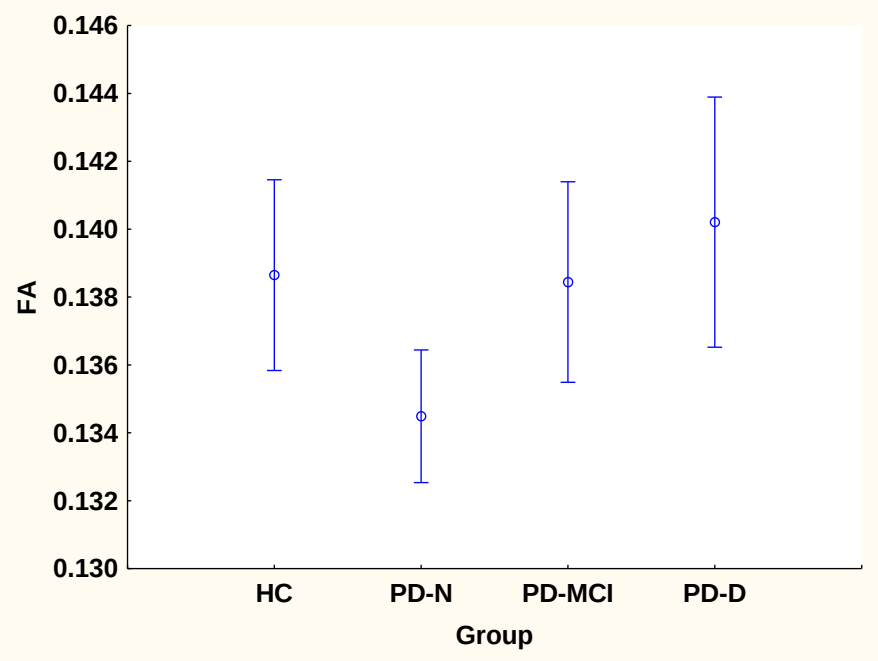

Fig 30B. DMN - rpIPL: Pairwise group differences (N-K): (HC = PD-N = PD-MCI = PD-D).

Figure 31

Differences between the means (±sem) of the FA of the MTG for the four groups controlling for age and education.

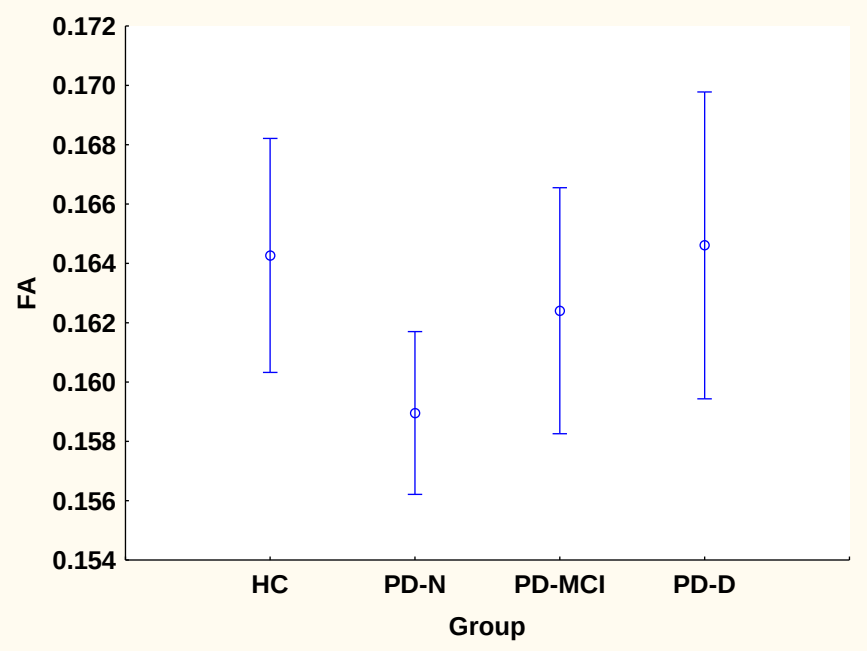

Fig 31A. DMN ANCOVA showing lMTG: Pairwise group differences (N-K): (HC = PD-N = PD-MCI = PD-D).

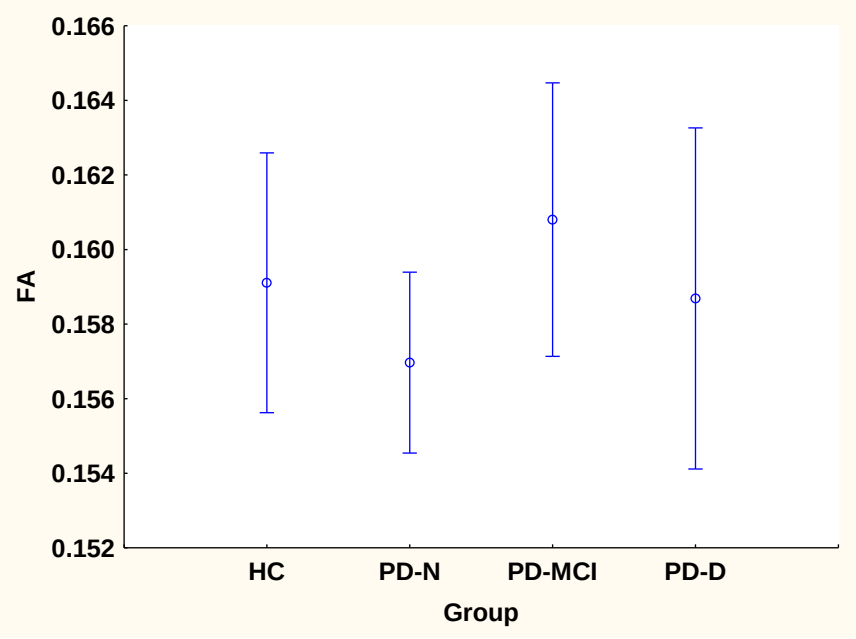

Fig 31B. DMN showing ANCOVA rMTG: Pairwise group differences (N-K): (HC = PD-N = PD-MCI = PD-D).

Figure 32

Differences between the means (+sem) of the FA of the FEF for the four groups controlling for age and education.

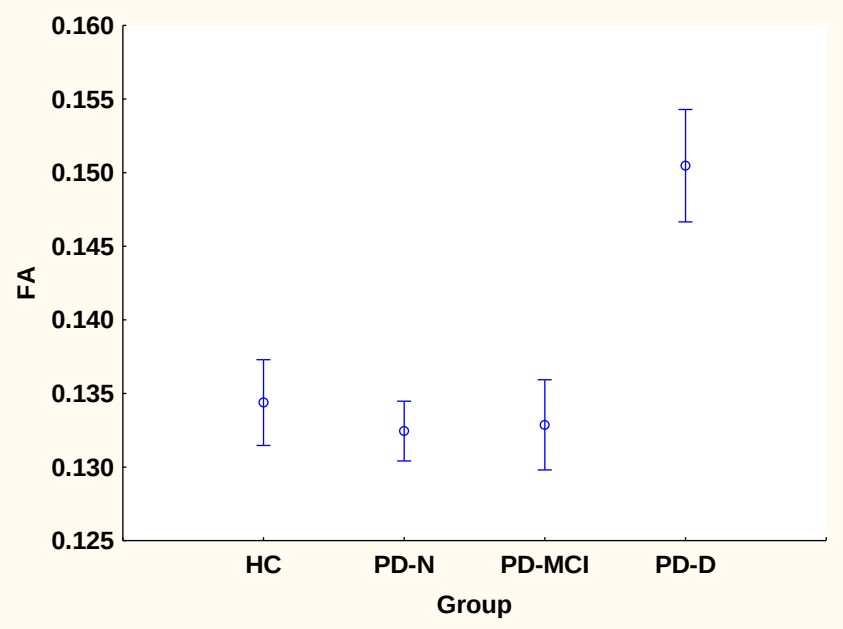

Fig 32A. DAN showing ANCOVA lFEF: Pairwise group differences (N-K): (HC = PD-N = PD-MCI) < PD-D.

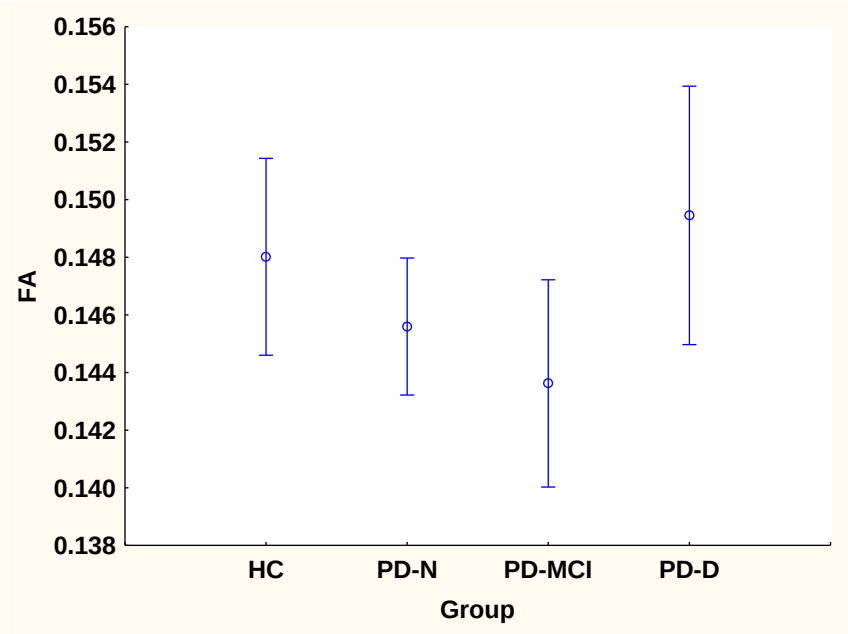

Fig 32B. DAN ANCOVA showing rFEF: Pairwise group differences (N-K): (HC = PD-N = PD-MCI = PD-D).

Figure 33

Differences between the means (+sem) of the FA of the aIPS for the four groups controlling for age and education.

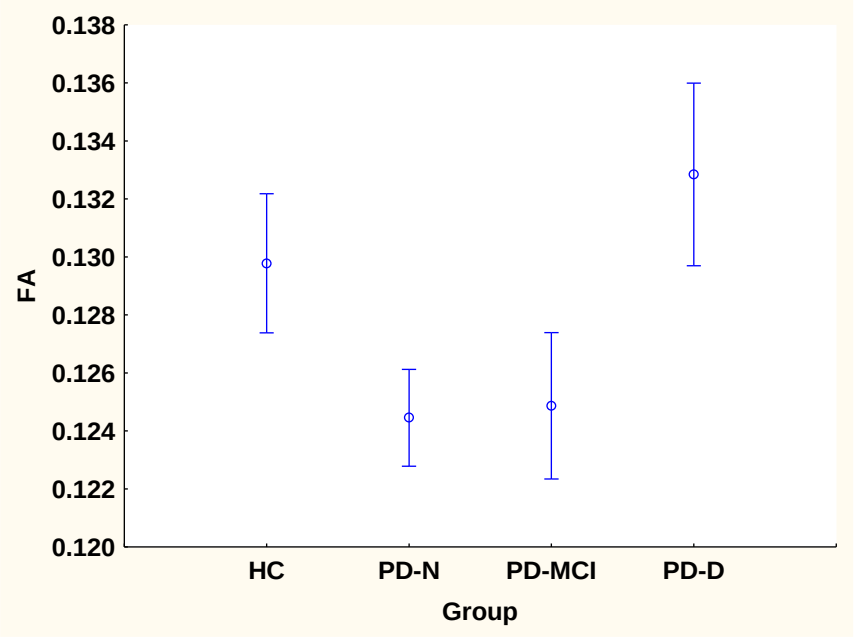

Fig 33A. DAN ANCOVA showing laIPS: Pairwise group differences (N-K): (HC = PD-N = PD-MCI = PD-D).

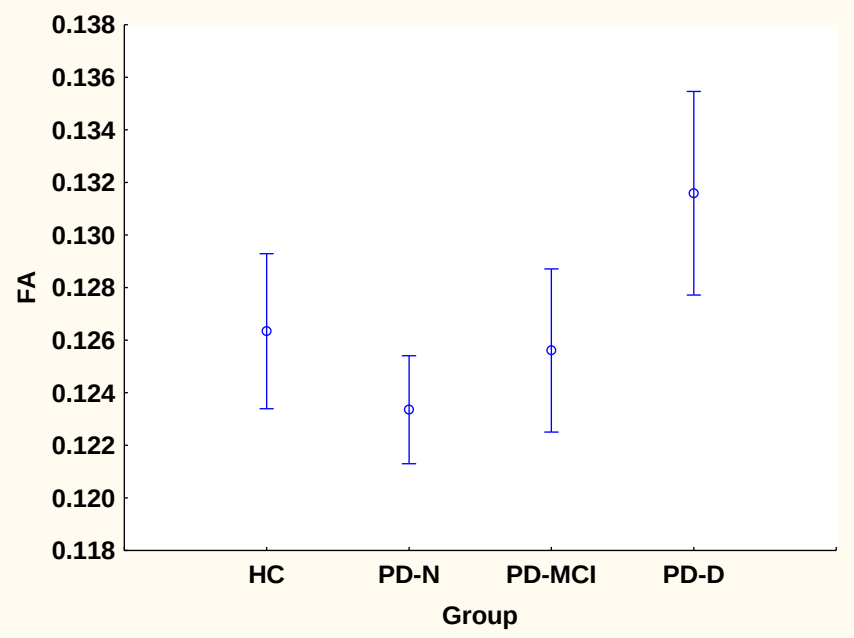

Fig 33B. DAN ANCOVA showing raIPS: Pairwise group differences (N-K): (HC = PD-N = PD-MCI = PD-D).

Figure 34

Differences between the means (+sem) of the FA of the pIPS for the four groups controlling for age and education.

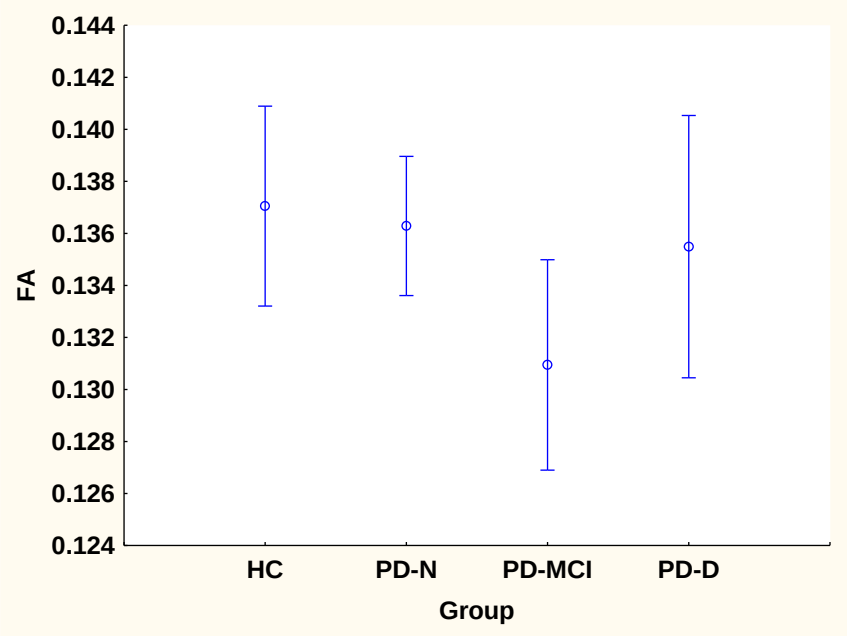

Fig 34A. DAN ANCOVA showing lpIPS: Pairwise group differences (N-K): (HC = PD-N = PD-MCI = PD-D).

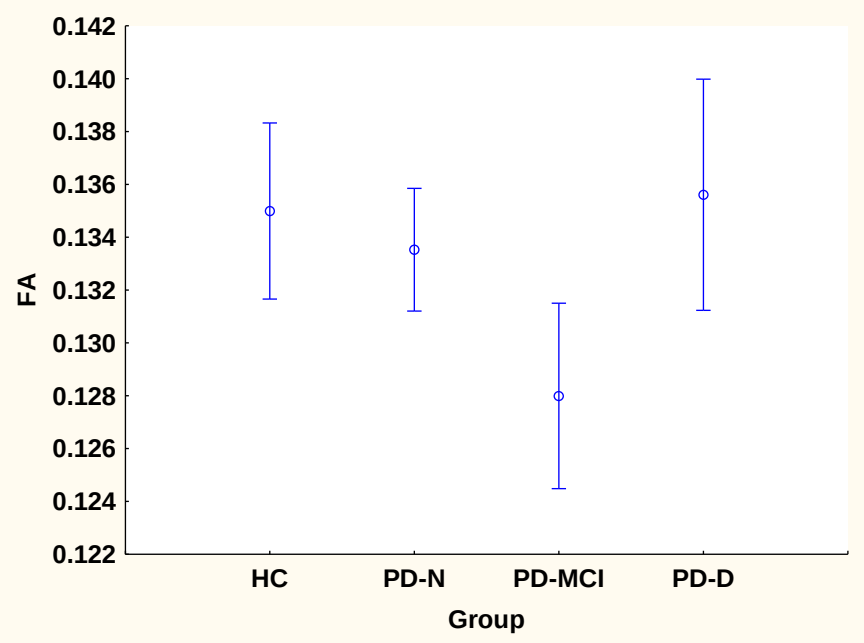

Fig 34B. DAN ANCOVA showing rpIPS: Adjacent pairwise group differences (N-K): (HC = PD-N = PD-MCI = PD-D).

Figure 35

Differences between the means (+sem) of the FA of the MT+ for the four groups controlling for age and education.

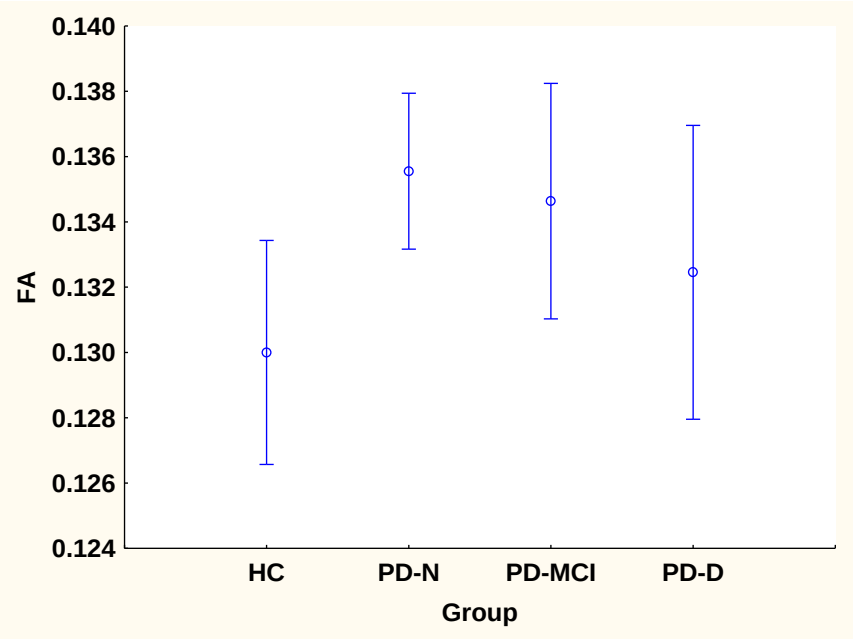

Fig 35A. DAN ANCOVA showing lMT+: Pairwise group differences (N-K): (HC = PD-N = PD-MCI = PD-D).

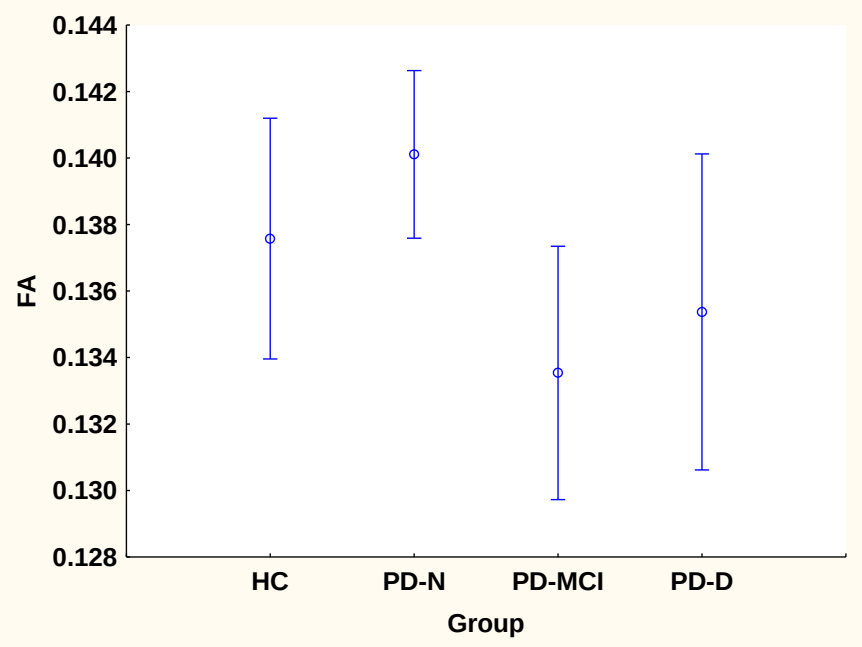

Fig 35B. DAN ANCOVA showing rMT+: Pairwise group differences (N-K): (HC = PD-N = PD-MCI = PD-D).

Figure 36

Differences between the means (+sem) of the FA of the ACC for the four groups controlling for age and education.

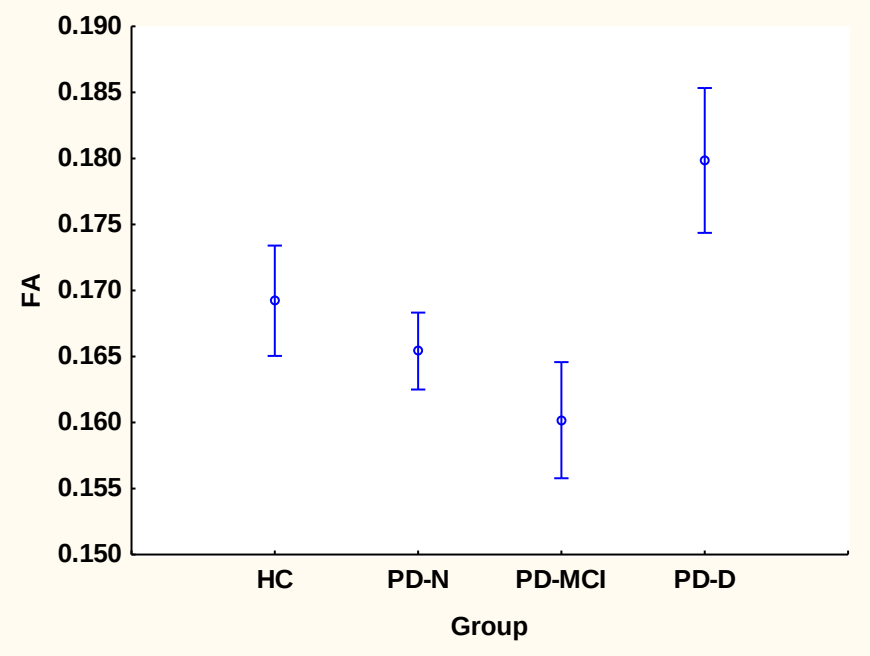

Fig 36A. SN ANCOVA showing lACC: Pairwise group differences (N-K): HC = PD-N = PD-MCI, (PD-N = PD-MCI) < PD-D.

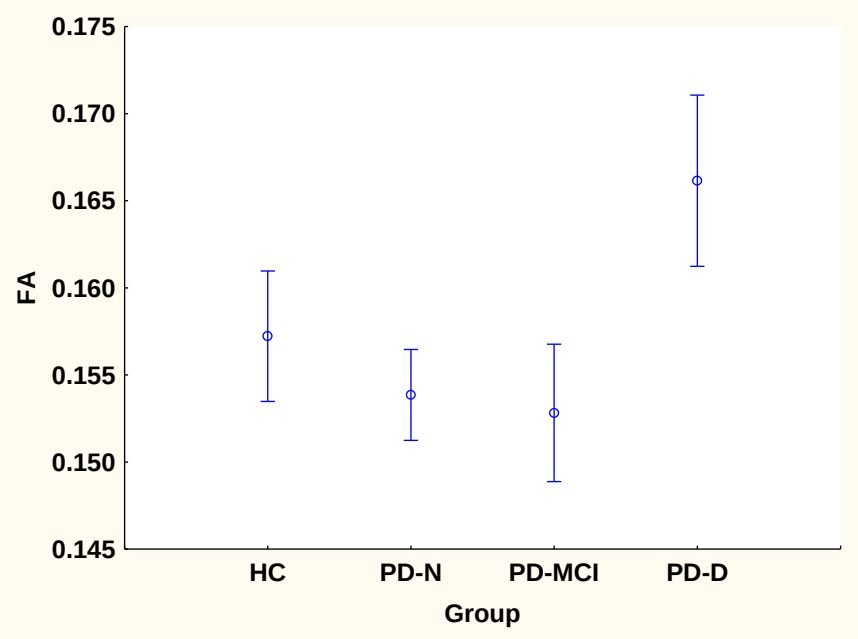

Fig 36B. SN ANCOVA showing rACC: Pairwise group differences (N-K): (HC = PD-N = PD-MCI = PD-D).

Figure 37

Differences between the means (+sem) of the FA of the INS for the four groups controlling for age and education.

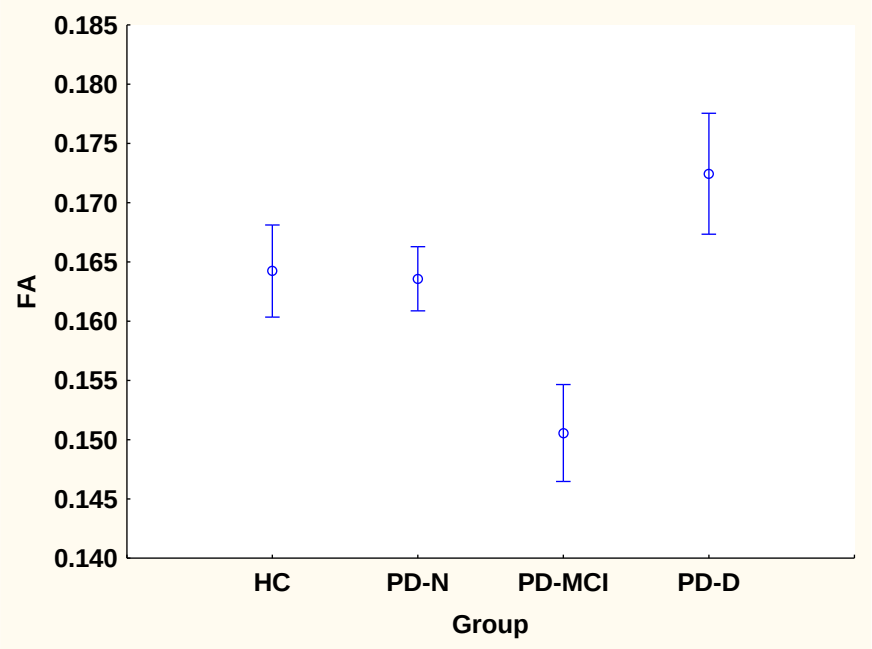

Fig 37A. SN ANCOVA showing lINS: Pairwise group differences (N-K): (HC = PD-N) < PD-D, (HC = PD-N) < PD-MCI, PD-MCI < PD-D.

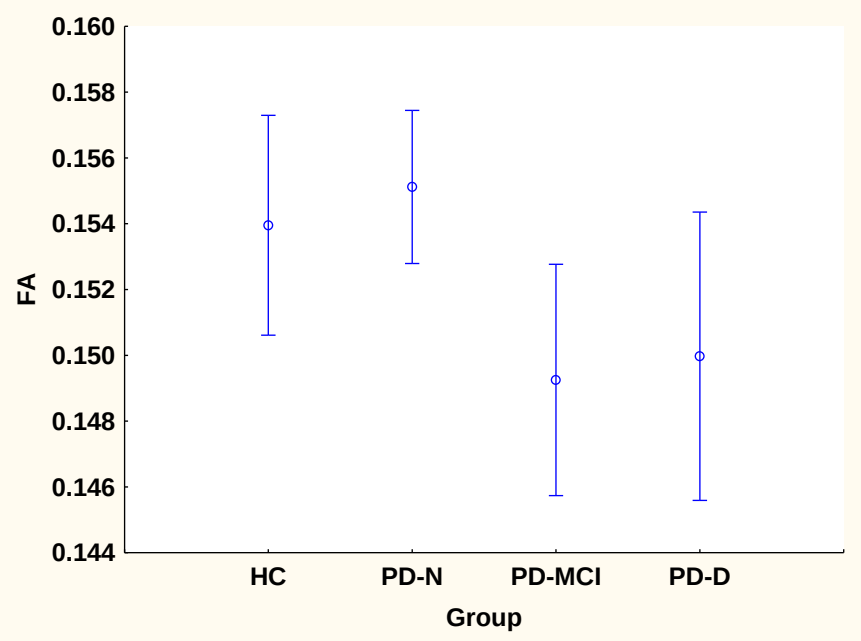

Fig 37B. SN ANCOVA showing rINS: Pairwise group differences (N-K): (HC = PD-N = PD-MCI = PD-D).

Figure 38

Differences between the means (+sem) of the FA of the dlPFC for the four groups controlling for age and education.

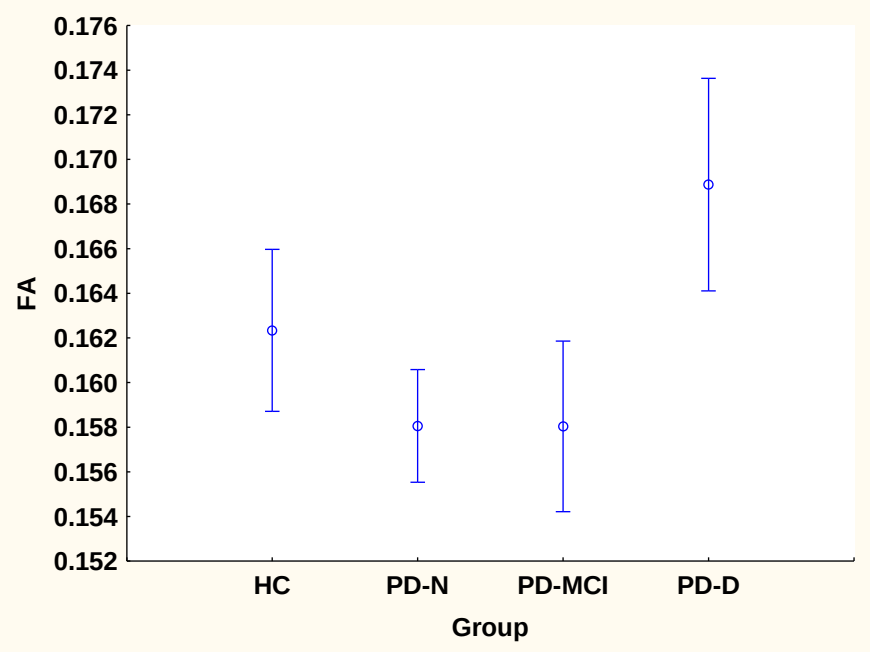

Fig 38A. CEN ANCOVA showing ldlPFC: Pairwise group differences (N-K): (HC = PD-N = PD-MCI = PD-D).

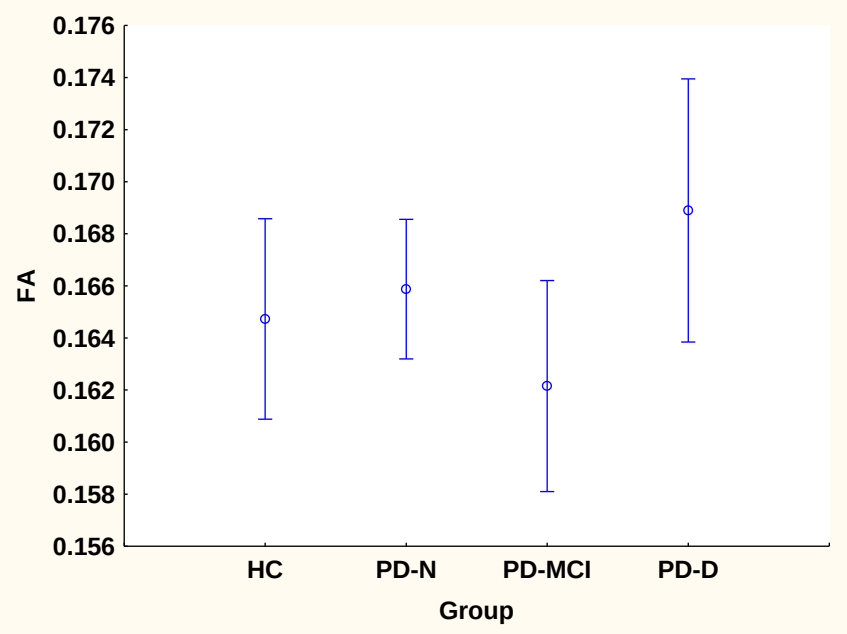

Fig 38B. CEN ANCOVA showing rdlPFC: Pairwise group differences (N-K): (HC = PD-N = PD-D = PD-MCI).

Figure 39

Differences between the means (+sem) of the FA of the aIPL for the four groups controlling for age and education.

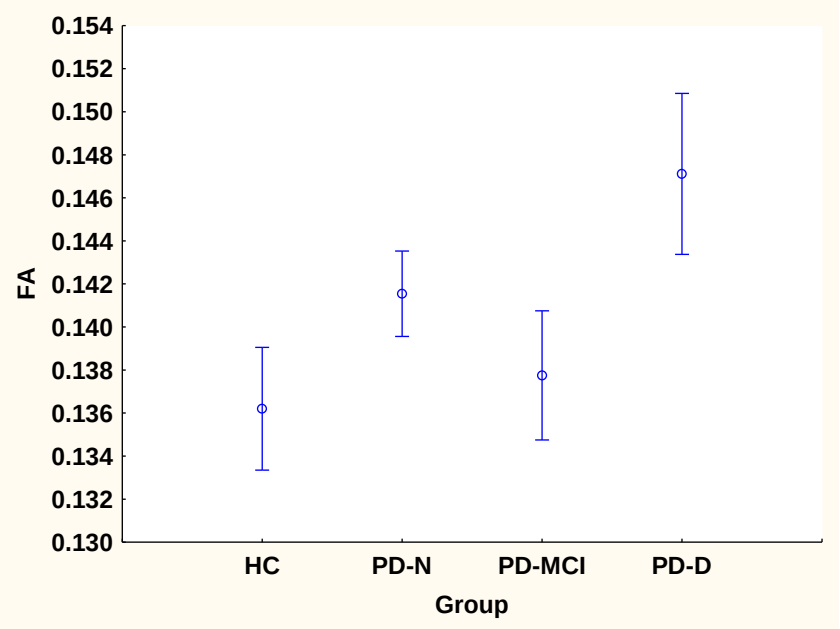

Fig 39A. CEN ANCOVA showing laIPL: Pairwise group differences (N-K): (HC = PD-N) < PD-D, (HC = PD-N = PD-MCI), PD-MCI < PD-D.

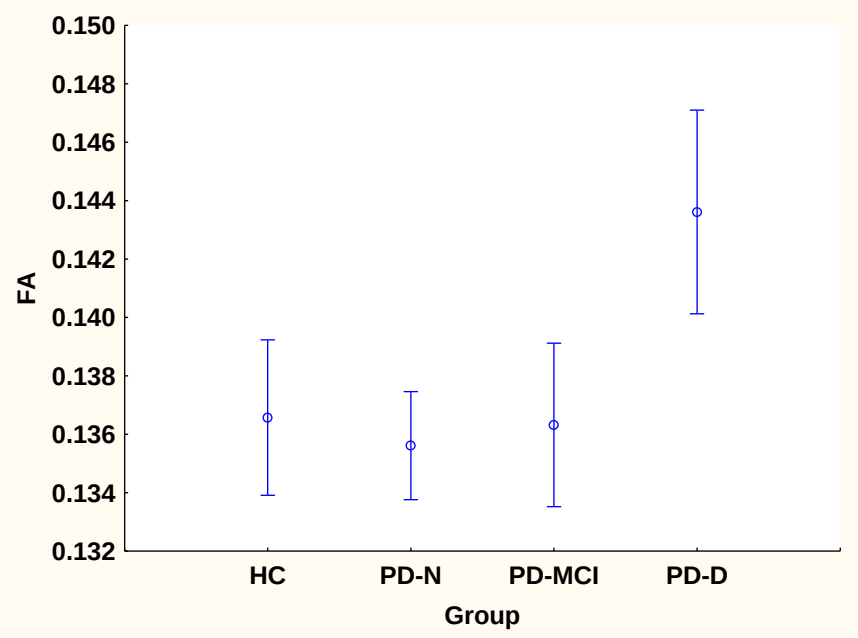

Fig 39B. CEN ANCOVA showing raIPL: Pairwise group differences (N-K): (HC = PD-N = PD-D = PD-MCI.

As shown in Table 31, age had no significant effect on any ROI except the right pIPL of the DMN. Education had no effect on any ROI, except the right INS of the SN and left pIPS of the DAN.

Significant group main effects were found in the left PCC of the DMN, the left FEF of the DAN, and the left INS of the SN. The group main effects for all other ROIs in the four networks were not significant. Post-hoc N-K tests revealed that the PD-D group had significantly higher FA values than the HC and PD-N group for left FEF, left INS, and left aIPL of the CEN, and higher value than the PD-N group only for the left ACC of the SN. The PD-D group also had significantly higher FA values than the PD-MCI group for the left ACC, left INS, and left aIPL. The PD-MCI group had significantly lower FA values than the HC and PD-N group for the left INS, and lower FA values than the HC group only for the left PCC. No significant differences were found between the PD-N and HC group for the left PCC, left FEF, left ACC, left INS, and left aIPL. There were no significant group differences in any other ROI across the four networks.

In summary, the PD-D group had higher FA value when compared to the HC or PD-N group, for a few nodes in the left hemisphere across the four networks, specifically the left FEF, left INS, left aIPL, and left ACC. However, the PD-MCI group, revealed an opposite change, with lower values compared to the HC and PD-N group, for some of these nodes. Two comments are relevant; first, only a few differences were apparent for FA, and lack of consistency may thus reflect some chance variation; secondly, voxels were selected using criteria to minimize white matter, so MD changes rather than FA changes might be expected to be more reliable measures of between group differences.

3.3 ANCOVA GM

ANCOVA (with age and education as covariates) and the Newman-Keuls post-hoc comparison tests were performed on the mean values of the Grey Matter (GM) voxels for each participant group in a particular ROI for each RSN. The GM voxels are the number of voxels identified in individuals in native space after removal of voxels reaching criteria for CSF and WM.

The ANCOVA for the group main effects for GM in the left and right ROIs of the four networks are summarized on Table 32 and the mean values for the four participant groups for each ROI in every RSN are shown in Figure 40 to Figure 52. The Newman-Keuls Test tables are presented in the Appendix.

Table 32

Grey Matter Voxels: Group main effect for the ANCOVA for each ROI for the four cognitive networks

	dlPFC		aIPL							
CEN	Left	Right	Left	Right						
	F (3,135) = 1.48, p = .2	F (3,135) = 2.0, p=.1	**F (3,135) = 3.6, p=.016**	F (3,135) = 2.04, p=.1						
SN	ACC		INS							
	Left	Right	Left	Right						
	F (3,135) = .58, p=.6	F (3,135) = 1.44, p=.2	F (3,135) = .62, p=.6	F (3,135) = .1.95, p =.1						
DAN	FEF		aIPS		pIPS		MT+			
	Left	Right	Left	Right	Left	Right	Left	Right		
	F (3,135) = 1.6, p = .2	F (3,135) = 1.17, p=.3	F (3,135) = 2.52, p=.1	**F (3,135) = 3.74, p<.01**	F (3,135) = 1.03, p=.4	F (3,135) = .93, p=.5	F (3,135) = .62, p=.6	F (3,135) = .377, p=.8		
DMN	PCC		dMPFC		vMPFC		pIPL		MTG	
	Left	Right	Left	Right	Left	Right	Left	Right	Left	Right
	F (3,135) = 2.7, p <.049	F (3,135) = .86, p=.5	**F (3,135) = 2.8, p<.04**	F (3,135) = .72, p=.5	F (3,135) = 1.8, p=.1	F (3,135) = .29, p=.8	F (3,135) = 1.08, p=.4	F (3,135) = .38, p=.8	F (3,135) = 1.72, p=.2	F (3,135) = 1.8, p=.2

All bolded F-ratios are significant. Age and education of participants were used as co-variates; age was significant ($p<0.05$), for the right dMPFC and left vMPFC in the DMN. Age was not significant for all other ROIs except the right aIPS of the DAN, and left aIPL for CEN; education was not significant for any ROI except right dMPFC of the DMN and the right ACC and left INS of the SN. For abbreviations, see Table 5.

Figure 40

Differences between the means (±sem) of the GM voxels of the PCC for the four groups controlling for age and education.

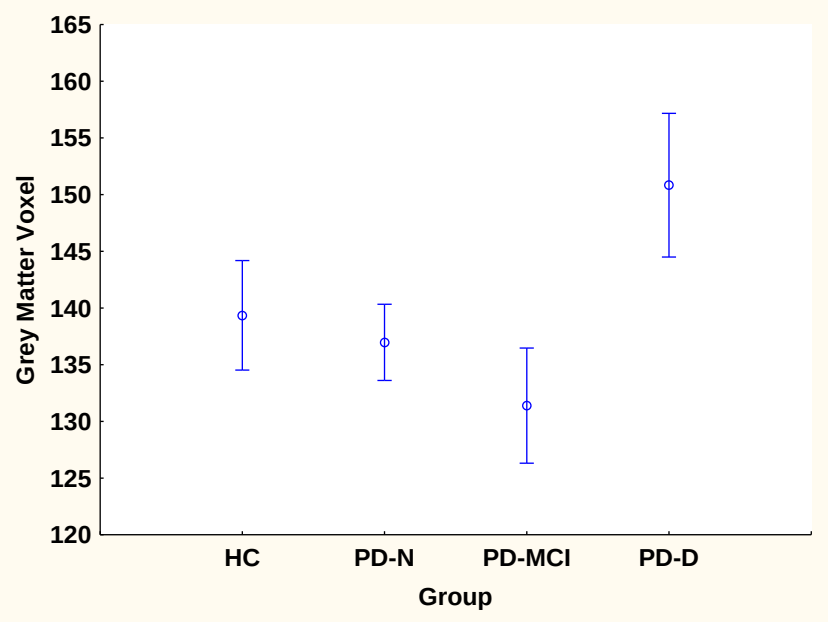

Fig 40A (these are number of voxels identified in individuals in native space after removal of voxels reaching criteria for CSF and WM). DMN ANCOVA showing lPCC: Pairwise group differences (N-K): (HC = PD-N = PD-D), (HC = PD-N = PD-MCI), PD-MCI <PD-D.

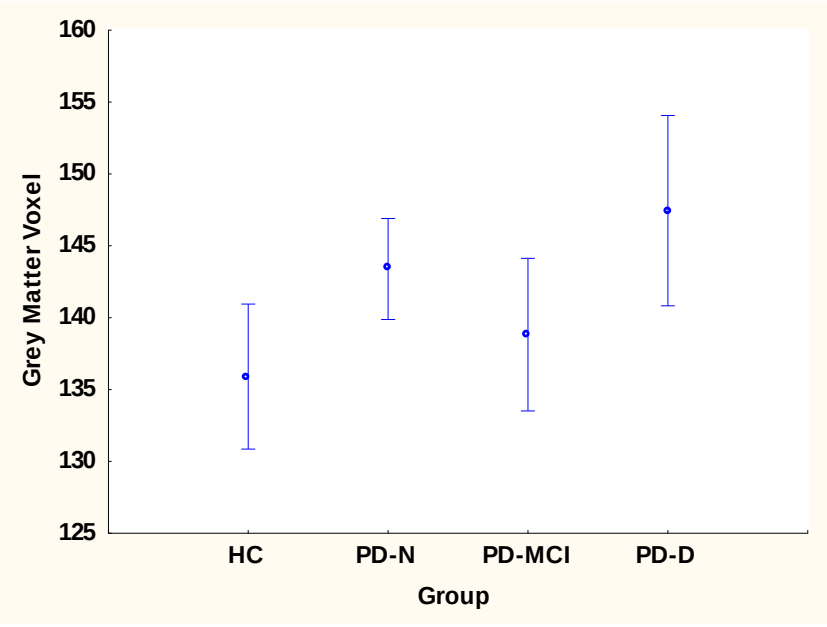

Fig 40B (these are number of voxels identified in individuals in native space after removal of voxels reaching criteria for CSF and WM). DMN ANCOVA showing rPCC: Pairwise group differences (N-K): (HC = PD-N = PD-MCI = PD-D).

Figure 41

Differences between the means (±sem) of the GM voxels of the dMPFC for the four groups controlling for age and education.

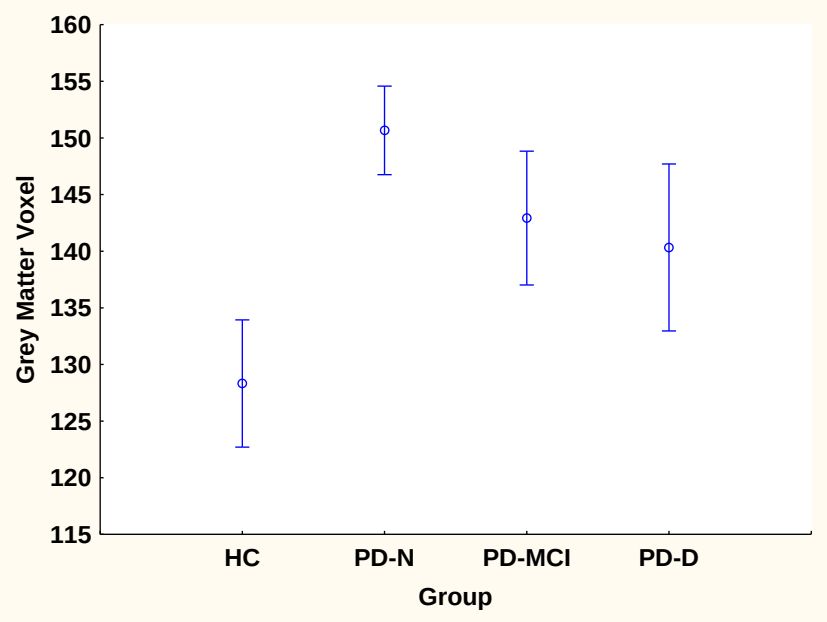

Fig 41A (these are number of voxels identified in individuals in native space after removal of voxels reaching criteria for CSF and WM). DMN ANCOVA showing ldMPFC: Pairwise group differences (N-K): (HC = PD-MCI = PD-D), (PD-N = PD-MCI = PD-D), HC < PD- N.

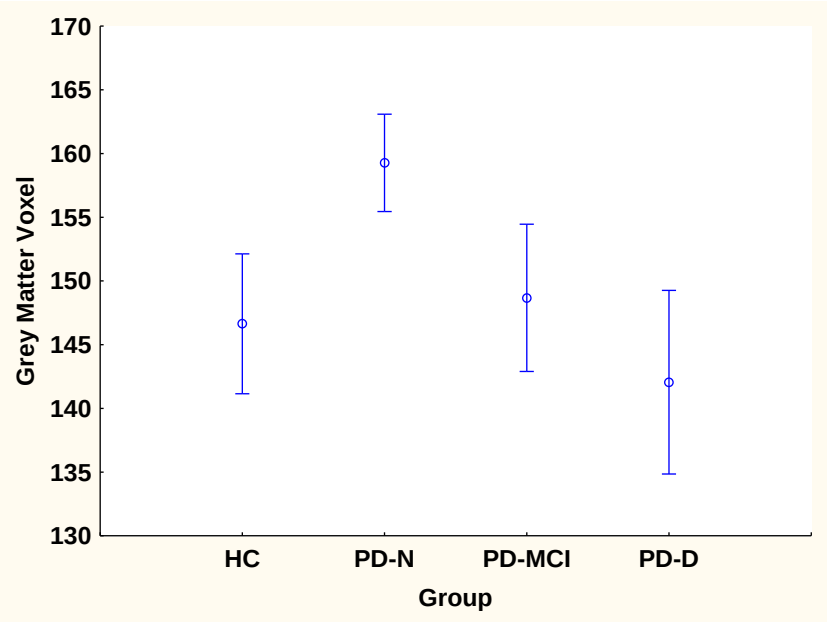

Fig 41B (these are number of voxels identified in individuals in native space after removal of voxels reaching criteria for CSF and WM). DMN ANCOVA showing rdMPFC: Pairwise group differences (N-K): (HC = PD-MCI = PD-D), (PD-N = PD-MCI = PD-D), HC < PD- N.

Figure 42

Differences between the means (±sem) of the GM voxels of the vMPFC for the four groups controlling for age and education.

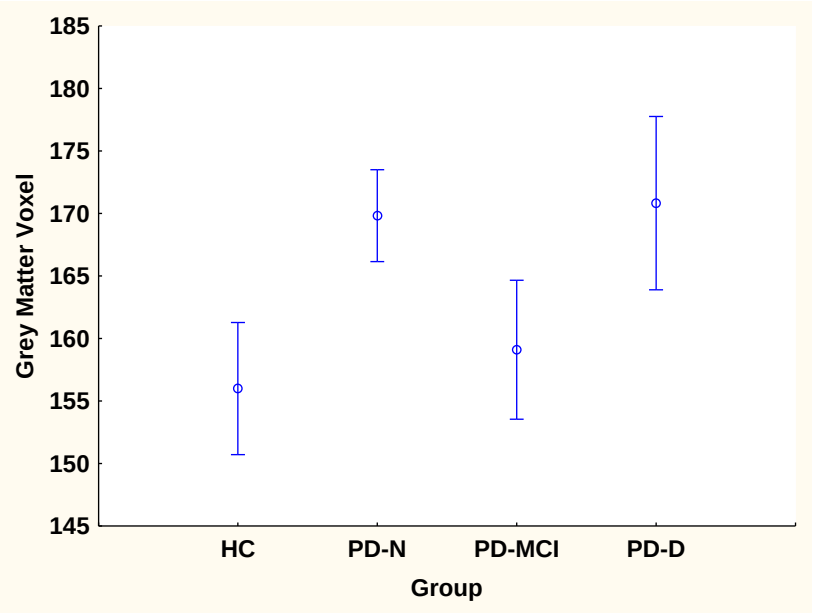

Fig 42A (these are number of voxels identified in individuals in native space after removal of voxels reaching criteria for CSF and WM). DMN ANCOVA showing lvMPFC: Pairwise group differences (N-K): (HC = PD-N = PD-MCI = PD-D)

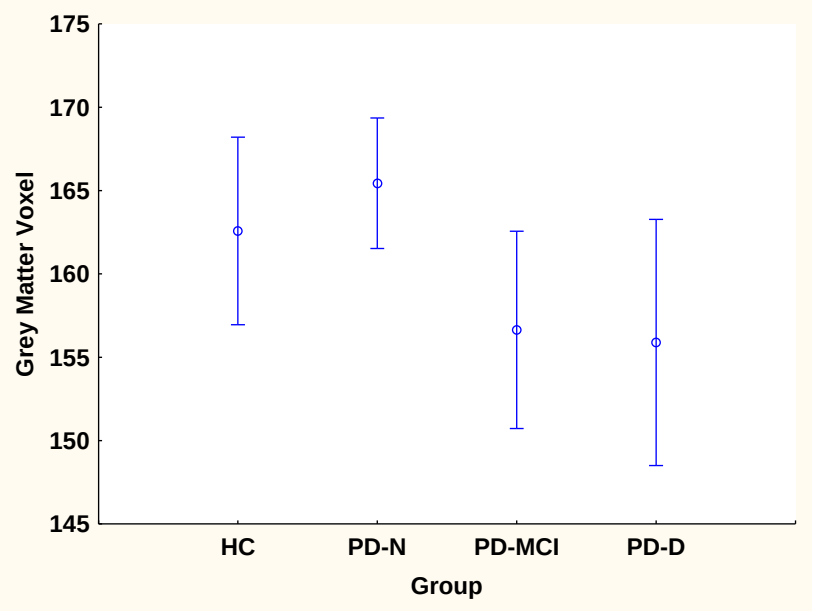

Fig 42B (these are number of voxels identified in individuals in native space after removal of voxels reaching criteria for CSF and WM). DMN ANCOVA showing rvMPFC: Pairwise group differences (N-K): (HC = PD-N = PD-MCI = PD-D.

Figure 43

Differences between the means (+sem) of the GM voxels of the pIPL for the four groups controlling for age and education.

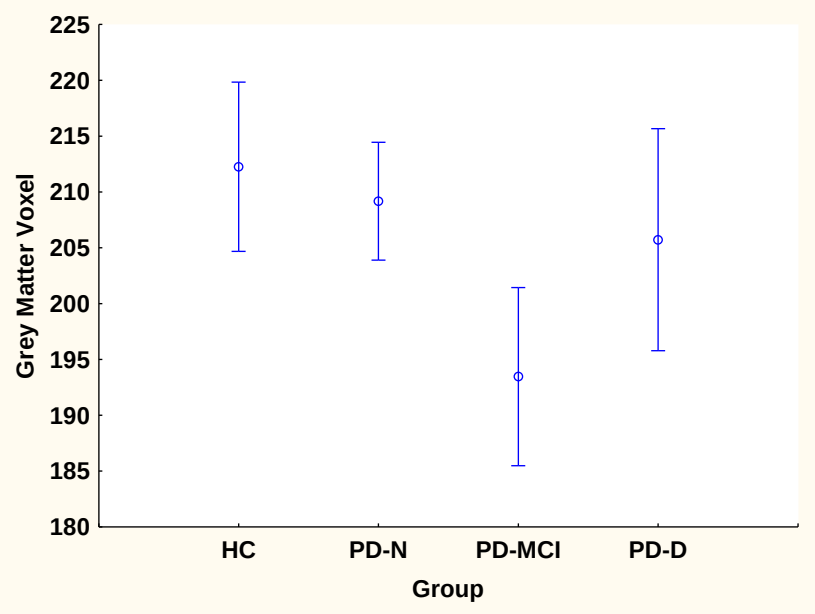

Fig 43A (these are number of voxels identified in individuals in native space after removal of voxels reaching criteria for CSF and WM). DMN ANCOVA showing lpIPL: Pairwise group differences (N-K): (HC = PD-N = PD-MCI = PD-D)

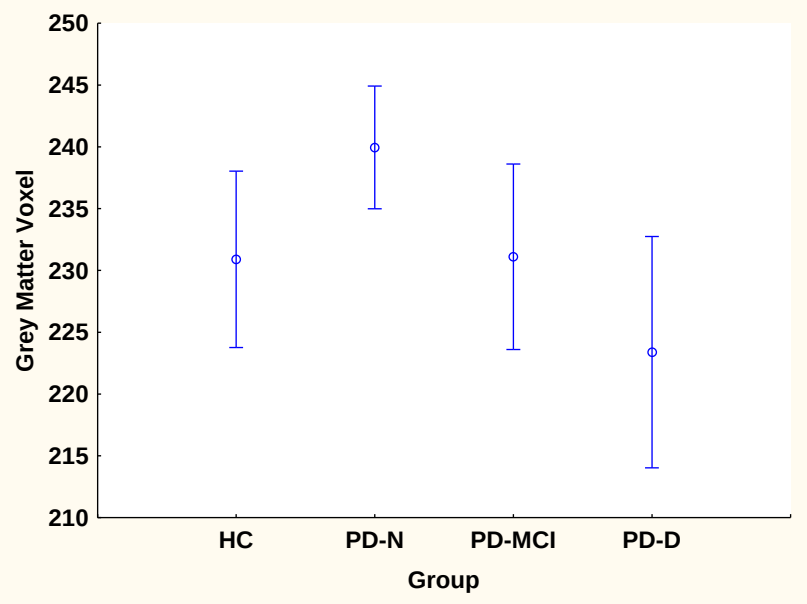

Fig 43B (these are number of voxels identified in individuals in native space after removal of voxels reaching criteria for CSF and WM). DMN ANCOVA showing rpIPL: Pairwise group differences (N-K): (HC = PD-N = PD-MCI = PD-D.

Figure 44

Differences between the means (+sem) of the GM voxels of the MTG for the four groups controlling for age and education.

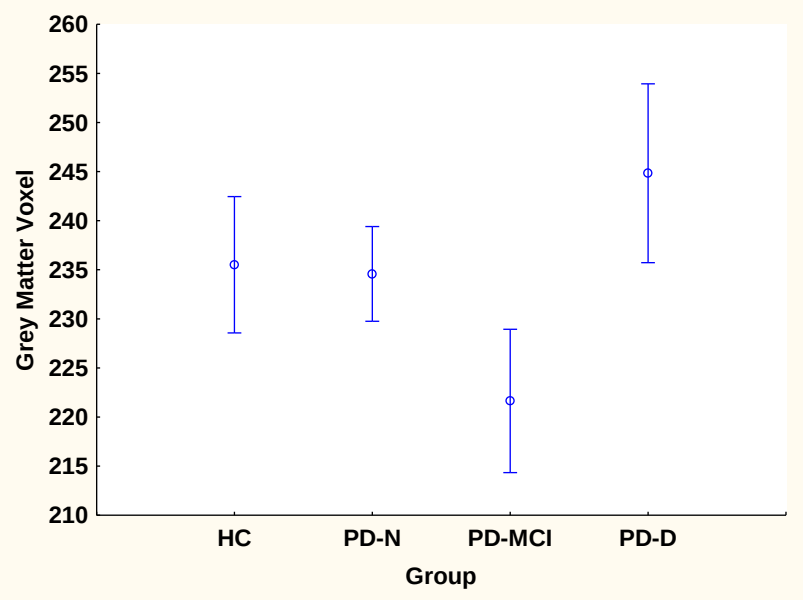

Fig 44A (these are number of voxels identified in individuals in native space after removal of voxels reaching criteria for CSF and WM). DMN ANCOVA showing lMTG: Pairwise group differences (N-K): (HC = PD-N = PD-MCI = PD-D)

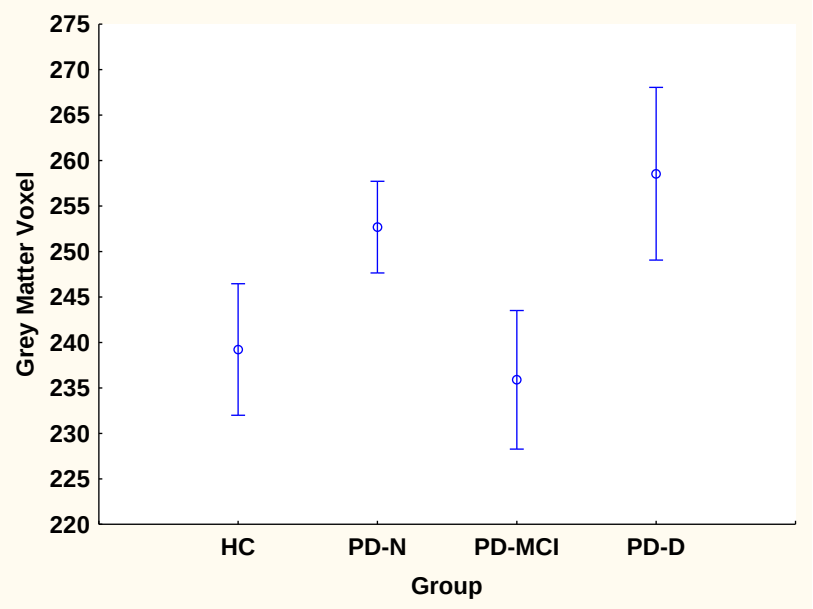

Fig 44B (these are number of voxels identified in individuals in native space after removal of voxels reaching criteria for CSF and WM). DMN ANCOVA showing rMTG: Pairwise group differences (N-K): (HC = PD-N = PD-MCI = PD-D).

Figure 45

Differences between the means (+sem) of the GM voxels of the FEF for the four groups controlling for age and education.

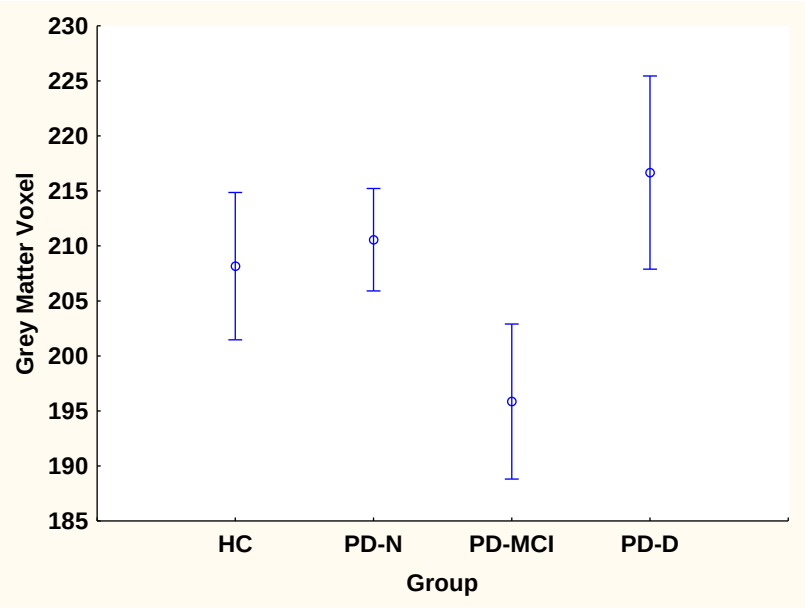

Fig 45A (these are number of voxels identified in individuals in native space after removal of voxels reaching criteria for CSF and WM). DAN ANCOVA showing lFEF: Pairwise group differences (N-K): (HC = PD-N = PD-MCI = PD-D)

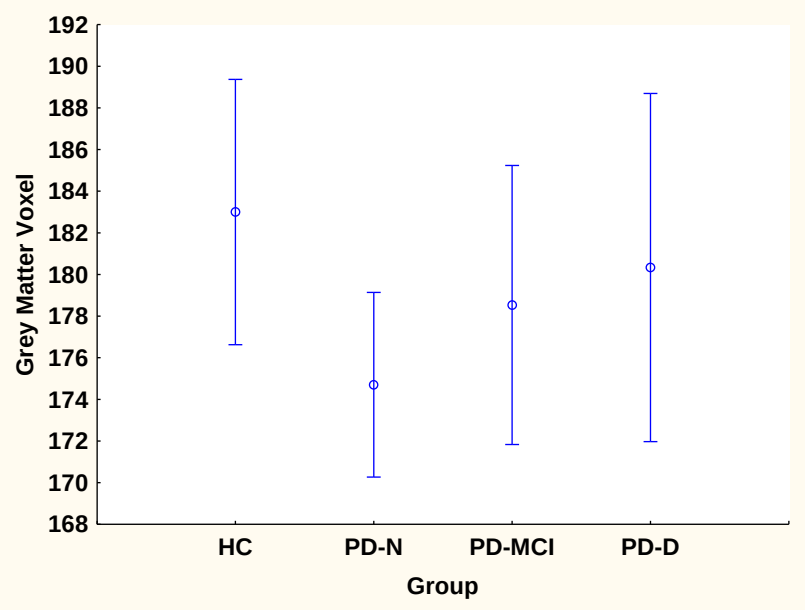

Fig 45B (these are number of voxels identified in individuals in native space after removal of voxels reaching criteria for CSF and WM). DAN ANCOVA showing rFEF: Pairwise group differences (N-K): (HC = PD-N = PD-MCI = PD-D.

Figure 46

Differences between the means (+sem) of the GM voxels of the aIPS for the four groups controlling for age and education.

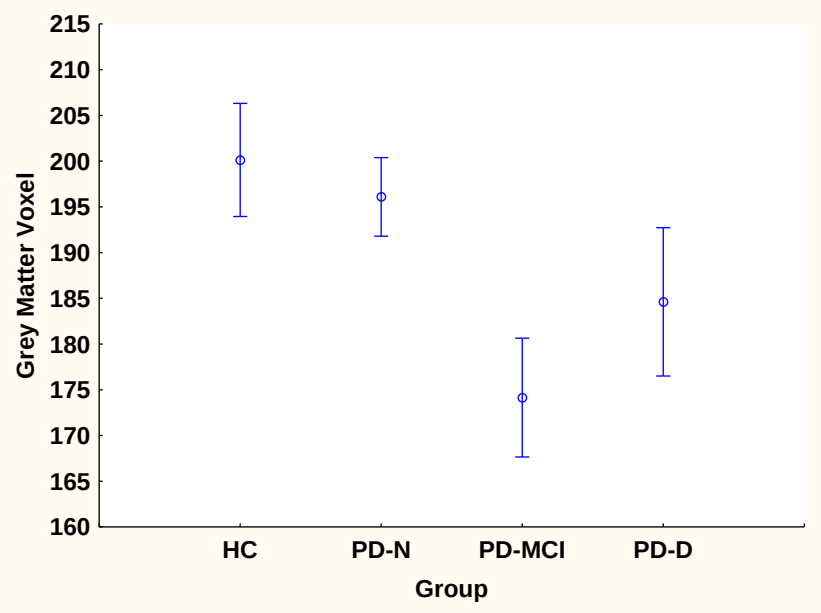

Fig 46A (these are number of voxels identified in individuals in native space after removal of voxels reaching criteria for CSF and WM). DAN ANCOVA showing laIPS: Pairwise group differences (N-K): (HC = PD-N < PD-MCI), (HC = PD-N = PD-D), (PD-MCI = PD-D).

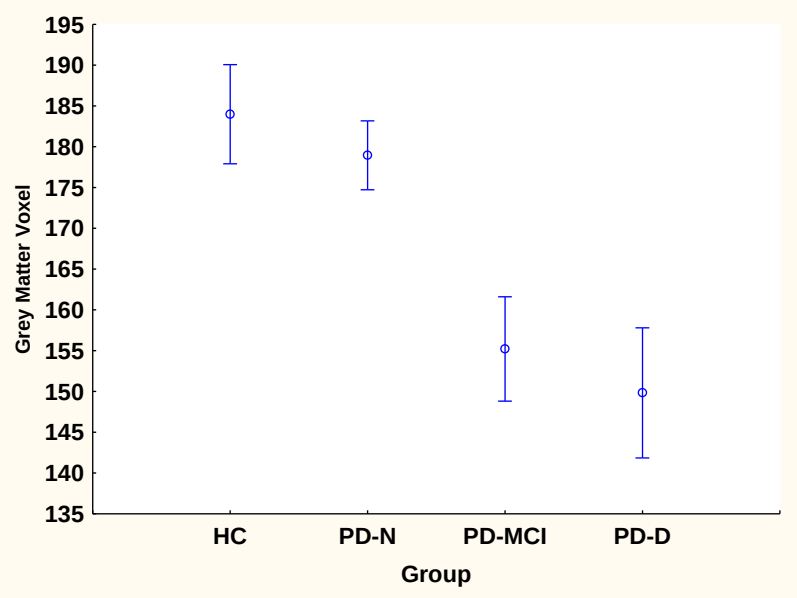

Fig 46B. (these are number of voxels identified in individuals in native space after removal of voxels reaching criteria for CSF and WM). DAN ANCOVA showing raIPS: Pairwise group differences (N-K): (HC = PD-N < PD-MCI = PD-D).

Figure 47

Differences between the means (+sem) of the GM voxels of the pIPS for the four groups controlling for age and education.

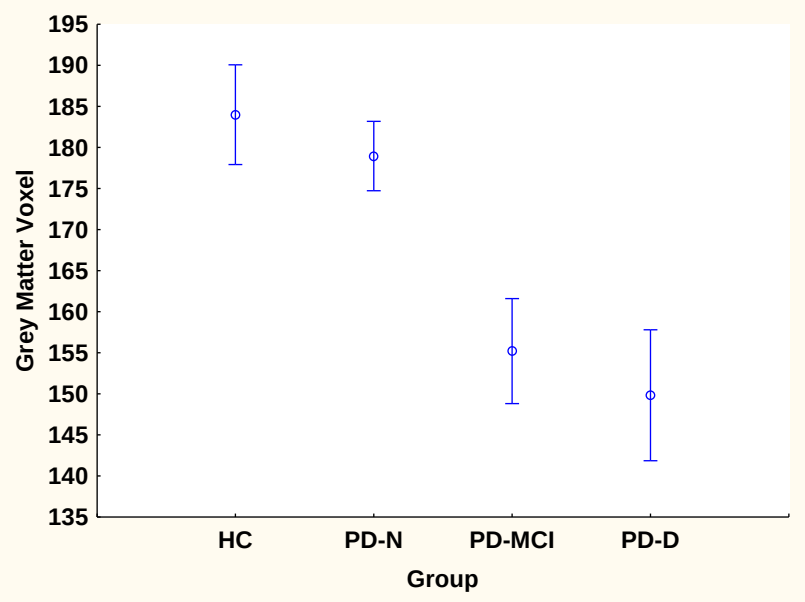

Fig 47A (these are number of voxels identified in individuals in native space after removal of voxels reaching criteria for CSF and WM). DAN ANCOVA showing lpIPS: Pairwise group differences (N-K): (HC = PD-N = PD-MCI = PD-D).

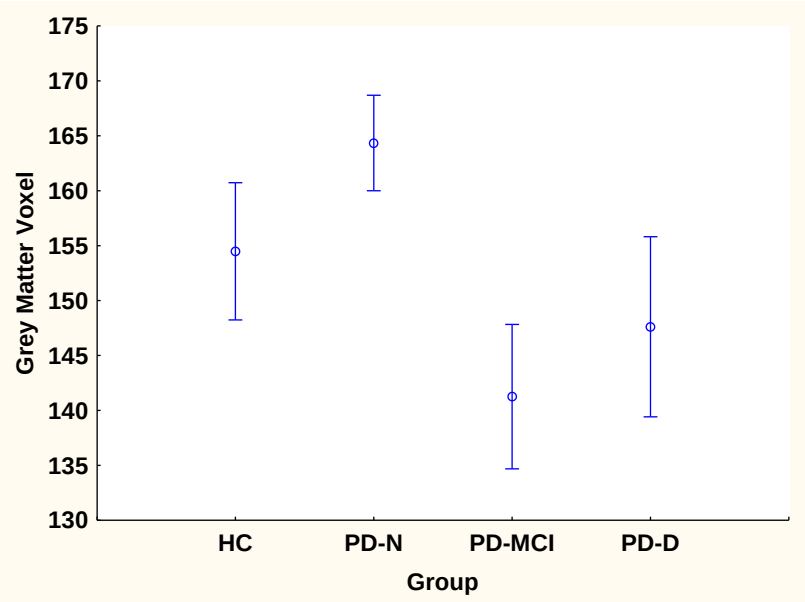

Fig 47B (these are number of voxels identified in individuals in native space after removal of voxels reaching criteria for CSF and WM). DAN ANCOVA showing rpIPS: Pairwise group differences (N-K): (HC = PD-N = PD-MCI = PD-D).

Figure 48

Differences between the means (+sem) of the GM voxels of the MT+ for the four groups controlling for age and education.

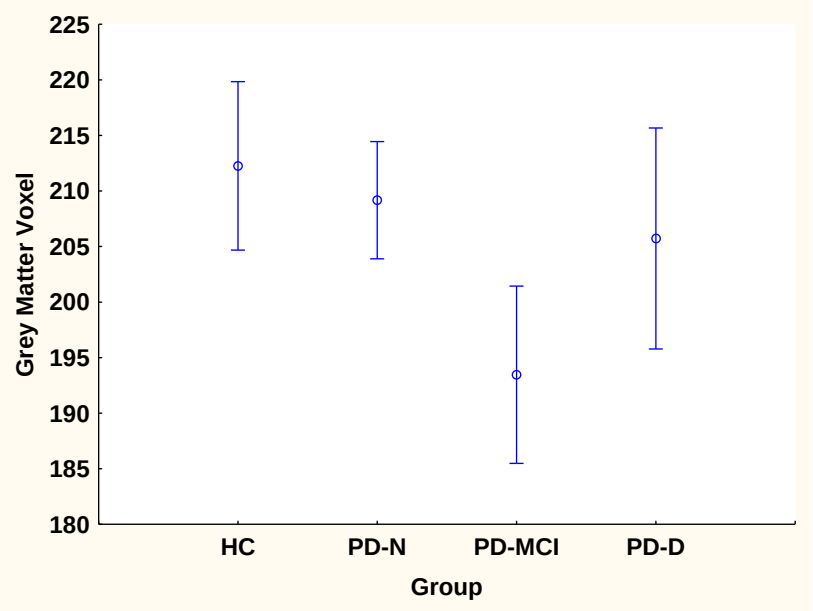

Fig 48A (these are number of voxels identified in individuals in native space after removal of voxels reaching criteria for CSF and WM). DAN ANCOVA showing lMT+: Pairwise group differences (N-K): (HC = PD-N = PD-MCI = PD-D).

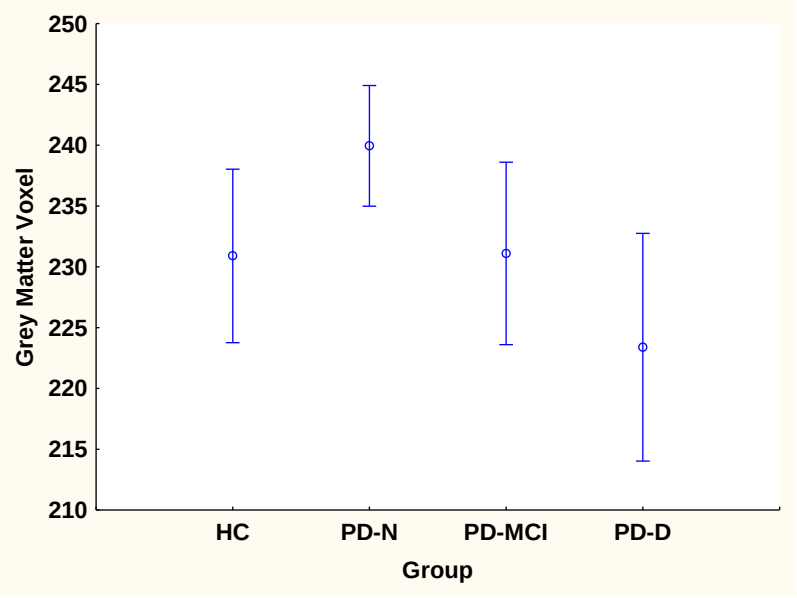

Fig 48B (these are number of voxels identified in individuals in native space after removal of voxels reaching criteria for CSF and WM). DAN ANCOVA showing rMT+: Pairwise group differences (N-K): (HC = PD-N = PD-MCI = PD-D).

Figure 49

Differences between the means (+sem) of the GM voxels of the ACC for the four groups controlling for age and education.

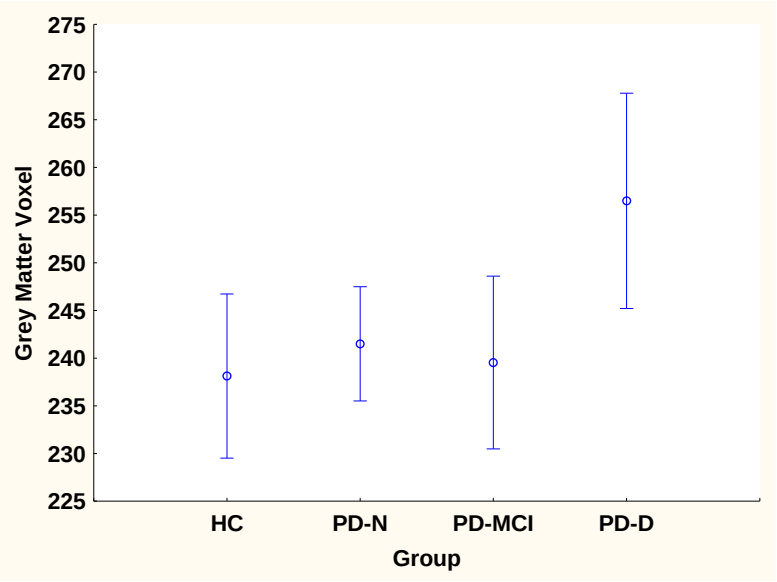

Fig 49A (these are number of voxels identified in individuals in native space after removal of voxels reaching criteria for CSF and WM). SN ANCOVA showing lACC: Pairwise group differences (N-K): (HC = PD-N = PD-MCI = PD-D).

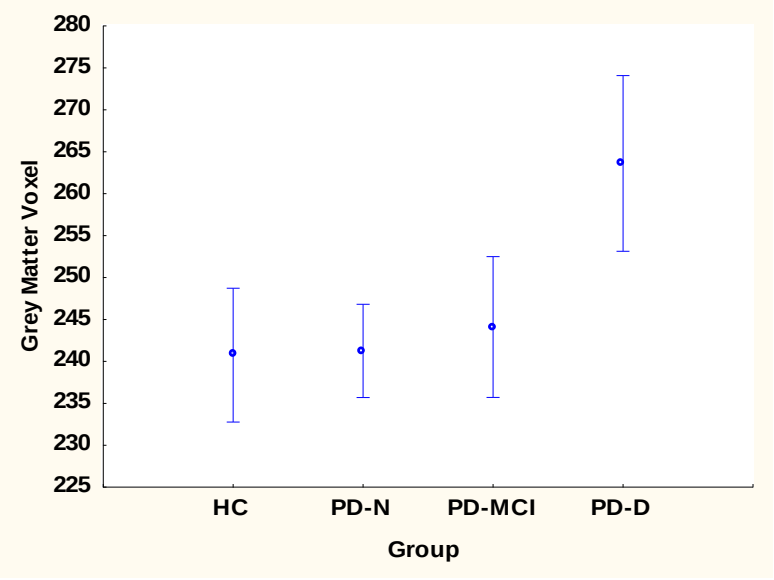

Fig 49B (these are number of voxels identified in individuals in native space after removal of voxels reaching criteria for CSF and WM). SN ANCOVA showing rACC: Pairwise group differences (N-K): (HC = PD-N = PD-MCI = PD-D).

Figure 50

Differences between the means (+sem) of the GM voxels of the INS for the four groups controlling for age and education.

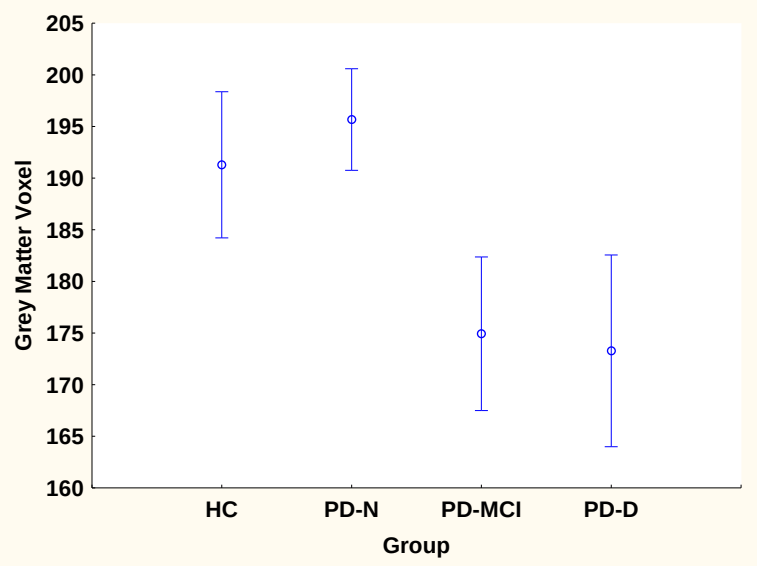

Fig 50A (these are number of voxels identified in individuals in native space after removal of voxels reaching criteria for CSF and WM). SN ANCOVA showing lINS: Pairwise group differences (N-K): (HC = PD-N = PD-MCI = PD-D).

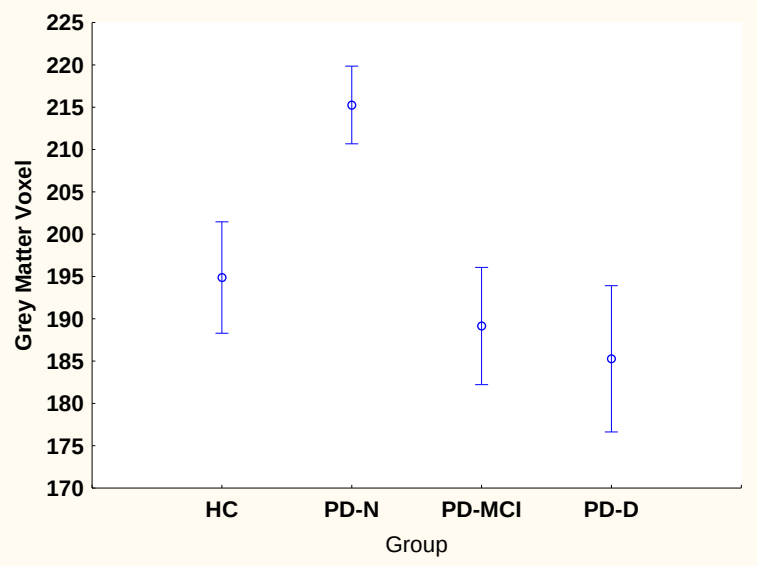

Fig 50B (these are number of voxels identified in individuals in native space after removal of voxels reaching criteria for CSF and WM). SN ANCOVA showing rINS: Pairwise group differences (N-K): HC < PD-N, (HC = PD-MCI = PD-D), PD-N <PD-MCI = PD-D, PD-N < PD-D.

Figure 51

Differences between the means (+sem) of the GM voxels of the dlPFC for the four groups controlling for age and education.

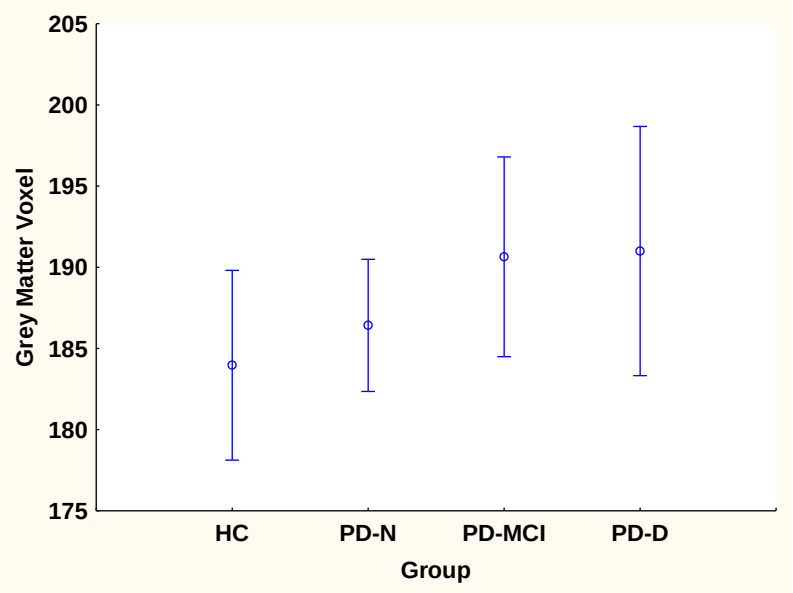

Fig 51A (these are number of voxels identified in individuals in native space after removal of voxels reaching criteria for CSF and WM) CEN ANCOVA showing ldlPFC: Pairwise group differences (N-K): (HC = PD-N = PD-MCI = PD-D).

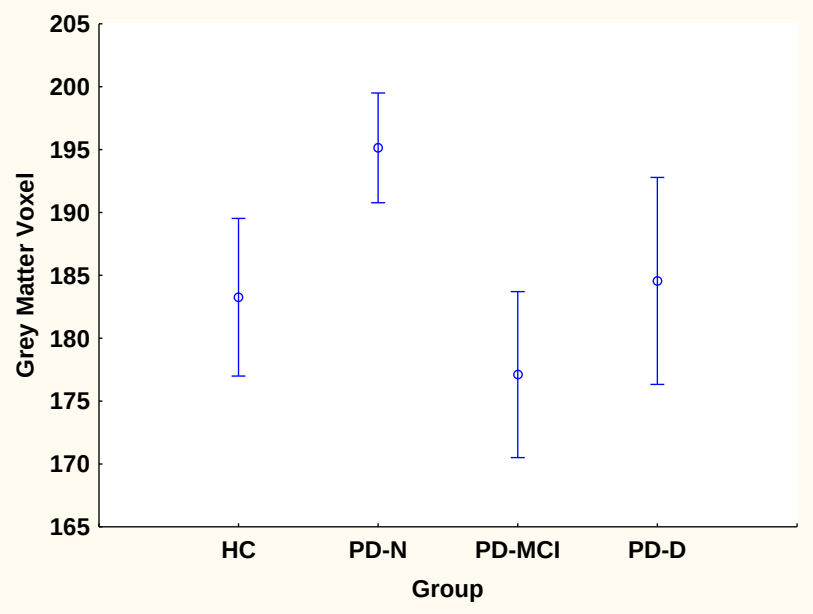

Fig 51B (these are number of voxels identified in individuals in native space after removal of voxels reaching criteria for CSF and WM). CEN ANCOVA showing rdlPFC: Pairwise group differences (N-K): (HC = PD-N = PD-MCI = PD-D)

Figure 52

Differences between the means (+sem) of the GM voxels of the aIPL for the four groups controlling for age and education.

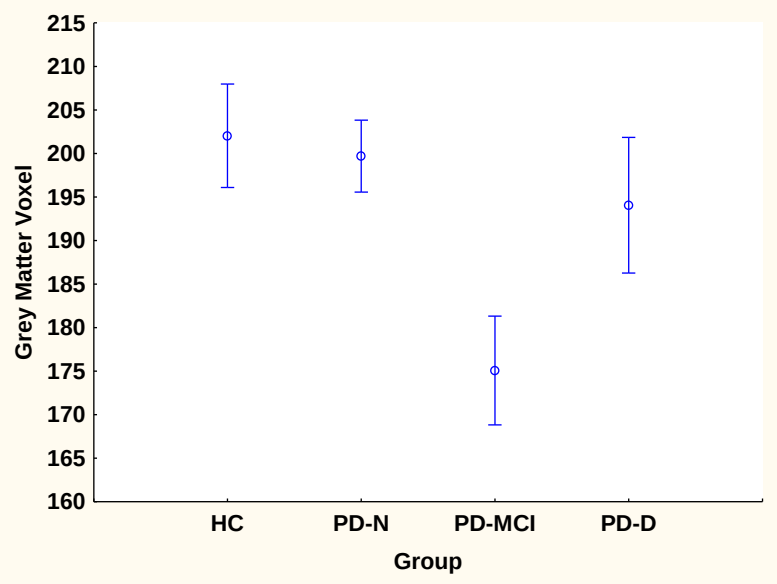

Fig 52A (these are number of voxels identified in individuals in native space after removal of voxels reaching criteria for CSF and WM). CEN ANCOVA showing laIPL: Pairwise group differences (N-K): (HC = PD-N) <PD-MCI, (HC = PD-N = PD-D), PD-MCI <PD-D.

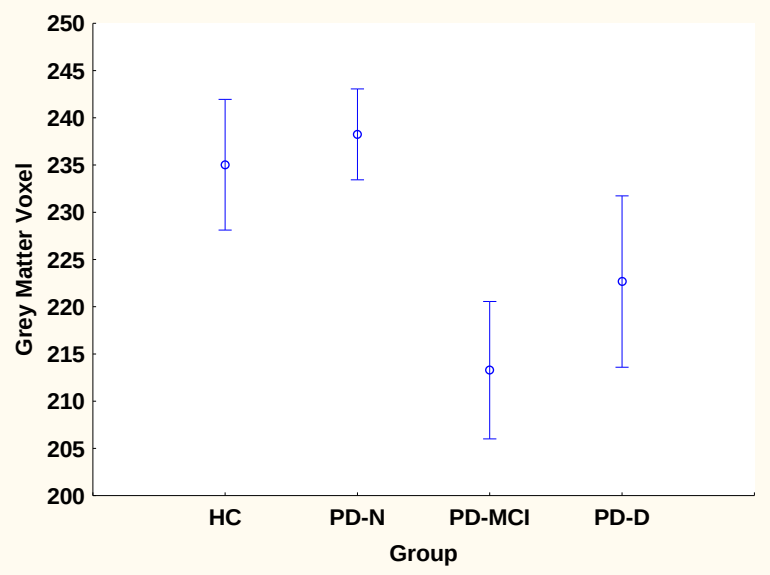

Fig 52B (these are number of voxels identified in individuals in native space after removal of voxels reaching criteria for CSF and WM). CEN ANCOVA showing raIPL: Pairwise group differences (N-K): (HC = PD-N = PD-MCI = PD-D).

ANCOVA GM VOXEL NUMBER for the ROIs

The ANCOVA for the group main effects for GM voxel number in the left and right ROIs of the four networks are summarized on Table X and the mean values for the four participant groups for each ROI are shown in Fig. X. As shown in Table X, age had no significant effect on the ROIs of the DMN except the right dMPFC and left vMPFC. Age was significant for some other ROIs except the left and right MT+ for DAN, left and right ACC for SN, and the right dlPFC and right aIPL for the CEN. Education had no effect for any ROI except the right ACC and left INS of the SN, as well as the right dMPFC of the DMN.

Significant group main effects were found in the left PCC and left dMPFC of the DMN, the right aIPS of the DAN, and the left aIPL of the CEN. The group main effects for all other ROIs in the four networks were not significant. On the whole, then, relatively few reliable differences emerged across the groups in terms of the number of voxels analysed for MD and FA across the groups for the ROIs of the four networks.

Post-hoc N-K tests revealed that the PD-D group had significantly lower number of grey matter voxels than the HC or PD-N for the right aIPS of the DAN, and lower value compared to PD-N only in the right INS of the SN. The PD-D group had significantly higher number of grey matter voxels than PD-MCI for the left PCC of the DMN and left aIPL of the CEN. The PD-MCI had significantly lower number of grey matter voxel than the HC and PD-N group for the left and right aIPS of the DAN, and lower value only for the PD-N in the right INS of the SN. The PD-N group had significantly higher number of grey matter voxels than the HC in the left and right dMPFC, and the right INS. There were no significant group differences in any other ROI across the four networks. To summarise, there were relatively few consistent differences in GM voxel number for the RSNs across the groups, with the direction of these changes varying across ROIs.

4. Discussion

4.1 Summary of Main Findings

Microstructural integrity of grey matter voxels in key nodes of four cognitive RSN, namely the DMN, DAN, SN, and the CEN, was investigated in three groups of patients with PD, that differed in terms of their cognitive status. The three patients groups, covering the full spectrum of cognitive ability, and were classified as PD-N, with cognition in the normal range, PD-MCI, which had cognitive impairment insufficient to cause dementia, and PD-D which met criteria for established dementia due to significant deficits in everyday independent function. These three PD groups were compared with a matched group of healthy controls (HC). The key nodes of the ROIs within these 4 networks were established by review of the general literature on RSNs to derive MNI-specified coordinates that were then reversed engineered to individual brain DTI images, co-registered to their TI images, so that person-specific DTI metrics could be subjected to statistical analysis.

Based on the mean of MD voxels from the DTI imaging, the PD-D group exhibited widespread loss of integrity (higher values) across the most nodes in the RSN, relative to HC and PD-N; notable exceptions occurred in the right pIPL of the DMN; the left FEF and right IPS of the DAN; and the left aIPL of the CEN, relative to HC only. The PD-MCI showed limited selective loss and the PD group with relatively preserved cognition (PD-N) had no detectable or minimal loss compared to the HC group.

Changes in the structural integrity for the RSNs in the PD-MCI group were found to be similar to the changes in the PD-D group, and worse than the structural integrity of the HC and PD-N group, in the left PCC and left MTG of the DMN, left and right ACC of the SN,

and right dlPFC of the CEN; but worse than PD-N only in the left INS of the SN and right MT+ of the DAN; worse than HC only, in the left IPL of the DMN.

The PD-MCI group showed improved structural integrity, when compared with PD-D, and displayed similar structural integrity to the HC and PD-N group, in the left and right dMPFC, right PCC, right vMPFC, and the right MTG of the DMN; and the right FEF, right aIPS, and left MT+ of the DAN.

The PD-N group had no detectable change of structural integrity, relative to HC, in all ROIs, across the 4 RSN.

For PD-D, it was expected that the DMN would most likely show the greatest change, as observed from past studies that have reported the effects of AD dementia, which has been shown to follow a disease pattern of brain atrophy that is also evident in PD (Weintraub et al., 2011). The current study confirmed this hypothesis by showing that the structural integrity for the PD-D group was consistently worse across the ROIs of the DMN in comparison with the PD-N and HC groups for the DMN.

This finding was consistent with previous functional magnetic resonance imaging (fMRI) connectivity studies that reported the regions of the DMN as a hub of sensitive microstructural change during the progression of dementia (Buckner et al., 2008; Brier et al., 2012; Broyd et al., 2009; Wen et al., 2013). The dysfunction of the DMN observed in the PD-D group showed similar patterns of DMN impairment in other dementias as well, particularly in AD studies (Broyd et al., 2009; Weintraub et al, 2012; Wu et al., 2011). Hence, damage to the DMN as a result of PD-D may have a role in the development of cognitive decline in PD, similar to AD. Prior PD studies on the effect of PD in DMN support this theory. Decreased FC in regions of the DMN in PD patients, specifically the PCC, IPL, and the MPFC has been

reported (Rektorova, Krajcociva, Marecek, & Miki, 2012; Tessitore et al., 2012; Van Eimeren et al., 2009)

The structural integrity of the ROIs across the 4 RSNs in PD-MCI could also suggest which nodes are likely to be most vulnerable when MCI occurs in PD. In particular, some ROIs of the DMN in PD-MCI were found to be similar to HC or PD-N group but others relatively similar to PD-D.

The structural integrity for the PD-N group across the 4 RSN show that it stays relatively intact, similar to the structural integrity of the HC group, paralleling previous studies using voxel-based morphometry (VBM), a neuroimaging technique that uses statistics to investigate the focal differences in brain anatomy (Whitwell, 2009), that shows there is little significant structural GM difference between cognitively unimpaired PD patients and HC. That is, PD patients, with generally intact cognitive ability (PD-N) also have generally intact GM cortical brain tissues (Melzer et. al., 2012; Tessitore et al., 2012; Weintraub et al., 2011). However, failure to show structural changes in PD may still mean that these patients have some functional deficits and indeed compensatory increases in network function.

The findings described above only reflect changes based on the evaluation of the MD values for the ROIs in the 4 RSN, and not on the FA values. The evaluation of the FA values in a few ROIs paradoxically suggested that PD-D group seemed to have better structural integrity than the ROIs in the other groups, indicated by higher FA values, which contradicts the findings observed from the assessment of the MD values. However, this discrepancy may be explained by chance variation, as the FA values were inconsistent across the 4 RSN, and by the criteria of the current study which minimized white matter voxels in order to study the grey matter voxels. Therefore, MD changes rather than FA changes would be expected to be a more consistent measure of group differences in the current study. This suggestion is

supported by Schwarz et al. (2013) that showed the FA as an inconsistent measure of the structural changes in PD, and MD as a more reliable measure to reveal microstructural changes, in a meta-analysis that investigated the DTI imaging of nigral degeneration.

The number of grey matter (GM) voxels analyzed for FA and MD was also investigated in the current study. It was shown that there were few reliable differences and changes were inconsistent across the groups, with the direction of these changes varying across ROIs. This similarity suggests that the reduction in MD for many ROIs in PD-D and for some nodes in PD-MCI reflect subtle structural change rather than whole-brain degeneration. Similarly, standard VBM analyses of T1 images from the whole brain suggest widespread GM degeneration in PD-D, in the temporal, parietal, and frontal cortex, which reaches statistical significance to a lesser extent in PD-MCI (Melzer et al., 2012). DTI imaging is more sensitive to microstructural changes than is T1.

The current study revealed that the microstructural changes in the ROIs of the 4 RSN were affected differently, depending on the cognitive status of participants. PD-D, in particular, showed degeneration of structural integrity in the ROIs across the 4 RSNs, and this finding was anticipated by the current study. However, the structural integrity of the ROIs in the PD-MCI group across the 4 RSNs did not change as expected, as the integrity of many ROIs was found to be similar to the integrity in the HC or PD-N group, which could signify those ROIs staying relatively intact in MCI or that the lack of structural changes in these ROIs shows it to be less sensitive to the MCI pathology. The PD-N group fails to show any significant structural changes in any ROIs across the 4 RSN, indicating that perhaps, PD patients retain structural integrity of the ROIs in the early stages of the disease before it converts to PD-MCI or PD-D. This finding can also be explained by the lack of sensitivity to

functional changes or compensation. Nonetheless, the current study showed that the microstructural changes in the RSNs of PD patients are clearly influenced by cognitive status.

4.2 Limitations and Future Directions

The current study evaluated structural changes of the ROIs in the RSNs, which could imply functional changes such as cognition or behavior as a result of PD. Dagher & Nagano-Saito (2007) stated that cognition in PD could be explained by direct neuronal loss in medial temporal and lateral prefrontal areas as a result of PD. Ibarretxe-Barrao, Tolosa, Junque, & Marti (2009) showed that lower hippocampal volume in patients with PD, relative to HC, correlated with deficits in verbal memory. Similarly, Biundo et al. (2011) also showed that brain atrophy in the middle and superior frontal gyrus in patients with PD leads to the development of implusive behaviours and in worse working memory. In a study of functional integrity of DMN in cognitively unimpaired PD patients, Tessitore et al. (2012) reported that there was a functional disruption of the DMN, in the absence of any significant structural differences, which showed that structural changes are not necessarily a pre-requisite for functional changes in PD. Nonetheless, the current study have shown significant structural changes in PD-D, which would imply that functional connectivity in those RSNs would be compromised; in PD-MCI, the more subtle changes could have a major impact on cognition or be compensated, the answer to which would require a combined structural / functional study. The changes observed in a combined study would suggest that interventions, such as cognitive training, could improve or delay the onset of cognitive impairment.

This study has included a comparison of the main nodes in the 4 RSN, but owing to time constraints, no association with any cognitive measures in the five cognitive domains was undertaken. Although it is possible to see the cognitive differences between groups based on the global cognitive domain Z scores as well as the individual Z scores for every cognitive

domain except language, statistical comparisons with individual cognitive tests and DTI measures could might reveal interesting associations. The sample size of the participants in the current study might also be an issue. There were relatively low numbers of participants, per group, with the exception of the PD-N group. Future research should ensure that there is a higher number of participants across all groups and examine the association between individual cognitive tests and the main nodes explored fully.

An issue with the current study was that it utilized Movement Disorders Task Force criteria for the diagnosis of MCI in PD participants remains uncertain, because they were not yet fully validated. Although consistent with the criteria suggested by Litvan et al. (2012) for the diagnosis of MCI in PD patients, more limited criteria were specified for PD-MCI in the current study. There is evidence that our specific criteria, as used in the current study, have done well in predicting conversion to PD-D and may be superior to many alternatives in that regard (Dalrymple-Alford, 2013; Wood et al., 2013). That is, diagnosis of MCI in PD patients used in the current study are likely to pick up many patients who are at high risk of conversion to dementia in the following 3 years, which the potential value for the ROI changes identified here.

4.3 Concluding Remarks

This study examined microstructural integrity of ROIs in four key brain networks, the DMN, DAN, SN, and CEN, in 3 groups of participants with PD, namely PD-N, PD-MCI, and PD-D, and a comparison group of healthy controls. The PD-D group was found to have the worse structural integrity for most ROIs across all the RSNs, relative to all groups. The structural integrity of the ROIs in the PD-MCI group showed selective change in some ROIs, but was similar to the structural integrity of the PD-N group or PD-D group in many ROIs. The PD-N group had no detectable or minimal change in the structural integrity of all the

ROIs across the four RSN, relative to healthy controls. The unique findings of this current study showed that subtle structural changes are evident in the RSNs, when patients reach a PD-MCI condition and that clear deficits in many regions are evident in PD-D. For future study, structural and functional changes for these RSNs should be explored to examine similarities between both measures.

5. References

Aarsland, D., Bronnick, K, Ehrt, U., De Deyn, P.P., Tekin, S., Emre, M., & Cummings, J.L. (2007). Neuropsychiatric symptoms in patients with Parkinson's disease and dementia: frequency, profile, and associated care giver stress. *J Neurol Neurosurg Psychiatry*, 78 (1), 36 – 42. doi:10.1136/jnnp.2005.083113,

Aarsland, D., & Kurz, M. W. (2010). The epidemiology of dementia associated with Parkinson disease. *J Neurol Sci, 289*(1-2), 18-22. doi: 10.1016/j.jns.2009.08.034

Arbuthnott, K., & Frank, J. (2000). Trail Making Test, Part B as a measure of executive control: validation using a switching-set paradigm. *J Clin Exp Neuropsychol*, *22* (4), 518 – 528. DOI:10.1076/1380-3395(200008)22:4;1-0;FT518

Allen, E. A., Erhardt, E. B., Damaraju, E., Gruner, W., Segall, J. M., Silva, R. F., . . . Calhoun, V. D. (2011). A baseline for the multivariate comparison of resting-state networks. *Front Syst Neurosci*, *5*, 2. doi: 10.3389/fnsys.2011.00002

Andrews-Hanna, J. R. (2012). The brain's default network and its adaptive role in internal mentation. *Neuroscientist, 18*(3), 251-270. doi: 10.1177/1073858411403316

Andrews-Hanna, J. R., Reidler, J. S., Sepulcre, J., Poulin, R., & Buckner, R. L. (2010). Functional-anatomic fractionation of the brain's default network. *Neuron, 65*(4), 550-562. doi: 10.1016/j.neuron.2010.02.005

Ashburner, J., & Friston, K. J. (2005). Unified segmentation. *Neuroimage, 26*(3), 839-851. doi: 10.1016/j.neuroimage.2005.02.018

Barone, P., Aarsland, D., Burn, D., Emre, M., Kulisevsky, J., & Weintraub, D. (2011). Cognitive impairment in nondemented Parkinson's disease. *Mov Disord, 26*(14), 2483-2495. doi: 10.1002/mds.23919

Benton, A., Hannay, H.J., & Varney, N.R. (1975). Visual perception of the line direction in patients with unilateral brain disease. *Neurology, 25* (10), 907 – 910. doi: 10.1212/WNL.25.10.907

Biundo, R., Formento-Dojot, P., Facchini, S., Vallelunga, A., Ghezzo, L., Foscolo, L., . . . Antonini, A. (2011). Brain volume changes in Parkinson's disease and their relationship with cognitive and behavioural abnormalities. *J Neurol Sci, 310*(1-2), 64-69. doi: 10.1016/j.jns.2011.08.001

Bluhm, R., Williamson, P., Lanius, R., Theberge, J., Densmore, M., Bartha, R., . . . Osuch, E. (2009). Resting state default-mode network connectivity in early depression using a seed region-of-interest analysis: decreased connectivity with caudate nucleus. *Psychiatry Clin Neurosci, 63*(6), 754-761. doi: 10.1111/j.1440-1819.2009.02030.x

Bosboom, J. L., Stoffers, D., & Wolters, E. (2004). Cognitive dysfunction and dementia in Parkinson's disease. *J Neural Transm, 111*(10-11), 1303-1315. doi: 10.1007/s00702-004-0168-1

Braga, R.M., Sharp, D.J., Leeson, C., Wise, R.J., & Leech, R. (2013). Echoes of the brain within default mode network , association, and heteromodal cortices. J Neurosci, 33 (35), 14031 – 14039). doi: 10.1523/JNEUROSCI.0570-13.2013

Bressler, S. L., & Menon, V. (2010). Large-scale brain networks in cognition: emerging methods and principles. *Trends Cogn Sci, 14*(6), 277-290. doi: 10.1016/j.tics.2010.04.004

Brett, M., Anton, J.L., Valabregue, R., & Poline, J.B. (2002). Region of interest analysis using an SPM toolbox [abstract]. Presented at the 8th International Conference on Functional Mapping of the Human Brain, June 2-6, 2002, Sendai, Japan.

Broeders, M., de Bie, R.M., Velseboer, D.C., Speelman, J.D., Muslimovic, D., & Schmand, B. (2013). Evolution of mild cognitive impairment in Parkinson's disease. *Neurology*, *81* (4) , 346 – 352. doi: 10.1212/WNL.0b013e31829c5c86.

Brier, M. R., Thomas, J. B., Snyder, A. Z., Benzinger, T. L., Zhang, D., Raichle, M. E., . . . Ances, B. M. (2012). Loss of intranetwork and internetwork resting state functional connections with Alzheimer's disease progression. *J Neurosci, 32*(26), 8890-8899. doi: 10.1523/JNEUROSCI.5698-11.2012

Buckner, R. L., Andrews-Hanna, J. R., & Schacter, D. L. (2008). The brain's default network: anatomy, function, and relevance to disease. *Ann N Y Acad Sci, 1124*, 1-38. doi: 10.1196/annals.1440.011

Buckner, R. L., Snyder, A. Z., Shannon, B. J., LaRossa, G., Sachs, R., Fotenos, A. F., . . . Mintun, M. A. (2005). Molecular, structural, and functional characterization of Alzheimer's disease: evidence for a relationship between default activity, amyloid, and memory. *J Neurosci, 25*(34), 7709-7717. doi: 10.1523/JNEUROSCI.2177-05.2005

Burns, A., & Iliffe, S. (2009). Alzheimer's disease. *BMJ, 338*, b158. doi: 10.1136/bmj.b158

Callahan, C. M., Arling, G., Tu, W., Rosenman, M. B., Counsell, S. R., Stump, T. E., & Hendrie, H. C. (2012). Transitions in care for older adults with and without dementia. *J Am Geriatr Soc, 60*(5), 813-820. doi: 10.1111/j.1532-5415.2012.03905.x

Camchong, J., MacDonald, A. W., 3rd, Bell, C., Mueller, B. A., & Lim, K. O. (2011). Altered functional and anatomical connectivity in schizophrenia. *Schizophr Bull, 37*(3), 640-650. doi: 10.1093/schbul/sbp131

Caviness, J. N., Driver-Dunckley, E., Connor, D. J., Sabbagh, M. N., Hentz, J. G., Noble, B., . . . Adler, C. H. (2007). Defining mild cognitive impairment in Parkinson's disease. *Mov Disord, 22*(9), 1272-1277. doi: 10.1002/mds.21453

Chan, L. L., Rumpel, H., Yap, K., Lee, E., Loo, H. V., Ho, G. L., . . . Tan, E. K. (2007). Case control study of diffusion tensor imaging in Parkinson's disease. *J Neurol Neurosurg Psychiatry, 78*(12), 1383-1386. doi: 10.1136/jnnp.2007.121525

Chou, K.L., Amick, M.M., Brandt, J., Camicoli, R., Frei, K…Uc, E.Y. (2010). A recommended scale for cognitive screening in clinical trials of Parkinson's disease. *Mov Disord, 25* (15), 2501 – 2507. DOI: 10.1002/mds.23362

Chua, T.C., Wen, W., Chen, X., Kochan, N., Slavin, M.J., Trollor, J.N., Brodaty, H., & Sachdev, P.S. (2009). Diffusion tensor imaging of the posterior cingulate is a useful biomarker of mild cognitive impairment. *Am J Geriatr Psychiatry, 17* (7), 602 – 613. doi: 10.1097/JGP.0b013e3181a76e0b.

Corbetta, M., & Shulman, G. L. (2002). Control of goal-directed and stimulus-driven attention in the brain. *Nat Rev Neurosci, 3*(3), 201-215. doi: 10.1038/nrn755

Cummings, J.L., Mega, M., Gray, K., Rosenberg-Thompson, S., Carusi, D.A., & Gornbein, J. (1994). The neuropsychiatric inventory: comprehensive assessment of psychopathology in dementia. *Neurology, 44*, 2309 – 2314. doi: 10.1212/WNL.44.12.2308

Dagher, A., & Nagano-Saito, A. (2007). Functional and anatomical magnetic resonance imaging in Parkinson's disease. *Mol Imaging Biol, 9*(4), 234-242. doi: 10.1007/s11307-007-0089-0

Dalrymple-Alford, J. C., Livingston, L., MacAskill, M. R., Graham, C., Melzer, T. R., Porter, R. J., . . . Anderson, T. J. (2011). Characterizing mild cognitive impairment in Parkinson's disease. *Mov Disord, 26*(4), 629-636. doi: 10.1002/mds.23592

Dalrymple-Alford, J.C., Livingstone, L., Melzer, T.R., Wood, K, J., Pitcher, T.L., Graham, C.F., Keenan, R.J., MacAskill, M.R. & Anderson, T.J. (2013). Current perspectives on Parkinson's disease: Cognition to the fore. *31st International Australasian Winter Conference on Brain Research*, Vol. 31 (Queenstown, New Zealand, 2013).

Dalrymple-Alford, J.C., MacAskill, M.R., Nakas, C.T., Livingston, L., Graham, C…Anderson, T.J. (2010). The MoCA: a well-suited screen for cognitive impairment in Parkinson disease. *Neurology*, *75* (19), 1717 – 1725. doi: 10.1212/WNL.0b013e3181fc29c9

Damoiseaux, J. S., Rombouts, S. A., Barkhof, F., Scheltens, P., Stam, C. J., Smith, S. M., & Beckmann, C. F. (2006). Consistent resting-state networks across healthy subjects. *Proc Natl Acad Sci U S A, 103*(37), 13848-13853. doi: 10.1073/pnas.0601417103

Deco, G., Jirsa, V.K., McIntosh, A.R. (2011). Emerging concepts for the dynamic organization of resting-state activity in the brain. *Nat Rev Neurosci*, *12* (1), 43 – 56. doi: 10.1038/nrn2961.

Delis, D. C., Kaplan, E., & Kramer, J. H. (2001a). *Delis-Kaplan Executive Function System (D-KEFS)*. San Antonio, TX: The Psychological Corporation.

Delis, D. C., Kaplan, E., & Kramer, J. H. (2001b). *Delis-Kaplan Executive Function System (D-KEFS) examiner's manual* (pp. 1-218). San Antonio, TX: The Psychological Corporation.

Delis, D. C., Kaplan, E., & Kramer, J. H. (2001c). *Delis-Kaplan Executive Function System (D-KEFS) technical manual* (pp. 1-132). San Antonio, TX: The Psychological Corporation.

Delis, D.C., Kramer, J.H., Kaplan, E., & Ober, B.A. (2000). *The California Verbal Learning Test*. (2nd Ed.). San Antonio: The Psychological Corporation.

De Vogelaere, F., Santens, P., Achten, E., Boon, P., & Vingerhoets, G. (2012). Altered default-mode network activation in mild cognitive impairment compared with healthy aging. *Neuroradiology, 54*(11), 1195-1206. doi: 10.1007/s00234-012-1036-6

Dubois, B., Feldman, H. H., Jacova, C., DeKosky, S. T., Barberger-Gateau, P., Cummings, J., . . . Jicha, G. (2007). Research criteria for the diagnosis of Alzheimer's disease: revising the NINCDS–ADRDA criteria. *The Lancet Neurology, 6*(8), 734-746. doi: 10.1016/s1474-4422(07)70178-3

Eickhoff, S. B., Laird, A. R., Grefkes, C., Wang, L. E., Zilles, K., & Fox, P. T. (2009). Coordinate-based activation likelihood estimation meta-analysis of neuroimaging data: a random-effects approach based on empirical estimates of spatial uncertainty. *Hum Brain Mapp, 30*(9), 2907-2926. doi: 10.1002/hbm.20718

Emre, M., Aarsland, D., Brown, R., Burn, D. J., Duyckaerts, C., Mizuno, Y., . . . Dubois, B. (2007). Clinical diagnostic criteria for dementia associated with Parkinson's disease. *Mov Disord, 22*(12), 1689-1707; quiz 1837. doi: 10.1002/mds.21507

Folstein, M.F., Folstein, S.E., & McHugh, P.R. (1975). “Mini-mental state”. A practical method for grading the cognitive stats of patients for the clinician. *J Psychiatr Res*, *12* (3), 189 – 198. http://dx.doi.org/10.1016/0022-3956(75)90026-6

Forjaz, M. J., Frades-Payo, B., Rodriguez-Blazquez, C., Ayala, A., Martinez-Martin, P., & Longitudinal Parkinson's Disease Patient Study. (2010). Should the SCOPA-COG be modified? A Rasch analysis perspective. *Eur J Neurol, 17*(2), 202-207. doi: 10.1111/j.1468-1331.2009.02791.x

Fornito, A., Harrison, B.J., Zalesky, A., & Simons, J.S. (2012). Competitive and cooperative dynamics of large-scale brain functional networks supporting recollection. *PloS One,* 109 (31), 12788 – 12793. doi:10.1073/pnas.1204185109.

Fox, M. D., & Raichle, M. E. (2007). Spontaneous fluctuations in brain activity observed with functional magnetic resonance imaging. *Nat Rev Neurosci, 8*(9), 700-711. doi: 10.1038/nrn2201

Fox, M. D., Snyder, A. Z., Vincent, J. L., Corbetta, M., Van Essen, D. C., & Raichle, M. E. (2005). The human brain is intrinsically organized into dynamic, anticorrelated functional networks. *Proc Natl Acad Sci U S A, 102*(27), 9673-9678. doi: 10.1073/pnas.0504136102

Fransson, P. (2006). How default is the default mode of brain function? Further evidence from intrinsic BOLD signal fluctuations. *Neuropsychologia, 44*(14), 2836-2845. doi: 10.1016/j.neuropsychologia.2006.06.017

Friston, K.J., Zarahn, E., Josephs, O., Henson, R.N., & Dale, A.M. (1999). Stochastic designs in event-related fMRI. *Neuroimage, 10* (5), 607 – 619. http://dx.doi.org/10.1006/nimg.1999.0498

Gancher, S.T. (2006). Scales for the Assessment of Movement Disorders. In RM. Herndon (eds). *Handbook of Neurologic Rating Scales*. (pp. 145-168). New York, United States: New York University Publishing.

Gao, W., & Lin, W. (2012). Frontal parietal control network regulates the anti-correlated default and dorsal attention networks. *Hum Brain Mapp, 33*(1), 192-202. doi: 10.1002/hbm.21204

Gattellaro, G., Minati, L., Grisoli, M., Mariani, C., Carella, F., Osio, M., . . . Bruzzone, M. G. (2009). White matter involvement in idiopathic Parkinson disease: a diffusion tensor imaging study. *AJNR Am J Neuroradiol, 30*(6), 1222-1226. doi: 10.3174/ajnr.A1556

Gaugler, J. E., Mittelman, M. S., Hepburn, K., & Newcomer, R. (2010). Clinically significant changes in burden and depression among dementia caregivers following nursing home admission. *BMC Med, 8*, 85. doi: 10.1186/1741-7015-8-85

Goldman, W.P., Baty, J.D., Buckles, V.D., Sahrmann, S., & Morris, J.C. (1998). Cognitive and motor functioning in Parkinson disease: subjects with and without questionable dementia. *Arch Neurol, 55* (5), 674 – 680. doi:10.1001/archneur.55.5.674.

Grady, C. L., Protzner, A. B., Kovacevic, N., Strother, S. C., Afshin-Pour, B., Wojtowicz, M., . . . McIntosh, A. R. (2010). A multivariate analysis of age-related differences in default mode and task-positive networks across multiple cognitive domains. *Cereb Cortex, 20*(6), 1432-1447. doi: 10.1093/cercor/bhp207

Green, R. E., Melo, B., Christensen, B., Ngo, L. A., Monette, G., & Bradbury, C. (2008). Measuring premorbid IQ in traumatic brain injury: an examination of the validity of the Wechsler Test of Adult Reading (WTAR). *J Clin Exp Neuropsychol, 30*(2), 163-172. doi: 10.1080/13803390701300524

Greicius, M. D., Krasnow, B., Reiss, A. L., & Menon, V. (2003). Functional connectivity in the resting brain: a network analysis of the default mode hypothesis. *Proc Natl Acad Sci U S A, 100*(1), 253-258. doi: 10.1073/pnas.0135058100

Greicius, M. D., Srivastava, G., Reiss, A. L., & Menon, V. (2004). Default-mode network activity distinguishes Alzheimer's disease from healthy aging: evidence from functional MRI. *Proc Natl Acad Sci U S A, 101*(13), 4637-4642. doi: 10.1073/pnas.0308627101

Greicius, M. D., Supekar, K., Menon, V., & Dougherty, R. F. (2009). Resting-state functional connectivity reflects structural connectivity in the default mode network. *Cereb Cortex, 19*(1), 72-78. doi: 10.1093/cercor/bhn059

Guttman, M., Kish, S.J., & Furukawa, Y. (2003). Current concepts in the diagnosis and management of Parkinson's disease. *CMAJ, 168*, 3, 293 – 301. Retrieved from http://www.cmaj.ca/content/168/3/293.full

Hafkemeijer, A., van der Grond, J., & Rombouts, S. A. (2012). Imaging the default mode network in aging and dementia. *Biochim Biophys Acta, 1822*(3), 431-441. doi: 10.1016/j.bbadis.2011.07.008

Harrison, B. J., Pujol, J., Lopez-Sola, M., Hernandez-Ribas, R., Deus, J., Ortiz, H., . . . Cardoner, N. (2008). Consistency and functional specialization in the default mode brain network. *Proc Natl Acad Sci U S A, 105*(28), 9781-9786. doi: 10.1073/pnas.0711791105

Hindle, J. V. (2010). Ageing, neurodegeneration and Parkinson's disease. *Age Ageing, 39*(2), 156-161. doi: 10.1093/ageing/afp223

Hobson, P., & Meara, J. (2004). Risk and incidence of dementia in a cohort of older subjects with Parkinson's disease in the United Kingdom. *Mov Disord, 19*(9), 1043-1049. doi: 10.1002/mds.20216

Hoehn, M. M., & Yahr, M. D. (1967). Parkinsonism: onset, progression, and mortality. *Neurology, 17*(5), 427-427. doi: 10.1212/wnl.17.5.427

Holdnack, H.A. (2001). *Wechsler Test of Adult Reading: WTAR*. San Antonio. The Psychological Corporation.

Hughes, A. J., Daniel, S. E., Kilford, L., & Lees, A. J. (1992). Accuracy of clinical diagnosis of idiopathic Parkinson's disease: a clinico-pathological study of 100 cases. *Journal of Neurology, Neurosurgery & Psychiatry, 55*(3), 181-184. doi: 10.1136/jnnp.55.3.181

Hughes, T. A., Ross, H. F., Mindham, R. H., & Spokes, E. G. (2004). Mortality in Parkinson's disease and its association with dementia and depression. *Acta Neurol Scand, 110*(2), 118-123. doi: 10.1111/j.1600-0404.2004.00292.x

Ibarretxe-Bilbao, N., Junque, C., Marti, M. J., & Tolosa, E. (2011). Brain structural MRI correlates of cognitive dysfunctions in Parkinson's disease. *J Neurol Sci, 310*(1-2), 70-74. doi: 10.1016/j.jns.2011.07.054

Isella, V., Mapelli, C., Morielli, N., Siri, C., De Gaspari, D., Pezzoli, G., . . . Appollonio, I. M. (2013). Diagnosis of possible Mild Cognitive Impairment in Parkinson's disease: Validity of the SCOPA-Cog. *Parkinsonism Relat Disord*. doi: 10.1016/j.parkreldis.2013.08.008

Jacobs, H. I., Radua, J., Luckmann, H. C., & Sack, A. T. (2013). Meta-analysis of functional network alterations in Alzheimer's disease: toward a network biomarker. *Neurosci Biobehav Rev, 37*(5), 753-765. doi: 10.1016/j.neubiorev.2013.03.009

Jankovic, J. (2008). Parkinson's disease: clinical features and diagnosis. *J Neurol Neurosurg Psychiatry, 79*(4), 368-376. doi: 10.1136/jnnp.2007.131045

Janvin, C. C., Larsen, J. P., Aarsland, D., & Hugdahl, K. (2006). Subtypes of mild cognitive impairment in Parkinson's disease: progression to dementia. *Mov Disord, 21*(9), 1343-1349. doi: 10.1002/mds.20974

Jellinger, K. A. (2013). Mild cognitive impairment in Parkinson disease: heterogenous mechanisms. *J Neural Transm, 120*(1), 157-167. doi: 10.1007/s00702-012-0771-5

Jeong, B., Choi, J., & Kim, J. W. (2012). MRI study on the functional and spatial consistency of resting state-related independent components of the brain network. *Korean J Radiol, 13*(3), 265-274. doi: 10.3348/kjr.2012.13.3.265

Jin, M., Pelak, V. S., & Cordes, D. (2012). Aberrant default mode network in subjects with amnestic mild cognitive impairment using resting-state functional MRI. *Magn Reson Imaging, 30*(1), 48-61. doi: 10.1016/j.mri.2011.07.007

Jurica, S.J., Leitten, C.L., & Mattis, S. (2001). *Dementia Rating Scale: Professional Manual*. Odessa, FL: Psychological Assessment Resources.

Kaplan, E., Gooodglass, H., & Weintraub, S. (1983). *Boston Naming Test*. Philadelphia: Lea and Febiger.

Koch, W., Teipel, S., Mueller, S., Buerger, K., Bokde, A. L., Hampel, H., . . . Meindl, T. (2010). Effects of aging on default mode network activity in resting state fMRI: does the method of analysis matter? *Neuroimage, 51*(1), 280-287. doi: 10.1016/j.neuroimage.2009.12.008

Kulisevsky, J., & Pagonabarraga, J. (2009). Cognitive impairment in Parkinson's disease: tools for diagnosis and assessment. *Mov Disord, 24*(8), 1103-1110. doi: 10.1002/mds.22506

Lansing, A.E., Ivnik, R.J., Cullum, C.M., & Randolph C. (1999). An empirically derived sort form of the Boston Naming Test. *Arch Clin Neuropsychol*, *14* (6), 481 – 487. http://dx.doi.org/10.1016/S0887-6177(98)00022-5

Le Bihan, D., Mangin, J.F., Poupon, C., Clark, C.A., Pappata, S., Molko, N., & Chabriat, H. (2001). Diffusion tensor imaging: concep.ts and applications. *J Majn Reson Imaging*, *13* (4), 534 – 546. DOI: 10.1002/jmri.1076.

Leech, R., & Sharp, D. J. (2013). The role of the posterior cingulate cortex in cognition and disease. *Brain*. doi: 10.1093/brain/awt162

Lemaitre, H., Crivello, F., Grassiot, B., Alperovitch, A., Tzourio, C., & Mazoyer, B. (2005). Age- and sex-related effects on the neuroanatomy of healthy elderly. *Neuroimage, 26*(3), 900-911. doi: 10.1016/j.neuroimage.2005.02.042

Li, R., Chen, K., Fleisher, A. S., Reiman, E. M., Yao, L., & Wu, X. (2011). Large-scale directional connections among multi resting-state neural networks in human brain: a functional MRI and Bayesian network modeling study. *Neuroimage, 56*(3), 1035-1042. doi: 10.1016/j.neuroimage.2011.03.010

Li, R., Wu, X., Fleisher, A. S., Reiman, E. M., Chen, K., & Yao, L. (2012). Attention-related networks in Alzheimer's disease: a resting functional MRI study. *Hum Brain Mapp, 33*(5), 1076-1088. doi: 10.1002/hbm.21269

Liao, W., Zhang, Z., Pan, Z., Mantini, D., Ding, J., Duan, X., . . . Chen, H. (2011). Default mode network abnormalities in mesial temporal lobe epilepsy: a study combining fMRI and DTI. *Hum Brain Mapp, 32*(6), 883-895. doi: 10.1002/hbm.21076

Litvan, I., Goldman, J. G., Troster, A. I., Schmand, B. A., Weintraub, D., Petersen, R. C., . . . Emre, M. (2012). Diagnostic criteria for mild cognitive impairment in Parkinson's disease: Movement Disorder Society Task Force guidelines. *Mov Disord, 27*(3), 349-356. doi: 10.1002/mds.24893

Liu, P., Zeng, F., Zhou, G., Wang, J., Wen, H., von Deneen, K. M., . . . Tian, J. (2013). Alterations of the default mode network in functional dyspepsia patients: a resting-state fmri study. *Neurogastroenterol Motil, 25*(6), e382-388. doi: 10.1111/nmo.12131

Liu, Z., Zhang, Y., Bai, L., Yan, H., Dai, R., Zhong, C., . . . Tian, J. (2012). Investigation of the effective connectivity of resting state networks in Alzheimer's disease: a functional MRI study combining independent components analysis and multivariate Granger causality analysis. *NMR Biomed, 25*(12), 1311-1320. doi: 10.1002/nbm.2803

Long, X. Y., Zuo, X. N., Kiviniemi, V., Yang, Y., Zou, Q. H., Zhu, C. Z., . . . Zang, Y. F. (2008). Default mode network as revealed with multiple methods for resting-state functional MRI analysis. *J Neurosci Methods, 171*(2), 349-355. doi: 10.1016/j.jneumeth.2008.03.021

Lustig, C., Snyder, A. Z., Bhakta, M., O'Brien, K. C., McAvoy, M., Raichle, M. E., . . . Buckner, R. L. (2003). Functional deactivations: change with age and dementia of the Alzheimer type. *Proc Natl Acad Sci U S A, 100*(24), 14504-14509. doi: 10.1073/pnas.2235925100

Mantini, D., Perrucci, M. G., Del Gratta, C., Romani, G. L., & Corbetta, M. (2007). Electrophysiological signatures of resting state networks in the human brain. *Proc Natl Acad Sci U S A, 104*(32), 13170-13175. doi: 10.1073/pnas.0700668104

Mars, R. B., Neubert, F. X., Noonan, M. P., Sallet, J., Toni, I., & Rushworth, M. F. (2012). On the relationship between the "default mode network" and the "social brain". *Front Hum Neurosci, 6*, 189. doi: 10.3389/fnhum.2012.00189

Matsui, H., Nishinaka, K., Oda, M., Niikawa, H., Kubori, T., & Udaka, F. (2007). Dementia in Parkinson's disease: diffusion tensor imaging. *Acta Neurol Scand, 116*(3), 177-181. doi: 10.1111/j.1600-0404.2007.00838.x

Marinus, J., Visser, M., Verwey, Verhey, N.A., Middelkoop…van Hilten, J.J. (2003). Assessment of cognition in Parkinson's disease. *Neurology, 61* (9), 1222 – 1228. doi: 10.1212/01.WNL.0000091864.39702.1C

Meijer, F.J., Bloem, B.R., Mahlknecht, P., Seppi, K., & Goraj, B. (2013). Update on diffusion MRI in Parkinson's disease and atypical parkinsonism. *J Neurol Sci, 332 (*1-2), *21 – 29.* doi:10.1016/j.jns.2013.06.032

Meindl, T., Teipel, S., Elmouden, R., Mueller, S., Koch, W., Dietrich, O., . . . Glaser, C. (2010). Test-retest reproducibility of the default-mode network in healthy individuals. *Hum Brain Mapp, 31*(2), 237-246. doi: 10.1002/hbm.20860

Meireles, J., & Massano, J. (2012). Cognitive impairment and dementia in Parkinson's disease: clinical features, diagnosis, and management. *Front Neurol, 3*, 88. doi: 10.3389/fneur.2012.00088

Melzer, T. R. (2011). Magnetic resonance imaging of cognition in Parkinson's disease (Thesis, Doctor of Philosophy). University of Otago. Retrieved from http://hdl.handle.net/10523/1719.

Melzer, T. R., Watts, R., MacAskill, M. R., Pitcher, T. L., Livingston, L., Keenan, R. J., . . . Anderson, T. J. (2012). Grey matter atrophy in cognitively impaired Parkinson's disease. *J Neurol Neurosurg Psychiatry, 83*(2), 188-194. doi: 10.1136/jnnp-2011-300828

Meyers, J.E, & Meyers, K.R. (1995). *Rey complex figure test and recognition trial: professional manual. Psychological Assessment resources*. USA: Florida.

Minoshima, S., Giordani, B., Brent, S., Frey, K.A., Foster, N.L., & Kuhl, D.E. (1997). Metabolic reduction in the posterior cingulate cortex in very early Alzheimer's disease. *Ann Neurology, 42*, 85 – 94. DOI: 10.1002/ana.410420114.

Mohammadi, B., Kollewe, K., Samii, A., Krampfl, K., Dengler, R., & Munte, T. F. (2009). Changes of resting state brain networks in amyotrophic lateral sclerosis. *Exp Neurol*, *217*(1), 147-153. doi: 10.1016/j.expneurol.2009.01.025

Molloy, D.W., Alemayehu, E., & Roberts, R. (1991). Reliability of a standard Mini-Mental State Examination compared with the traditional Mini-Mental State Examination. Am J Psychiatry, 148 (1), 102 – 105. Retrieved from http://ajp.psychiatryonline.org/article.aspx?articleid=167366

Molloy, D.W., & Standish, T.I. (1997). A guide to the standardized mini-mental state examination. *Int Psychogeriatr, 9* (Suppl 1), 87 – 94. Retrieved from http://www.dementia-assessment.com.au/guidelines/Guide_Standardised_MMSE.pdf

Morris, J.C. (1993). The Clinical Dementia Rating (CDR): current version and scoring rules. *Neurology, 43* (11), 2412, - 2414. http://dx.doi.org/10.1212/WNL.43.11.2412-a

Nasreddine, Z.S., Phillips, N.A., Bedirian, V., Charbonneau, S., Whitehead, V., Collin I…Chertkow, H. (2005). The Montreal cognitive assessment, MoCa: a brief screening tool mor mild cognitive impairment. *J Am Geriatr Soc*, *53* (4), 695 – 699. DOI: 10.1111/j.1532-5415.2005.53221.x

Niendam, T. A., Laird, A. R., Ray, K. L., Dean, Y. M., Glahn, D. C., & Carter, C. S. (2012). Meta-analytic evidence for a superordinate cognitive control network subserving diverse executive functions. *Cogn Affect Behav Neurosci, 12*(2), 241-268. doi: 10.3758/s13415-011-0083-5

Pangman, V. C., Sloan, J., & Guse, L. (2000). An examination of psychometric properties of the mini-mental state examination and the standardized mini-mental state examination: implications for clinical practice. *Appl Nurs Res, 13*(4), 209-213. doi: 10.1053/apnr.2000.9231

Petrella, J.R., Sheldon, F.C., Prince, S.E., Calhoun, V.D., & Doraiswamy, P.M. (2011). Default mode network connectivity in stable vs progressive mild cognitive impairment. *Neurology, 76* (6), 511 – 517. doi: 10.1212/WNL.0b013e31820af94e

Piatt, A.L., Fields, J.A., Paolo, A.M., Troster, Al. (2004). Action verbal fluency normative data for the elderly. *Brain Lang, 89* (3), 580 – 583. doi: 10.1093/arclin/14.1.62

Posada, I. J., Benito-Leon, J., Louis, E. D., Trincado, R., Villarejo, A., Medrano, M. J., & Bermejo-Pareja, F. (2011). Mortality from Parkinson's disease: a population-based prospective study (NEDICES). *Mov Disord, 26*(14), 2522-2529. doi: 10.1002/mds.23921

Qi, R., Zhang, L.J., Xu, Q., Zhong, J., Wu, S., Zhang, Z…Lu, G. (2012). Selective impairments of Resting-State Networks in Minimal Hepatic Encephalopathy. *PloS One*, 7 (5), e3740. DOI: 10.1371/journal.pone.0037400.

Raichle, M. E. (2011). The restless brain. *Brain Connect, 1*(1), 3-12. doi: 10.1089/brain.2011.0019

Raichle, M.E., MacLeod, A.M., Snyder, A.Z., Powers, W.J., Gusnard, D.A., & Shulman, G.L. (2001). A default mode of brain function. *Proc Natl Acad Sci USA, 98* (2), 676 – 682. doi: 10.1073/pnas.98.2.676.

Reitan, R. M. (1958). Validity of the Trail Making test as an indicator of organic brain damage. *Percept. Mot Skills*, **8**, 271 - 276. doi: 10.2466/PMS.8.7.271-276

Reisberg, B. (1988), Functional assessment staging (FAST). *Psychopharmacol Bull, 24* (4), 653 – 659.

Reisberg, B., Ferris, S.H., deLeon, M.J., & Crook, T. (1982). The global deterioration scale for assessment of primary degenerative dementias. *Am J Psychiatry, 139* (9), 1136 – 1139. Retrieved from http://ajp.psychiatryonline.org/article.aspx?articleid=161950

Reisberg, B., Finkel, S., Overall, J., Schmidt-Gollas, N., Kanowski, S…Erzigkeit, H. (2001). The Alzheimer's disease activities of daily living international scale (ADL-IS). *Int Psychogeriatr, 13* (2), 163 – 181. http://dx.doi.org/10.1017/S1041610201007566

Rektorova, I., Krajcovicova, L., Marecek, R., & Mikl, M. (2012). Default mode network and extrastriate visual resting state network in patients with Parkinson's disease dementia. *Neurodegener Dis, 10*(1-4), 232-237. doi: 10.1159/000334765

Robertson, I.H., Ward, T., Ridgeway, V. & Nimmo Smith, I. (1996). The structure of normal human attention: the test of everyday attention. *J Int Neuropsychol Soc, 2* (6), 523 – 534. http://dx.doi.org/10.1017/S1355617700001697

Rombouts, S. A., Barkhof, F., Goekoop, R., Stam, C. J., & Scheltens, P. (2005). Altered resting state networks in mild cognitive impairment and mild Alzheimer's disease: an fMRI study. *Hum Brain Mapp, 26*(4), 231-239. doi: 10.1002/hbm.20160

Rosazza, C., & Minati, L. (2011). Resting-state brain networks: literature review and clinical applications. *Neurol Sci, 32*(5), 773-785. doi: 10.1007/s10072-011-0636-y

Rosen, W.G., Mohs, R.C., & Davis, K.L. (1984). A new rating scale for Alzheimer's disease. *Am J Psychiatry, 14* (11), 1356 – 1364. Retrieved from http://ajp.psychiatryonline.org/article.aspx?articleid=161950

Schapira, A., & Jenner, P. (2011). Etiology and pathogenesis of Parkinson's disease. *Mov Disord, 26* (6), 1049-1055. doi: 10.1002/mds.23732.

Scheeringa, R., Bastiaansen, M. C., Petersson, K. M., Oostenveld, R., Norris, D. G., & Hagoort, P. (2008). Frontal theta EEG activity correlates negatively with the default mode network in resting state. *Int J Psychophysiol, 67*(3), 242-251. doi: 10.1016/j.ijpsycho.2007.05.017

Scherfler, C., Frauscher, B., Schocke, M., Iranzo, A., Gschliesser, V., Seppi, K., . . . Group, S. (2011). White and gray matter abnormalities in idiopathic rapid eye movement sleep behavior disorder: a diffusion-tensor imaging and voxel-based morphometry study. *Ann Neurol, 69*(2), 400-407. doi: 10.1002/ana.22245

Schopf, V., Kasess, C. H., Lanzenberger, R., Fischmeister, F., Windischberger, C., & Moser, E. (2010). Fully exploratory network ICA (FENICA) on resting-state fMRI data. *J Neurosci Methods, 192*(2), 207-213. doi: 10.1016/j.jneumeth.2010.07.028

Schuff, N. (2009). Potential role of high-field MRI for studies in Parkinson's disease. *Mov Disord, 24 Suppl 2*, S684-690. doi: 10.1002/mds.22647

Schwarz, S. T., Abaei, M., Gontu, V., Morgan, P. S., Bajaj, N., & Auer, D. P. (2013). Diffusion tensor imaging of nigral degeneration in Parkinson's disease: A region-of-interest and voxel-based study at 3 T and systematic review with meta-analysis. *Neuroimage Clin, 3*, 481-488. doi: 10.1016/j.nicl.2013.10.006

Seeley, W. W., Menon, V., Schatzberg, A. F., Keller, J., Glover, G. H., Kenna, H., . . . Greicius, M. D. (2007). Dissociable intrinsic connectivity networks for salience processing

and executive control. *J Neurosci*, *27*(9), 2349-2356. doi: 10.1523/JNEUROSCI.5587-06.2007

Shehzad, Z., Kelly, A. M., Reiss, P. T., Gee, D. G., Gotimer, K., Uddin, L. Q., . . . Milham, M. P. (2009). The resting brain: unconstrained yet reliable. *Cereb Cortex*, *19*(10), 2209-2229. doi: 10.1093/cercor/bhn256

Skudlarski, P., Jagannathan, K., Calhoun, V., Hampson, M., & Skudlarska, B.A., & Pearlson, G. (2008). Measuring brain connectivity: diffusion tensor imaging validates resting state temporal correlations. *Neuroimage., 43* (5), 554- 561. doi: 10.1016/j.neuroimage.2008.07.063.

Smith, S. M., Jenkinson, M., Woolrich, M. W., Beckmann, C. F., Behrens, T. E., Johansen-Berg, H., . . . Matthews, P. M. (2004). Advances in functional and structural MR image analysis and implementation as FSL. *Neuroimage, 23 Suppl 1*, S208-219. doi: 10.1016/j.neuroimage.2004.07.051

Spreng, R. N. (2012). The fallacy of a "task-negative" network. *Front Psychol, 3*, 145. doi: 10.3389/fpsyg.2012.00145

Spreng, R.N., & Grady, C.L. (2010). Patterns of brain activity supporting autobiographical memory, prospection, and theory of mind, and their relationship to the default mode network. *J Cogn Neurosci*, *22* (6), 1112 – 1123. doi: 10.1162/jocn.2009.21282.

Song, M., Du, H., Wu, N., Hou, B., Wu, G., Wang, J…Jiang, T. (2011). Impaired resting state functional integrations within the default mode network of generalized tonic-clonic seizures. *PloS One, 6* (2), e17294. DOI: 10.1371/journal.pone.0017294.

Sridharan, D., Levitin, D. J., & Menon, V. (2008). A critical role for the right fronto-insular cortex in switching between central-executive and default-mode networks. *Proc Natl Acad Sci U S A, 105*(34), 12569-12574. doi: 10.1073/pnas.0800005105

Svenningsson, P., Westman, E., Ballard, C., & Aarsland, D. (2012). Cognitive impairment in patients with Parkinson's disease: diagnosis, biomarkers, and treatment. *The Lancet Neurology, 11*(8), 697-707. doi: 10.1016/s1474-4422(12)70152-7

Thal, D.R., Del Tredici, K, & Braak, H (2004). Neurodegeneration in normal brain aging and disease. Sci Aging Knowledge Environ, 23, pe26. doi: 10.1126/sageke.2004.23.pe26.

Teipel, S. J., Bokde, A. L., Meindl, T., Amaro, E., Jr., Soldner, J., Reiser, M. F., . . . Hampel, H. (2010). White matter microstructure underlying default mode network connectivity in the human brain. *Neuroimage, 49*(3), 2021-2032. doi: 10.1016/j.neuroimage.2009.10.067

Tessitore, A., Esposito, F., Vitale, C., Santangelo, G., Amboni, M., Russo, A., Corbo D., Cirillo, G., Barone, P., & Tedeschi, G. (2012). Default mode network connectivity in cognitively unimpaired patients with Parkinson disease. *Neurology, 79* (23), 2226 – 2232. doi: 10.1212/WNL.0b013e31827689d6.

Tomasi, D., & Volkow, N. D. (2011). Association between functional connectivity hubs and brain networks. *Cereb Cortex, 21*(9), 2003-2013. doi: 10.1093/cercor/bhq268

Turkeltaub, P. E., Eden, G. F., Jones, K. M., & Zeffiro, T. A. (2002). Meta-Analysis of the Functional Neuroanatomy of Single-Word Reading: Method and Validation. *Neuroimage, 16*(3), 765-780. doi: 10.1006/nimg.2002.1131

van Eimeren, T., Monchi, O., Ballanger, B., Strafella, A.P. (2009). Dysfunction of the default mode network in Parkinson disease: a functional magnetic resonance imaging study. *Arch Neurol, 66* (7), 877 – 883. doi: 10.1001/archneurol.2009.97.

van den Heuvel, M. P., & Hulshoff Pol, H. E. (2010). Exploring the brain network: a review on resting-state fMRI functional connectivity. *Eur Neuropsychopharmacol, 20*(8), 519-534. doi: 10.1016/j.euroneuro.2010.03.008

Vertesi, A., Lever, J.A., Molloy, D.W., Sanderson, B., Tuttle, I., & Prinicipi, E. (2001). Standardized Mini-Mental State Examination: use and interpretation. *Can Fam Physician, 47*, 2018 – 2023. Retrieved from http://www.cfp.ca/content/47/10/2018.full.pdf

Vincent, J. L., Kahn, I., Snyder, A. Z., Raichle, M. E., & Buckner, R. L. (2008). Evidence for a frontoparietal control system revealed by intrinsic functional connectivity. *J Neurophysiol, 100*(6), 3328-3342. doi: 10.1152/jn.90355.2008

Wang, Z., Lu, G., Zhang, Z., Zhong, Y., Jiao, Q., Zhang, Z., . . . Liu, Y. (2011). Altered resting state networks in epileptic patients with generalized tonic-clonic seizures. *Brain Res, 1374*, 134-141. doi: 10.1016/j.brainres.2010.12.034

Warrington E.K., & James, M. (1991). *The visual object and space perception battery* (VOSP). England: Thames Valley Corporation.

Wechsler, D. (1997). *Wechsler adult intelligence scale* (WAIS-III). Psychological Cooperation: USA.

Weintraub, D., Dietz, N., Duda, J. E., Wolk, D. A., Doshi, J., Xie, S. X., . . . Siderowf, A. (2012). Alzheimer's disease pattern of brain atrophy predicts cognitive decline in Parkinson's disease. *Brain, 135*(Pt 1), 170-180. doi: 10.1093/brain/awr277

Wen, X., Wu, X., Li, R., Fleisher, A. S., Reiman, E. M., Wen, X., . . . Yao, L. (2013). Alzheimer's disease-related changes in regional spontaneous brain activity levels and inter-region interactions in the default mode network. *Brain Res, 1509*, 58-65. doi: 10.1016/j.brainres.2013.03.007

Werheid K., Hoppe, C., Thorne, A., Muller, U., Mungersdorf, M., & von Cramon, D.Y. (2002). The adaptive digit-ordering test: clinical application, reliability, and validity of a verbal working memory test. *Arch Clin Neuropsychol*, *17* (6), 547 – 565. http://dx.doi.org/10.1016/S0887-6177(01)00134-2

White, T. P., Joseph, V., Francis, S. T., & Liddle, P. F. (2010). Aberrant salience network (bilateral insula and anterior cingulate cortex) connectivity during information processing in schizophrenia. *Schizophr Res, 123*(2-3), 105-115. doi: 10.1016/j.schres.2010.07.020

Whitwell, J. L. (2009). Voxel-based morphometry: an automated technique for assessing structural changes in the brain. *J Neurosci, 29*(31), 9661-9664. doi: 10.1523/JNEUROSCI.2160-09.2009

Williams-Gray, C. H., Foltynie, T., Brayne, C. E., Robbins, T. W., & Barker, R. A. (2007). Evolution of cognitive dysfunction in an incident Parkinson's disease cohort. *Brain, 130*(Pt 7), 1787-1798. doi: 10.1093/brain/awm111

Wirdefeldt, K., Adami, H. O., Cole, P., Trichopoulos, D., & Mandel, J. (2011). Epidemiology and etiology of Parkinson's disease: a review of the evidence. *Eur J Epidemiol, 26 Suppl 1*, S1-58. doi: 10.1007/s10654-011-9581-6

Wood, K., Livingston, L., Melzer, T.R., Pitcher, T.L., MacAskill, M.R., Dalrymple-Alford, J.C. (2013). Criteria for Parkinson's disease with mild cognitive impairment associated with increased progression to dementia. *31st International Australasian Winter Conference on Brain Research*, Vol. 31 (Queenstown, New Zealand, 2013).

Wu, J. T., Wu, H. Z., Yan, C. G., Chen, W. X., Zhang, H. Y., He, Y., & Yang, H. S. (2011). Aging-related changes in the default mode network and its anti-correlated networks: a resting-state fMRI study. *Neurosci Lett, 504*(1), 62-67. doi: 10.1016/j.neulet.2011.08.059

Yeo, B. T., Krienen, F. M., Sepulcre, J., Sabuncu, M. R., Lashkari, D., Hollinshead, M., . . . Buckner, R. L. (2011). The organization of the human cerebral cortex estimated by intrinsic functional connectivity. *J Neurophysiol, 106*(3), 1125-1165. doi: 10.1152/jn.00338.2011

Yesavage, J.A., Brink, T.L., Rose, T.L., Lum,O., Huang, V…Leirer, V.O. (1982). Development and validation of a geriatric depression screening scale: a preliminary report. *J Psychiatry Res, 17* (1), 37 – 49. http://dx.doi.org/10.1016/0022-3956(82)90033-4

Zhou, Y., Liang, M., Tian, L., Wang, K., Hao, Y., Liu, H., . . . Jiang, T. (2007). Functional disintegration in paranoid schizophrenia using resting-state fMRI. *Schizophr Res, 97*(1-3), 194-205. doi: 10.1016/j.schres.2007.05.029

Appendix 1: Newman-Keuls Tests

DMN Newman-Keuls Test

DMN Newman-Keuls Test (lPCC)

FA

Newman-Keuls test; variable FA (lPCC) Approximate Probabilities for Post Hoc Tests Error: Between MSE = .00039, df = 135.00

	Group	{1} - .15179	{2} - .14318	{3} - .13613	{4} - .14729
1	HC		0.226863	0.014705	0.389822
2	PD-N	0.226863		0.177808	0.432517
3	PD-MCI	0.014705	0.177808		0.083379
4	PD-D	0.389822	0.432517	0.083379	

*red = significant, p <0.05

MD

Newman-Keuls test; variable MD (lPCC) Approximate Probabilities for Post Hoc Tests Error: Between MSE = .00000, df = 135.00

	Group	{1} - .00090	{2} - .00091	{3} - .00098	{4} - .00100
1	HC		0.748937	0.003110	0.000087
2	PD-N	0.748937		0.003196	0.000184
3	PD-MCI	0.003110	0.003196		0.280764
4	PD-D	0.000087	0.000184	0.280764	

*red = significant, p <0.05

Grey Matter

Newman-Keuls test; variable Grey Matter Voxel (lPCC GM) Approximate Probabilities for Post Hoc Tests Error: Between MSE = 723.07, df = 135.00

	Group	{1} - 139.35	{2} - 136.97	{3} - 131.39	{4} - 150.83
1	HC		0.736576	0.500129	0.105607
2	PD-N	0.736576		0.431802	0.123647
3	PD-MCI	0.500129	0.431802		0.031175
4	PD-D	0.105607	0.123647	0.031175	

*red = significant, p <0.05

DMN Newman-Keuls Test (rPCC)

FA

Newman-Keuls test; variable FA (rPCC) Approximate Probabilities for Post Hoc Tests Error: Between MSE = .00039, df = 135.00					
	Group	**{1} - .14596**	**{2} - .13997**	**{3} - .13552**	**{4} - .14383**
1	HC		0.481684	0.184262	0.682110
2	PD-N	0.481684		0.391360	0.457452
3	PD-MCI	0.184262	0.391360		0.245513
4	PD-D	0.682110	0.457452	0.245513	

MD

Newman-Keuls test; variable MD (rPCC) Approximate Probabilities for Post Hoc Tests Error: Between MSE = .00000, df = 135.00					
	Group	**{1} - .00092**	**{2} - .00091**	**{3} - .00096**	**{4} - .00103**
1	HC		0.743895	0.078061	0.000030
2	PD-N	0.743895		0.092138	0.000011
3	PD-MCI	0.078061	0.092138		0.003751
4	PD-D	0.000030	0.000011	0.003751	

*red = significant, p <0.05

Grey Matter

Newman-Keuls test; variable Grey Matter Voxel (rPCC GM) Approximate Probabilities for Post Hoc Tests Error: Between MSE = 789.51, df = 135.00					
	Group	**{1} - 135.90**	**{2} - 143.39**	**{3} - 138.82**	**{4} - 147.44**
1	HC		0.570382	0.693778	0.403349
2	PD-N	0.570382		0.537572	0.584411
3	PD-MCI	0.693778	0.537572		0.475121
4	PD-D	0.403349	0.584411	0.475121	

DMN Newman-Keuls Test (ldMPFC)

FA

Newman-Keuls test; variable FA (ldMPFC) Approximate Probabilities for Post Hoc Tests
Error: Between MSE = .00060, df = 135.00

	Group	{1} - .15385	{2} - .15266	{3} - .14990	{4} - .15358
1	HC		0.981673	0.928661	0.967236
2	PD-N	0.981673		0.668874	0.886984
3	PD-MCI	0.928661	0.668874		0.836192
4	PD-D	0.967236	0.886984	0.836192	

MD

Newman-Keuls test; variable MD (ldMPFC) Approximate Probabilities for Post Hoc Tests
Error: Between MSE = .00000, df = 135.00

	Group	{1} - .00111	{2} - .00109	{3} - .00117	{4} - .00139
1	HC		0.794308	0.283000	0.000028
2	PD-N	0.794308		0.376057	0.000011
3	PD-MCI	0.283000	0.376057		0.000279
4	PD-D	0.000028	0.000011	0.000279	

*red = significant, p <0.05

Grey Matter

Newman-Keuls test; variable Grey Matter Voxel (ldMPFC GM) Approximate Probabilities for Post Hoc Tests Error: Between MSE = 977.65, df = 135.00

	Group	{1} - 128.32	{2} - 150.67	{3} - 142.93	{4} - 140.33
1	HC		0.034034	0.179408	0.145321
2	PD-N	0.034034		0.347802	0.421684
3	PD-MCI	0.179408	0.347802		0.753023
4	PD-D	0.145321	0.421684	0.753023	

*red = significant, p <0.05

DMN Newman-Keuls Test (rdMPFC)

FA

Newman-Keuls test; variable FA (rdMPFC) Approximate Probabilities for Post Hoc Tests
Error: Between MSE = .00053, df = 135.00

	Group	{1} - .14966	{2} - .16002	{3} - .15044	{4} - .15211
1	HC		0.323966	0.897758	0.914454
2	PD-N	0.323966		0.258327	0.194801
3	PD-MCI	0.897758	0.258327		0.783864
4	PD-D	0.914454	0.194801	0.783864	

MD

Newman-Keuls test; variable MD (rdMPFC) Approximate Probabilities for Post Hoc Tests
Error: Between MSE = .00000, df = 135.00

	Group	{1} - .00109	{2} - .00101	{3} - .00111	{4} - .00125
1	HC		0.096302	0.699037	0.004231
2	PD-N	0.096302		0.100573	0.000015
3	PD-MCI	0.699037	0.100573		0.005255
4	PD-D	0.004231	0.000015	0.005255	

*red = significant, p <0.05

Grey Matter

Newman-Keuls test; variable Grey Matter Voxel (rdMPFC GM) Approximate Probabilities for Post Hoc Tests Error: Between MSE = 934.06, df = 135.00

	Group	{1} - 146.65	{2} - 159.27	{3} - 148.68	{4} - 142.06
1	HC		0.260690	0.800878	0.569142
2	PD-N	0.260690		0.189094	0.142098
3	PD-MCI	0.800878	0.189094		0.689638
4	PD-D	0.569142	0.142098	0.689638	

DMN Newman-Keuls Test (lvMPFC)

FA

Newman-Keuls test; variable FA (lvMPFC) Approximate Probabilities for Post Hoc Tests
Error: Between MSE = .00089, df = 135.00

	Group	{1} - .17875	{2} - .17017	{3} - .16153	{4} - .16793
1	HC		0.274596	0.124985	0.352071
2	PD-N	0.274596		0.513456	0.774727
3	PD-MCI	0.124985	0.513456		0.415218
4	PD-D	0.352071	0.774727	0.415218	

MD

Newman-Keuls test; variable MD (lvMPFC) Approximate Probabilities for Post Hoc Tests
Error: Between MSE = .00000, df = 135.00

	Group	{1} - .00097	{2} - .00096	{3} - .00101	{4} - .00105
1	HC		0.681381	0.123128	0.017492
2	PD-N	0.681381		0.124257	0.009187
3	PD-MCI	0.123128	0.124257		0.235257
4	PD-D	0.017492	0.009187	0.235257	

*red = significant, p <0.05

Grey Matter

Newman-Keuls test; variable Grey Matter Voxel (lvMPFC GM) Approximate Probabilities for Post Hoc Tests Error: Between MSE = 865.18, df = 135.00

	Group	{1} - 156.00	{2} - 169.83	{3} - 159.11	{4} - 170.83
1	HC		0.175519	0.688809	0.222958
2	PD-N	0.175519		0.167036	0.896925
3	PD-MCI	0.688809	0.167036		0.285516
4	PD-D	0.222958	0.896925	0.285516	

DMN Newman-Keuls Test (rvMPFC)

FA

Newman-Keuls test; variable FA (rvMPFC) Approximate Probabilities for Post Hoc Tests
Error: Between MSE = .00089, df = 135.00

	Group	{1} - .17737	{2} - .16616	{3} - .16149	{4} - .16263
1	HC		0.154973	0.182364	0.147160
2	PD-N	0.154973		0.824003	0.653612
3	PD-MCI	0.182364	0.824003		0.885496
4	PD-D	0.147160	0.653612	0.885496	

MD

Newman-Keuls test; variable MD (rvMPFC) Approximate Probabilities for Post Hoc Tests
Error: Between MSE = .00000, df = 135.00

	Group	{1} - .00093	{2} - .00095	{3} - .00100	{4} - .00106
1	HC		0.541335	0.028843	0.000021
2	PD-N	0.541335		0.052200	0.000138
3	PD-MCI	0.028843	0.052200		0.030693
4	PD-D	0.000021	0.000138	0.030693	

*red = significant, p <0.05

Grey Matter

Newman-Keuls test; variable Grey Matter Voxel (rvMPFC GM) Approximate Probabilities for Post Hoc Tests Error: Between MSE = 981.68, df = 135.00

	Group	{1} - 162.58	{2} - 165.44	{3} - 156.64	{4} - 155.89
1	HC		0.729597	0.472475	0.697012
2	PD-N	0.729597		0.536414	0.655060
3	PD-MCI	0.472475	0.536414		0.927318
4	PD-D	0.697012	0.655060	0.927318	

DMN Newman-Keuls Test (lpIPL)

FA

Newman-Keuls test; variable FA (lpIPL) Approximate Probabilities for Post Hoc Tests Error: Between MSE = .00035, df = 135.00

	Group	{1} - .14024	{2} - .13390	{3} - .13908	{4} - .13543
1	HC		0.566370	0.811973	0.587610
2	PD-N	0.566370		0.541096	0.755397
3	PD-MCI	0.811973	0.541096		0.456198
4	PD-D	0.587610	0.755397	0.456198	

MD

Newman-Keuls test; variable MD (lpIPL) Approximate Probabilities for Post Hoc Tests Error: Between MSE = .00000, df = 135.00

	Group	{1} - .00098	{2} - .00101	{3} - .00105	{4} - .00108
1	HC		0.225964	0.034843	0.001886
2	PD-N	0.225964		0.203478	0.045611
3	PD-MCI	0.034843	0.203478		0.267832
4	PD-D	0.001886	0.045611	0.267832	

*red = significant, p <0.05

Grey Matter

Newman-Keuls test; variable Grey Matter Voxel (lpIPL GM) Approximate Probabilities for Post Hoc Tests Error: Between MSE = 1780.5, df = 135.00

	Group	{1} - 212.26	{2} - 209.17	{3} - 193.46	{4} - 205.72
1	HC		0.781572	0.329689	0.826982
2	PD-N	0.781572		0.335031	0.756618
3	PD-MCI	0.329689	0.335031		0.270758
4	PD-D	0.826982	0.756618	0.270758	

DMN Newman-Keuls Test (rpIPL)

FA

Newman-Keuls test; variable FA (rpIPL) Approximate Probabilities for Post Hoc Tests Error: Between MSE = .00024, df = 135.00					
	Group	**{1} - .13865**	**{2} - .13449**	**{3} - .13844**	**{4} - .14021**
1	HC		0.571985	0.960657	0.705054
2	PD-N	0.571985		0.337883	0.507986
3	PD-MCI	0.960657	0.337883		0.904035
4	PD-D	0.705054	0.507986	0.904035	

MD

Newman-Keuls test; variable MD (rpIPL) Approximate Probabilities for Post Hoc Tests Error: Between MSE = .00000, df = 135.00					
	Group	**{1} - .00097**	**{2} - .00096**	**{3} - .00099**	**{4} - .00102**
1	HC		0.718963	0.344978	0.117304
2	PD-N	0.718963		0.392774	0.089297
3	PD-MCI	0.344978	0.392774		0.300673
4	PD-D	0.117304	0.089297	0.300673	

Grey Matter

Newman-Keuls test; variable Grey Matter Voxel (rpIPL GM) Approximate Probabilities for Post Hoc Tests Error: Between MSE = 1576.8, df = 135.00					
	Group	**{1} - 230.90**	**{2} - 239.95**	**{3} - 231.11**	**{4} - 223.39**
1	HC		0.663032	0.984480	0.473124
2	PD-N	0.663032		0.398371	0.389231
3	PD-MCI	0.984480	0.398371		0.741541
4	PD-D	0.473124	0.389231	0.741541	

DMN Newman-Keuls Test (lMTG)

FA

Newman-Keuls test; variable FA (lMTG) Approximate Probabilities for Post Hoc Tests
Error: Between MSE = .00048, df = 135.00

	Group	{1} - .16427	{2} - .15896	{3} - .16240	{4} - .16461
1	HC		0.629250	0.747572	0.953415
2	PD-N	0.629250		0.551455	0.763228
3	PD-MCI	0.747572	0.551455		0.923390
4	PD-D	0.953415	0.763228	0.923390	

MD

Newman-Keuls test; variable MD (lMTG) Approximate Probabilities for Post Hoc Tests
Error: Between MSE = .00000, df = 135.00

	Group	{1} - .00097	{2} - .00098	{3} - .00105	{4} - .00109
1	HC		0.836770	0.036467	0.000474
2	PD-N	0.836770		0.023865	0.000542
3	PD-MCI	0.036467	0.023865		0.137320
4	PD-D	0.000474	0.000542	0.137320	

*red = significant, p <0.05

Grey Matter

Newman-Keuls test; variable Grey Matter Voxel (lMTG GM) Approximate Probabilities for Post Hoc Tests Error: Between MSE = 1493.3, df = 135.00

	Group	{1} - 235.52	{2} - 234.58	{3} - 221.64	{4} - 244.83
1	HC		0.926686	0.361531	0.360687
2	PD-N	0.926686		0.204432	0.572992
3	PD-MCI	0.361531	0.204432		0.103842
4	PD-D	0.360687	0.572992	0.103842	

DMN Newman-Keuls Test (rMTG)

FA

Newman-Keuls test; variable FA (rMTG) Approximate Probabilities for Post Hoc Tests
Error: Between MSE = .00038, df = 135.00

	Group	{1} - .15911	{2} - .15697	{3} - .16080	{4} - .15869
1	HC		0.907974	0.740961	0.934471
2	PD-N	0.907974		0.877073	0.736651
3	PD-MCI	0.740961	0.877073		0.910352
4	PD-D	0.934471	0.736651	0.910352	

MD

Newman-Keuls test; variable MD (rMTG) Approximate Probabilities for Post Hoc Tests
Error: Between MSE = .00000, df = 135.00

	Group	{1} - .00097	{2} - .00098	{3} - .00101	{4} - .00108
1	HC		0.727986	0.178884	0.000170
2	PD-N	0.727986		0.154264	0.000375
3	PD-MCI	0.178884	0.154264		0.015689
4	PD-D	0.000170	0.000375	0.015689	

*red = significant, p <0.05

Grey Matter

Newman-Keuls test; variable Grey Matter Voxel (rMTG GM) Approximate Probabilities for Post Hoc Tests Error: Between MSE = 1623.4, df = 135.00

	Group	{1} - 239.23	{2} - 252.69	{3} - 235.89	{4} - 258.56
1	HC		0.205284	0.753829	0.163400
2	PD-N	0.205284		0.254173	0.580854
3	PD-MCI	0.753829	0.254173		0.142843
4	PD-D	0.163400	0.580854	0.142843	

DAN Newman-Keuls

Newman-Keuls Test (lFEF)

FA

Newman-Keuls test; variable FA (lFEF) Approximate Probabilities for Post Hoc Tests Error: Between MSE = .00026, df = 135.00

	Group	{1} - .13438	{2} - .13245	{3} - .13287	{4} - .15048
1	HC		0.893701	0.724351	0.000174
2	PD-N	0.893701		0.921206	0.000151
3	PD-MCI	0.724351	0.921206		0.000131
4	PD-D	0.000174	0.000151	0.000131	

*red = significant, p <0.05

MD

Newman-Keuls test; variable MD (lFEF) Approximate Probabilities for Post Hoc Tests Error: Between MSE = .00000, df = 135.00

	Group	{1} - .00105	{2} - .00104	{3} - .00104	{4} - .00110
1	HC		0.975778	0.939967	0.103768
2	PD-N	0.975778		0.892127	0.255516
3	PD-MCI	0.939967	0.892127		0.204317
4	PD-D	0.103768	0.255516	0.204317	

Grey Matter

Newman-Keuls test; variable Grey Matter Voxel (lFEF GM) Approximate Probabilities for Post Hoc Tests Error: Between MSE = 1388.2, df = 135.00

	Group	{1} - 208.16	{2} - 210.56	{3} - 195.86	{4} - 216.67
1	HC		0.806996	0.210586	0.662140
2	PD-N	0.806996		0.292677	0.534532
3	PD-MCI	0.210586	0.292677		0.147504
4	PD-D	0.662140	0.534532	0.147504	

Newman-Keuls Test (rFEF)

FA

Newman-Keuls test; variable FA (rFEF) Approximate Probabilities for Post Hoc Tests Error: Between MSE = .00036, df = 135.00					
	Group	**{1} - .14802**	**{2} - .14560**	**{3} - .14362**	**{4} - .14945**
1	HC		0.629570	0.655885	0.774522
2	PD-N	0.629570		0.694306	0.722191
3	PD-MCI	0.655885	0.694306		0.650994
4	PD-D	0.774522	0.722191	0.650994	

MD

Newman-Keuls test; variable MD (rFEF) Approximate Probabilities for Post Hoc Tests Error: Between MSE = .00000, df = 135.00					
	Group	**{1} - .00096**	**{2} - .00098**	**{3} - .00102**	**{4} - .00110**
1	HC		0.603981	0.208785	0.000201
2	PD-N	0.603981		0.241264	0.000840
3	PD-MCI	0.208785	0.241264		0.013972
4	PD-D	0.000201	0.000840	0.013972	

*red = significant, p <0.05

Grey Matter

Newman-Keuls test; variable Grey Matter Voxel (rFEF GM) Approximate Probabilities for Post Hoc Tests Error: Between MSE = 1258.2, df = 135.00					
	Group	**{1} - 183.00**	**{2} - 174.70**	**{3} - 178.54**	**{4} - 180.33**
1	HC		0.811760	0.882098	0.775646
2	PD-N	0.811760		0.682086	0.819155
3	PD-MCI	0.882098	0.682086		0.847658
4	PD-D	0.775646	0.819155	0.847658	

Newman-Keuls Test (laIPS)

FA

Newman-Keuls test; variable FA (laIPS) Approximate Probabilities for Post Hoc Tests Error: Between MSE = .00018, df = 135.00					
	Group	**{1} - .12978**	**{2} - .12445**	**{3} - .12487**	**{4} - .13284**
1	HC		0.285068	0.163047	0.384355
2	PD-N	0.285068		0.906547	0.080483
3	PD-MCI	0.163047	0.906547		0.060852
4	PD-D	0.384355	0.080483	0.060852	

MD

Newman-Keuls test; variable MD (laIPS) Approximate Probabilities for Post Hoc Tests Error: Between MSE = .00000, df = 135.00					
	Group	**{1} - .00104**	**{2} - .00109**	**{3} - .00110**	**{4} - .00115**
1	HC		0.096404	0.103022	0.000610
2	PD-N	0.096404		0.706690	0.067220
3	PD-MCI	0.103022	0.706690		0.064677
4	PD-D	0.000610	0.067220	0.064677	

*red = significant, p <0.05

Grey Matter

Newman-Keuls test; variable Grey Matter Voxel (laIPS GM) Approximate Probabilities for Post Hoc Tests Error: Between MSE = 1183.1, df = 135.00					
	Group	**{1} - 200.13**	**{2} - 196.09**	**{3} - 174.14**	**{4} - 184.61**
1	HC		0.656492	0.021754	0.201249
2	PD-N	0.656492		0.041167	0.205659
3	PD-MCI	0.021754	0.041167		0.248586
4	PD-D	0.201249	0.205659	0.248586	

*red = significant, p <0.05

Newman-Keuls Test (raIPS)

FA

Newman-Keuls test; variable FA (raIPS) Approximate Probabilities for Post Hoc Tests Error: Between MSE = .00027, df = 135.00					
	Group	**{1} - .12634**	**{2} - .12336**	**{3} - .12561**	**{4} - .13159**
1	HC		0.769846	0.865558	0.225715
2	PD-N	0.769846		0.603196	0.227716
3	PD-MCI	0.865558	0.603196		0.350984
4	PD-D	0.225715	0.227716	0.350984	

MD

Newman-Keuls test; variable MD (raIPS) Approximate Probabilities for Post Hoc Tests Error: Between MSE = .00000, df = 135.00					
	Group	**{1} - .00109**	**{2} - .00109**	**{3} - .00113**	**{4} - .00120**
1	HC		0.901400	0.281051	0.001374
2	PD-N	0.901400		0.162425	0.001128
3	PD-MCI	0.281051	0.162425		0.031237
4	PD-D	0.001374	0.001128	0.031237	

*red = significant, p <0.05

Grey Matter

Newman-Keuls test; variable Grey Matter Voxel (raIPS GM) Approximate Probabilities for Post Hoc Tests Error: Between MSE = 1144.7, df = 135.00					
	Group	**{1} - 184.00**	**{2} - 178.95**	**{3} - 155.21**	**{4} - 149.83**
1	HC		0.571731	0.003608	0.000763
2	PD-N	0.571731		0.007828	0.003172
3	PD-MCI	0.003608	0.007828		0.546550
4	PD-D	0.000763	0.003172	0.546550	

*red = significant, p <0.05

Newman-Keuls Test (lpIPS)

FA

Newman-Keuls test; variable FA (lpIPS) Approximate Probabilities for Post Hoc Tests Error: Between MSE = .00046, df = 135.00					
	Group	**{1} - .13705**	**{2} - .13629**	**{3} - .13094**	**{4} - .13549**
1	HC		0.892256	0.700522	0.958786
2	PD-N	0.892256		0.610739	0.887996
3	PD-MCI	0.700522	0.610739		0.420396
4	PD-D	0.958786	0.887996	0.420396	

MD

Newman-Keuls test; variable MD (lpIPS) Approximate Probabilities for Post Hoc Tests Error: Between MSE = .00000, df = 135.00					
	Group	**{1} - .00108**	**{2} - .00107**	**{3} - .00113**	**{4} - .00119**
1	HC		0.758543	0.104306	0.001290
2	PD-N	0.758543		0.129778	0.000782
3	PD-MCI	0.104306	0.129778		0.058711
4	PD-D	0.001290	0.000782	0.058711	

*red = significant, p <0.05

Grey Matter

Newman-Keuls test; variable Grey Matter Voxel (lpIPS GM) Approximate Probabilities for Post Hoc Tests Error: Between MSE = 1376.6, df = 135.00					
	Group	{1} - 169.55	{2} - 170.64	{3} - 153.29	{4} - 151.33
1	HC		0.911146	0.096582	0.150099
2	PD-N	0.911146		0.178589	0.198283
3	PD-MCI	0.096582	0.178589		0.841891
4	PD-D	0.150099	0.198283	0.841891	

Newman-Keuls Test (rpIPS)

FA

Newman-Keuls test; variable FA (rpIPS) Approximate Probabilities for Post Hoc Tests Error: Between MSE = .00034, df = 135.00					
	Group	**{1} - .13499**	**{2} - .13353**	**{3} - .12799**	**{4} - .13561**
1	1		0.764671	0.325556	0.900251
2	2	0.764671		0.258324	0.905368
3	3	0.325556	0.258324		0.404581
4	4	0.900251	0.905368	0.404581	

MD

Newman-Keuls test; variable MD (rpIPS) Approximate Probabilities for Post Hoc Tests Error: Between MSE = .00000, df = 135.00					
	Group	**{1} - .00110**	**{2} - .00107**	**{3} - .00114**	**{4} - .00119**
1	1		0.415107	0.313815	0.068348
2	2	0.415107		0.162299	0.012990
3	3	0.313815	0.162299		0.226421
4	4	0.068348	0.012990	0.226421	

*red = significant, p <0.05

Grey Matter

Newman-Keuls test; variable Grey Matter Voxel (rpIPS GM) Approximate Probabilities for Post Hoc Tests Error: Between MSE = 1210.5, df = 135.00					
	Group	**{1} - 154.48**	**{2} - 164.34**	**{3} - 141.25**	**{4} - 147.61**
1	HC		0.282651	0.319327	0.453927
2	PD-N	0.282651		0.057406	0.161953
3	PD-MCI	0.319327	0.057406		0.488225
4	PD-D	0.453927	0.161953	0.488225	

Newman-Keuls Test (lMT+)

FA

Newman-Keuls test; variable FA (lMT+) Approximate Probabilities for Post Hoc Tests Error: Between MSE = .00036, df = 135.00

	Group	{1} - .13000	{2} - .13555	{3} - .13464	{4} - .13245
1	HC		0.688046	0.627337	0.626020
2	PD-N	0.688046		0.855631	0.811876
3	PD-MCI	0.627337	0.855631		0.664932
4	PD-D	0.626020	0.811876	0.664932	

MD

Newman-Keuls test; variable MD (lMT+) Approximate Probabilities for Post Hoc Tests Error: Between MSE = .00000, df = 135.00

	Group	{1} - .00093	{2} - .00091	{3} - .00096	{4} - .00107
1	HC		0.423301	0.248856	0.000022
2	PD-N	0.423301		0.123872	0.000008
3	PD-MCI	0.248856	0.123872		0.000020
4	PD-D	0.000022	0.000008	0.000020	

*red = significant, p <0.05

Grey Matter

Newman-Keuls test; variable Grey Matter Voxel (lMT+ GM) Approximate Probabilities for Post Hoc Tests Error: Between MSE = 1780.5, df = 135.00

	Group	{1} - 212.26	{2} - 209.17	{3} - 193.46	{4} - 205.72
1	HC		0.781572	0.329689	0.826982
2	PD-N	0.781572		0.335031	0.756618
3	PD-MCI	0.329689	0.335031		0.270758
4	PD-D	0.826982	0.756618	0.270758	

Newman-Keuls Test (rMT+)

FA

Newman-Keuls test; variable FA (rMT+) Approximate Probabilities for Post Hoc Tests Error: Between MSE = .00041, df = 135.00					
	Group	**{1} - .13758**	**{2} - .14011**	**{3} - .13354**	**{4} - .13537**
1	HC		0.633727	0.727775	0.678454
2	PD-N	0.633727		0.603783	0.645958
3	PD-MCI	0.727775	0.603783		0.730051
4	PD-D	0.678454	0.645958	0.730051	

MD

Newman-Keuls test; variable MD (rMT+) Approximate Probabilities for Post Hoc Tests Error: Between MSE = .00000, df = 135.00					
	Group	**{1} - .00096**	**{2} - .00094**	**{3} - .00101**	**{4} - .00101**
1	HC		0.444759	0.053002	0.021234
2	PD-N	0.444759		0.010970	0.006108
3	PD-MCI	0.053002	0.010970		0.986721
4	PD-D	0.021234	0.006108	0.986721	

*red = significant, p <0.05

Grey Matter

Newman-Keuls test; variable Grey Matter Voxel (rMT+ GM) Approximate Probabilities for Post Hoc Tests Error: Between MSE = 1576.8, df = 135.00					
	Group	**{1} - 230.90**	**{2} - 239.95**	**{3} - 231.11**	**{4} - 223.39**
1	HC		0.663032	0.984480	0.473124
2	PD-N	0.663032		0.398371	0.389231
3	PD-MCI	0.984480	0.398371		0.741541
4	PD-D	0.473124	0.389231	0.741541	

SN Newman-Keuls

Newman-Keuls Test (lACC)

FA

Newman-Keuls test; variable FA (lACC) Approximate Probabilities for Post Hoc Tests Error: Between MSE = .00054, df = 135.00

	Group	{1} - .16923	{2} - .16541	{3} - .16018	{4} - .17985
1	HC		0.534482	0.303355	0.083479
2	PD-N	0.534482		0.393641	0.048959
3	PD-MCI	0.303355	0.393641		0.007388
4	PD-D	0.083479	0.048959	0.007388	

*red = significant, p <0.05

MD

Newman-Keuls test; variable MD (lACC) Approximate Probabilities for Post Hoc Tests Error: Between MSE = .00000, df = 135.00

	Group	{1} - .00099	{2} - .00096	{3} - .00105	{4} - .00108
1	HC		0.292792	0.039634	0.005924
2	PD-N	0.292792		0.005329	0.000218
3	PD-MCI	0.039634	0.005329		0.307801
4	PD-D	0.005924	0.000218	0.307801	

*red = significant, p <0.05

Grey Matter

Newman-Keuls test; variable Grey Matter Voxel (lACC GM) Approximate Probabilities for Post Hoc Tests Error: Between MSE = 2297.2, df = 135.00

	Group	{1} - 238.13	{2} - 241.50	{3} - 239.54	{4} - 256.50
1	HC		0.961567	0.911414	0.466144
2	PD-N	0.961567		0.876540	0.235436
3	PD-MCI	0.911414	0.876540		0.371949
4	PD-D	0.466144	0.235436	0.371949	

Newman-Keuls Test (rACC)

FA

Newman-Keuls test; variable FA (rACC) Approximate Probabilities for Post Hoc Tests
Error: Between MSE = .00044, df = 135.00

	Group	{1} - .15722	{2} - .15386	{3} - .15282	{4} - .16615
1	HC		0.540585	0.703284	0.104807
2	PD-N	0.540585		0.851176	0.065595
3	PD-MCI	0.703284	0.851176		0.073043
4	PD-D	0.104807	0.065595	0.073043	

MD

Newman-Keuls test; variable MD (rACC) Approximate Probabilities for Post Hoc Tests
Error: Between MSE = .00000, df = 135.00

	Group	{1} - .00092	{2} - .00095	{3} - .00101	{4} - .00105
1	HC		0.343512	0.002060	0.000009
2	PD-N	0.343512		0.014760	0.000106
3	PD-MCI	0.002060	0.014760		0.082214
4	PD-D	0.000009	0.000106	0.082214	

*red = significant, p <0.05

Grey Matter

Newman-Keuls test; variable Grey Matter Voxel (rACC GM) Approximate Probabilities for Post Hoc Tests Error: Between MSE = 1974.7, df = 135.00

	Group	{1} - 240.74	{2} - 241.25	{3} - 244.11	{4} - 263.61
1	1		0.965431	0.955584	0.206879
2	2	0.965431		0.807443	0.136471
3	3	0.955584	0.807443		0.096140
4	4	0.206879	0.136471	0.096140	

Newman-Keuls Test (lINS)

FA

Newman-Keuls test; variable FA (lINS) Approximate Probabilities for Post Hoc Tests Error: Between MSE = .00047, df = 135.00

	Group	{1} - .16424	{2} - .16358	{3} - .15056	{4} - .17245
1	HC		0.908845	0.043666	0.150281
2	PD-N	0.908845		0.022485	0.266271
3	PD-MCI	0.043666	0.022485		0.000744
4	PD-D	0.150281	0.266271	0.000744	

*red = significant, p <0.05

MD

Newman-Keuls test; variable MD (lINS) Approximate Probabilities for Post Hoc Tests Error: Between MSE = .00000, df = 135.00

	Group	{1} - .00125	{2} - .00120	{3} - .00133	{4} - .00138
1	HC		0.383973	0.075409	0.018761
2	PD-N	0.383973		0.022039	0.001997
3	PD-MCI	0.075409	0.022039		0.354095
4	PD-D	0.018761	0.001997	0.354095	

*red = significant, p <0.05

Grey Matter

Newman-Keuls test; variable Grey Matter Voxel (rINS GM) Approximate Probabilities for Post Hoc Tests Error: Between MSE = 1343.4, df = 135.00

	Group	{1} - 194.87	{2} - 215.27	{3} - 189.14	{4} - 185.28
1	HC		0.034904	0.553526	0.581750
2	PD-N	0.034904		0.018907	0.010382
3	PD-MCI	0.553526	0.018907		0.689315
4	PD-D	0.581750	0.010382	0.689315	

Newman-Keuls Test (rINS)

FA

Newman-Keuls test; variable FA (rINS) Approximate Probabilities for Post Hoc Tests Error: Between MSE = .00035, df = 135.00

	Group	{1} - .15395	{2} - .15512	{3} - .14925	{4} - .14997
1	HC		0.812395	0.603192	0.416957
2	PD-N	0.812395		0.629469	0.545863
3	PD-MCI	0.603192	0.629469		0.883331
4	PD-D	0.416957	0.545863	0.883331	

MD

Newman-Keuls test; variable MD (rINS) Approximate Probabilities for Post Hoc Tests Error: Between MSE = .00000, df = 135.00

	Group	{1} - .00122	{2} - .00117	{3} - .00127	{4} - .00136
1	HC		0.147853	0.294100	0.002282
2	PD-N	0.147853		0.033577	0.000016
3	PD-MCI	0.294100	0.033577		0.021019
4	PD-D	0.002282	0.000016	0.021019	

*red = significant, p <0.05

Grey Matter

Newman-Keuls test; variable Grey Matter Voxel (rINS GM) Approximate Probabilities for Post Hoc Tests Error: Between MSE = 1343.4, df = 135.00

	Group	{1} - 194.87	{2} - 215.27	{3} - 189.14	{4} - 185.28
1	HC		0.034904	0.553526	0.581750
2	PD-N	0.034904		0.018907	0.010382
3	PD-MCI	0.553526	0.018907		0.689315
4	PD-D	0.581750	0.010382	0.689315	

CEN Newman-Keuls

Newman-Keuls Test (ldlPFC)

FA

Newman-Keuls test; variable FA (ldlPFC) Approximate Probabilities for Post Hoc Tests
Error: Between MSE = .00041, df = 135.00

	Group	{1} - .16234	{2} - .15806	{3} - .15804	{4} - .16887
1	HC		0.421923	0.698809	0.220631
2	PD-N	0.421923		0.997053	0.105544
3	PD-MCI	0.698809	0.997053		0.176320
4	PD-D	0.220631	0.105544	0.176320	

MD

Newman-Keuls test; variable MD (ldlPFC) Approximate Probabilities for Post Hoc Tests
Error: Between MSE = .00000, df = 135.00

	Group	{1} - .00107	{2} - .00108	{3} - .00115	{4} - .00121
1	HC		0.720641	0.065172	0.000252
2	PD-N	0.720641		0.060243	0.000559
3	PD-MCI	0.065172	0.060243		0.063173
4	PD-D	0.000252	0.000559	0.063173	

*red = significant, p <0.05

Grey Matter

Newman-Keuls test; variable Grey Matter Voxel (ldlPFC GM) Approximate Probabilities for Post Hoc Tests Error: Between MSE = 1059.3, df = 135.00

	Group	{1} - 183.97	{2} - 186.42	{3} - 190.64	{4} - 191.00
1	HC		0.774987	0.716846	0.845451
2	PD-N	0.774987		0.622949	0.854965
3	PD-MCI	0.716846	0.622949		0.966820
4	PD-D	0.845451	0.854965	0.966820	

Newman-Keuls Test (rdlPFC)

FA

Newman-Keuls test; variable FA (rdlPFC) Approximate Probabilities for Post Hoc Tests
Error: Between MSE = .00046, df = 135.00

	Group	{1} - .16473	{2} - .16588	{3} - .16215	{4} - .16890
1	HC		0.839386	0.648725	0.741432
2	PD-N	0.839386		0.787685	0.593091
3	PD-MCI	0.648725	0.787685		0.631530
4	PD-D	0.741432	0.593091	0.631530	

MD

Newman-Keuls test; variable MD (rdlPFC) Approximate Probabilities for Post Hoc Tests
Error: Between MSE = .00000, df = 135.00

	Group	{1} - .00102	{2} - .00102	{3} - .00107	{4} - .00113
1	HC		0.984398	0.169722	0.006981
2	PD-N	0.984398		0.344711	0.012398
3	PD-MCI	0.169722	0.344711		0.098170
4	PD-D	0.006981	0.012398	0.098170	

*red = significant, p <0.05

Grey Matter

Newman-Keuls test; variable Grey Matter Voxel (rdlPFC GM) Approximate Probabilities for Post Hoc Tests Error: Between MSE = 1218.2, df = 135.00

	Group	{1} - 183.26	{2} - 195.14	{3} - 177.11	{4} - 184.56
1	HC		0.400416	0.504069	0.887934
2	PD-N	0.400416		0.203789	0.250252
3	PD-MCI	0.504069	0.203789		0.697418
4	PD-D	0.887934	0.250252	0.697418	

Newman-Keuls Test (laIPL)

FA

Newman-Keuls test; variable FA (laIPL) Approximate Probabilities for Post Hoc Tests Error: Between MSE = .00025, df = 135.00

	Group	{1} - .13620	{2} - .14155	{3} - .13775	{4} - .14711
1	HC		0.407881	0.710993	0.045073
2	PD-N	0.407881		0.364418	0.183428
3	PD-MCI	0.710993	0.364418		0.065071
4	PD-D	0.045073	0.183428	0.065071	

*red = significant, p <0.05

MD

Newman-Keuls test; variable MD (laIPL) Approximate Probabilities for Post Hoc Tests Error: Between MSE = .00000, df = 135.00

	Group	{1} - .00105	{2} - .00102	{3} - .00107	{4} - .00111
1	HC		0.235731	0.710570	0.200295
2	PD-N	0.235731		0.264572	0.019614
3	PD-MCI	0.710570	0.264572		0.179664
4	PD-D	0.200295	0.019614	0.179664	

*red = significant, p <0.05

Grey Matter

Newman-Keuls test; variable Grey Matter Voxel (laIPL GM) Approximate Probabilities for Post Hoc Tests Error: Between MSE = 1093.2, df = 135.00

	Group	{1} - 202.03	{2} - 199.70	{3} - 175.07	{4} - 194.06
1	HC		0.789444	0.010741	0.631049
2	PD-N	0.789444		0.013156	0.517282
3	PD-MCI	0.010741	0.013156		0.029508
4	PD-D	0.631049	0.517282	0.029508	

*red = significant, p <0.05

Newman-Keuls Test (raIPL)

FA

Newman-Keuls test; variable FA (raIPL) Approximate Probabilities for Post Hoc Tests Error: Between MSE = .00022, df = 135.00

	Group	{1} - .13657	{2} - .13561	{3} - .13632	{4} - .14361
1	HC		0.967050	0.948525	0.071492
2	PD-N	0.967050		0.855584	0.170213
3	PD-MCI	0.948525	0.855584		0.148373
4	PD-D	0.071492	0.170213	0.148373	

MD

Newman-Keuls test; variable FA (raIPL) Approximate Probabilities for Post Hoc Tests Error: Between MSE = .00022, df = 135.00

	Group	{1} - .13657	{2} - .13561	{3} - .13632	{4} - .14361
1	HC		0.967050	0.948525	0.071492
2	PD-N	0.967050		0.855584	0.170213
3	PD-MCI	0.948525	0.855584		0.148373
4	PD-D	0.071492	0.170213	0.148373	

Grey Matter

Newman-Keuls test; variable Grey Matter Voxel (raIPL GM) Approximate Probabilities for Post Hoc Tests Error: Between MSE = 1482.4, df = 135.00

	Group	{1} - 235.03	{2} - 238.25	{3} - 213.29	{4} - 222.67
1	HC		0.751380	0.081696	0.223390
2	PD-N	0.751380		0.066657	0.274783
3	PD-MCI	0.081696	0.066657		0.355659
4	PD-D	0.223390	0.274783	0.355659	